5-1-2019

Moisture Absorption and Desorption Effects on Mechanical Behavior in Specialty Polyamide Products

Michelle Denison Brown
Lehigh University, sleepyzombiecow@gmail.com

Moisture Absorption and Desorption Effects on Mechanical Behavior in Specialty Polyamide Products

by

Michelle D. Brown

A Thesis

Presented to the Graduate and Research Committee

of Lehigh University

in Candidacy for the Degree of

Master of Science

in

Polymer Science & Engineering, Material Science & Engineering

Lehigh University

May 2019

Certificate of Approval

This thesis is accepted and approved in partial fulfillment of the requirements for the Master of Science.

_____
Date

_____
Thesis Advisor

_____
Co-Advisor

_____
Chairperson of Department

Acknowledgements

I would like to extend my deepest appreciation to EMS-GRIVORY for giving me the opportunity to complete the Master's program at Lehigh University as well as providing resources to complete my thesis project during normal business hours in addition to all hours of night and weekends.

My sincerest gratitude to the QA Lab for conducting all the viscosity testing for my thesis project and to the QA/MT Manager, Heather Bass, for proctoring my classes and co-advising this project.

My heartfelt thankfulness to my family for their loving support and to my husband, Sonny Brown, for your patience and understanding in this journey.

My eternal gratefulness to God for giving me the strength and perseverance to complete this achievement.

Table of Contents

List of Tables

List of Figures

Abstract

Nylon manufacturers provide one-size-fits-all recommendation for drying resin regarding temperature and time. This directive is generic considering the various types of nylons produced for various applications in automotive, sports, leisure, domestic appliances, and optics. Field experts and consultants provide vague points on the importance of drying nylons before processing, what temperatures to use, and how to avoid over drying. Determining an effective drying method for nylon resins and parts begins with understanding the degradation mechanisms associated with water absorption. The degradation mechanisms include plasticization, hydrolysis, and thermal oxidation. Another factor to consider is the effect of additives, fillers, and chemical structure on absorption behavior. This information provides a base for the qualitative analysis of water absorption and desorption behavior on specialty polyamides products such as unreinforced PA6, 50% glass reinforced PA6, 50% glass reinforced PA66+PA6, PA MACM12, 50% glass reinforced PA12, PA6I/6T, and 50% glass reinforced PA66+PA6I/X. These products share behavior indicative of their polyamide base as well as exhibit unique characteristics influenced by their composition.

CHAPTER 1: Introduction

1.1 Overview

Specialty nylons or polyamides exhibit qualities comparable to metal or glass with improved heat, chemical, and dimensional stability making them versatile in many commercial and domestic applications. Additives, fillers, uniquely formulated polymerization process, or combination of these factors contribute to its enhanced properties. Despite its robust composition, polyamides are susceptible to moisture which compromises durability in part manufacturing or field use. Drying becomes an important aspect of the production process. Data sheets, journals, seminars, and periodicals in the polymer field provide unspecific guidelines for drying polymers. Academic research studies about drying is minimal. Studies on related topics such as moisture absorption and heat aging are vast. The expert articles generally agree with the research studies. The articles provide highlights without delving into the details research provides. Plasticization studies support articles pointing out the importance of drying material before use to prevent lower performance properties. Hydrolysis studies support articles advising against processing wet material. Thermal oxidation studies support articles warning against drying material for too long or at too high a temperature. Several articles and studies indicate temperatures above the glass transition point yield better drying results.

Water diffusivity in absorption and desorption present value in characterizing a drying process. Several studies demonstrate various methods for determining water diffusion in polyamide. Knowledge of how water diffuses into the polymer matrix is just as important as how it diffuses out during desorption. KF titration and mass change

measurement methods for measuring moisture content are equally important in gauging the water content in material or samples.

1.2 Problem Definition

The complex composition of specialty nylons presents a challenge in determining water absorption and desorption behavior. Most research studies cover PA6 and PA66 behavior under moisture absorption and heat aging conditions which show agreement among each other. Polyamides under study are in their pure form which does not translate to behavior with additives, fillers, specialized formulation, aromatic structures, and cyclic structures. Amorphous polyamides are a specialty nylon with glass transition temperatures between 130°C and 150°C. The direct relationship between moisture absorption, the amorphous regions, and damaging effects at elevated temperatures presents a dilemma for these types of products.

1.3 Research Objective

Further study into absorption and desorption behavior needs to include characterizing other types of polyamides. Variation in behavior based on the polyamide structure should provide guidance in determining a more specific and effective drying method. Effectiveness of the method should be based on recovery of the original properties.

1.4 Theoretical Framework

1.4.1 Dependent Variables

Target monitoring on the absorption behavior in the presence of moisture and desorption behavior to eliminate water content for each polyamide under study.

1.4.2 Independent Variables

Absorption treatment methods include 100°C water, 23°C water, 23°C + 50% relative humidity environment, and 70°C + 62% relative humidity environment. Desorption treatment method utilizes 80°C, 100°C, 120°C, and 140°C exposure.

1.4.3 Moderating Variables

Weight change measurements at different intervals in both adsorption and desorption phases determine the exposure time.

1.4.4 Intervening Variables

Adverse physical effects exhibited by the samples immediately terminates the phase treatment for the product under test.

1.4.5 Assumptions

- Drying temperatures should be at or above the glass transition temperature
- Specialty polyamide products require longer absorption and desorption times due to additives and fillers inhibiting diffusion

1.4.6 Limitations

- Desorption treatment is limited to oven dryers.
- Experiment must be a simple methodology to be transferable to a manufacturing environment.
- Evaluation tests must be traceable to an established standard, such as ISO and ASTM, to comply with a manufacturing facility's quality system requirements.

1.5 Research Methodology

1.5.1 Research Type

Project is a qualitative analysis.

1.5.2 Sampling

Polyamide under study include unreinforced PA6, 50% glass reinforced PA6, 50% glass reinforced PA66+PA6, PA MACM12, 50% glass reinforced PA12, PA6I/6T, and 50% glass reinforced PA66+PA6I/X.

1.5.3 Data Analysis Methods

Evaluation based on qualitative comparative analysis.

CHAPTER 2: Literature Review

2.1 Introduction

Polyamides (PA), also called nylons, are a thermoplastic polymer found in automotive, sports and leisure, industrial, and domestic applications. Favorable qualities include excellent chemical resistance, high mechanical properties, dampening behavior [1], wear resistance against parts [2], and low manufacturing cost. Unfavorable quality is its hygroscopic nature. This makes it susceptible to absorb moisture from the air and undergo hydrolysis. Hydrolysis leads to molecular degradation by breaking the polymer chain [3]. This results in physical and chemical changes. Temperature, moisture level, and time affect degree of change. Changes range from the less destructive plasticization process to the most destructive hydrolysis degradation process. Plasticization increases molecular chain mobility and reduces relaxation time [4]. This is the first stage in the degradation process. Degradation results in mechanical property changes such as glass transition temperature reduction [5], viscosity reduction [6], tensile stress and modulus reduction [7], tensile elongation increase [7], and fracture toughness increase ([4], [8], [9]). Moisture is a common problem during part manufacturing. Injection molding wet material causes hydrolysis which compromises part integrity and deteriorates mechanical properties [10]. Other problems include poor part surface features such as splay, discoloration, and voids in addition to processing incidents such as outgassing and foaming ([11], [12]). Drying can reduce or prevent moisture effects. There is a risk of drying too long or at too high temperatures. Polyamides, like any thermoplastic, are vulnerable to thermal oxidative degradation below the melt point, decomposition around the melt point, and pyrolysis above the melt point if not properly monitored [6].

Degradation in an oxidative environment have similar effects as in a hydrolysis environment. This includes the molecular weight decreases while molar weight distribution widens, melt viscosity reduction, melt flow index reduction ([13], [14], [15]), and strength reduction. Many articles on drying hygroscopic polymers are available in the polymer manufacturing field. The articles provide some insight on into drying polyamides and generalized overview on optimum parameters. No direct method to determine an optimized drying process is available. Academic studies directly related to drying is sparse. Analysis on moisture absorption as well as extreme effects of thermal oxidation and hydrolysis are abundant. All sources provide valuable information but presents itself as a puzzle. Drying method for polyamides comes from extracting key information between polymer expert articles and academic degradation studies and developing a test approach.

2.1.1 Manufacturer Data Sheets and Expert Advice

Manufacturers make available technical data sheets for their products. Data sheets provide material description with key features, processing parameters, characterization properties, and drying recommendations. Most of the characterization properties include dry and conditioned values. Dry values represent data at moisture content equivalent to when it was molded. Conditioned values represent data at some level of moisture the material absorbs at 50% relative humidity [16]. Review of PA6 technical data sheets from five manufacturers, such as DuPont™ [17], BASF™ [18], Solvay™ [19], DSM™ ([20], [21]), and EMS-GRIVORY™ [22], shows differences in recommendations. Moisture content for processing the resin ranges from 0.1 % to 0.2 %. The water absorption at saturation by three manufacturers is between 9 % and 9.5 %.

The humidity absorption by two manufacturers ranges between 2.8 % to 3.3 %. All agree with drying temperature of 80 °C. Four out of five recommend two to four hours of drying, whereas one recommend four to 12 hours. All agree with using a desiccant or dehumidifying dryer. Two list a vacuum dryer as another option. One does not recommend using a hot air oven or hopper dryer. The conclusion is two to four hours of drying at 80 °C to bring the moisture content down to 0.1 % to 0.2 %. Conclusion seems reasonable until consulting with polymer expert articles.

Drying is an important factor in removing plasticization effects. There are many suggestions on this topic. One suggestion is three to four hours between 120 °F (49 °C) and 240°F (116 °C). Longer drying time results in increased viscosity or lower melt flow. Correcting incomplete mold fill or short shots requires processing adjustments as needed ([11], [12]). Another suggestion is utilizing elevated temperatures. Temperature should be below the softening or melt point for semi-crystalline polyamides and close to the softening or glass transition for amorphous polyamides. This increases the rate of drying with the risk oxidation [23]. Another recommendation is drying at temperature above the boiling point of water (100 °C) with circulating air [24]. Another is to dry between 160 °F (71 °C) and 180 °F (82 °C). These recommendations open more options for drying polyamides. Determining the best option presents a challenge. This requires a better understanding of moisture effects on polyamides.

The maximum moisture content for processability applies to unfilled material. Filled material absorb less moisture. General guideline is to reduce the maximum moisture content of 0.2% by the filler content percentage. For example, 33 % glass filled material displaces the matrix by 33 % and reduces moisture absorption by 33 %. The

adjusted maximum moisture content for 33 % glass filled nylon would be 0.134 %. Another point is the minimum moisture should be 0.05 %. Processability becomes more difficult at very low moisture content [25].

2.1.2 Moisture Measurement Methods

Knowing the difference in moisture content measurements is the key to understanding the effects of high or low moisture. The studies investigated use either Karl Fisher (KF) titration or mass change. Both are acceptable methods for measuring water content. KF titration measures only the water content. Mass change measures total weight change. This includes both water and volatile impurities [26]. Mass change is not as precise as KF titration but is suitable for production environment [12]. Both methods can alter the sample. Secondary methods for measuring moisture content are nondestructive [27] and include electrical, microwave, nuclear, and optical devices. Test measurement is instant and ideal for production environments. The high potential for measurement errors make them not recommended for accurate measurements [28]. The two standardized methods for research studies are ISO 15512 and ISO 62. ISO 15512 [29] is a water content method that utilizes Karl Fisher titration with an accuracy of 0.01% down to 0.01% water content. This is a coulometric technique based on iodine reduction where 10.71 C corresponds to 1 mg of water in accordance with Faraday's Law. It is applicable to both granules and parts. ISO 62 [30] is a water absorption method based on change in mass. This method applies to determination of water loss after drying.

2.2 Nylon's Hygroscopic Nature

Polyamides are well known in the manufacturing and academic fields to be very hygroscopic. Moisture from the air absorbs into the molecular structure [31]. Aromatic polyamides, such as polyphthalamides, absorb less moisture or at a much slower rate than aliphatic polyamides [12]. The absorbed water encourages mobility of the polymer chains. This leads to a decrease in mechanical strength and glass transition temperature. This process called plasticization is reversible by drying. The absorbed water at saturation is more destructive. The polymer chains cleave leading to ductile-brittle transition of mechanical strength [32]. This process called hydrolysis is not irreversible.

Solubility, diffusivity, and activity are factors affecting polyamide's ability to absorb water. Hydrogen bonding between water and polar functional groups drives the solubility of water into the surface layer. Free volume availability within the polymer matrix encourages diffusivity of water into the core [33]. Water concentration, or activity, affects water uptake. Low activity drives the water uptake linearly in accordance with Henry's Law. High water activity shows nonlinear contribution due to water clustering [34].

2.3 Moderate to Extreme Moisture Effects

Several studies investigate behavior changes in different polyamides, such as PA6, PA66, PA46, PA11, and PA12, under moderate to extreme conditions. Moderate conditions induce physical changes such as plasticization. Extreme conditions induce chemical changes such as hydrolysis and thermal oxidation. The level of behavior change depends on amount of water absorbed. Polyamides absorb water only into the amorphous region resulting in ductile behavior. The crystalline region does not absorb water but can fragment under hydrolysis resulting in brittle behavior.

2.3.1 Plasticization

Plasticization occurs when the absorbed water binds with hydrophilic functional groups on the polyamide chain. Water continues to penetrate the material by forming clusters between the polymer chain. Several studies investigate the effects of plasticization on polyamide properties. Plasticization results in decrease in stiffness, decrease in strength, increase in strain and increase in swelling.

Clavería et. al. [35] studied the influence of realistic in-service environmental conditions on the dimensional stability of PA6 and PA66 components working life. The component is a base support plate inserted into the mechanical structure of an induction cooktop. The critical dimensions are the screw holes on the assembly frame and the general flatness. Material dried for three hours at 100°C before injection molding. Sample of each material was tested under five difference conditions with different exposure times. One set stabilized under laboratory conditions at 20 °C and 65% environmental humidity for 24 hours. Second set saturated to 100% moisture by submersion in distilled water for 24 hours at 20 °C. This represents an extremely humid situation at a medium temperature. Measurements completed when removed from the water. Third set subjected to a temperature of 50 °C for 48 h in an oven to represent medium/high temperature conditions. Measurements completed when removed from the oven at a real surface temperature of 33 °C. This represents high temperature storage conditions. This is the most critical in the assembly chain with respect to the temperature. Fourth set subjected to a temperature of 100 °C for 48 hours then stabilized at 20 °C and 72% humidity for 24 hours. This represents in-use temperature variations where the maximum temperature is 100 °C then cools to a standard temperature later. Fifth set

subjected to temperature of 100 °C. All sets simulate expected and extreme manufacturing, storage and working conditions. The analysis applies to structural elements with mechanical and dimensional sensitivity to the environmental humidity and processing temperature. These characteristics are crucial in the component's design stage for functionality and assembly. The PA6 component demonstrated a higher capacity to absorb moisture and a higher capacity to release moisture than the PA66 component. The PA6 component exhibited flatness errors four times greater than established design tolerances. The PA6 assembly dimensions stayed within dimensional tolerances under average and extreme humidity conditions and average temperature conditions. More significant change observed at extreme temperature conditions. The PA66 components are more stable in all conditions.

Monson et.al. [36] characterized dimensional changes from moisture uptake in PA6, PA66, and PA46 parts. Molded plates of each product immersed in deionized water for approximately 370 hours until reaching mass saturation. Density increased less than 1 % compared to initial measurements. Plaque dimensions expanded equally in all directions. Dimensional changes coincided with mass changes. Absorption amount depended on thickness. Thicker plates took longer to reach water absorption equilibrium compared to thinner plates. The diffusion coefficient showed independence from sample thickness. Level of absorption affected by amide content. PA46 containing the highest amide content absorbed the most water in shorter amount of time compared to PA6 and PA66.

Obeid et. al. [37] studied swelling in PA6 parts. Tensile modulus exhibited a sharp drop at the initial part of the absorption process then stabilized without further

significant drop. Decline in stiffness is due to plasticization. The stiffness of the material reaches its minimum well before maximum saturation. Swelling observed during the diffusion process. This is due to inhomogeneous absorption where the outer layers absorb more moisture than the dryer inner layer.

Miri et. al. [38] evaluated moisture effects on the α, β, and γ crystalline form of PA6 above the glass transition temperature where amorphous chains are more mobile. The experiment consisted of casting 80μm film samples for testing. The initial film is predominant mesomorphic β form. The α and γ crystalline forms created by different treatments of the β film. The film samples subjected to different conditioning methods to increase moisture content identified as the humid group. Film samples of each form stored in a vacuum desiccator identified as the dry group. The moisture content, evaluated by thermogravimetric analysis, is 8.8%. The kinetic of water release is consistent among all three forms for the humid group. The crystalline structure, evaluated by wide angle X-ray scattering (WAXS), showed no change between the dry and humid samples for each form. This indicated the moisture in the humid samples are stored in the amorphous region. Tensile stress-strain testing performed at 25°C for the three films α, β, and γ in dry and humid states. Yield stress is lower for the humid samples. The dry samples exhibited periodic stress oscillations during neck propagation. This is due to periodic adiabatic heat release associated with structural changes. Additional tensile testing conducted on the dry groups at 110°C to understand the role of the amorphous phase. Result compared humid group tested at 25°C. Comparison of dry sample tested at 110°C and humid sample at 25°C showed similar yield stress values as well as strain hardening behavior from increased amorphous chain mobility. The plastic

deformation past the yield point is due to fragmentation of the crystalline lamellae in addition to unraveling of folded chains.

Baschek et. al. [39] studied loss factor, shear modulus, and thermal expansion in dry and wet samples of PA12 and PA6. Wet samples prepared by water immersion at room temperature for up to six days. Dry samples placed under vacuum in an oven for 24 hours at 100 °C. PA6 exhibited similar behavior to PA12 at low water content. Reduction of first loss factor peak, increase in the second loss factor peak, slight increase in shear modulus, and slight decrease in thermal expansion observed at low water content. PA6 changed significantly especially around 250 K at the higher moisture content. The first and second loss factor peaks disappear while a third peak appears around 250 K. The shear modulus increases further then drops significantly around 250 K. Thermal expansion increases significantly around 250 K.

Chaichanawong et. al. [40] studied moisture effects on PA66 mechanical properties with 0 wt.%, 10 wt.%, 20 wt.% and 30 wt.% short glass fiber. Tensile specimens prepared by injection molding then dried at 100°C. Specimens immersed in distilled water up to 60 days to achieve water saturation. Moisture uptake monitored during the immersion period using weight change. Rapid absorption observed in the initial seven days. Consistent absorption then saturation observed in the final 30 to 60 days. Tensile and flexural properties measured after 0 days, 10 days, 30 days, and 60 days of immersion. Modulus of elasticity, yield strength, and flexural strength decreased with increased absorption. Tensile elongation increased with increased absorption. Results show change from brittle to ductile fracture after 30 or more days. Surface fractures examined by scanning electron microscope after tensile testing. Crystalline

regions form from the polar attraction between amide groups in the polymer chain. This causes the chain to fold over itself. These regions resist being pulled apart resulting in higher strength and stiffness. The polar nature of water from immersion causes attraction to the amide group which weakens the attraction between amide groups within the polymer chain. This reduces the crystalline regions. The higher glass fiber samples exhibited smaller change in mechanical properties compared to the samples with little to no glass fiber.

2.3.2 Hydrolysis

Extreme degradation effects include hydrolysis and thermal oxidation. Hydrolysis degradation occurs with high moisture and heat. Several studies on polyamide behavior under hydrolysis show similar results. Effects show lowering of melt viscosity and increasing melt flow. Molecular weight decreases but the distribution broadens. This indicates the presence of oligomers, monomers, and cross-linked material. Tensile elongation increases tensile strength decreases and fracture toughness increases under hydrolysis. Rate of degradation increases with increasing temperature and moisture content [41]. Tensile strength, elongation, and fracture toughness decreases with long exposure times under thermal oxidation. Temperatures between the glass transition and melt temperature induces oxidation on the material surface [42].

Bernstein and Gillien [43] studied hydrolysis effects on nylon straps over a 2.5-year period. Tensile property change monitored after storage in 80 °C circulating air oven, 80 °C with 100% relative humidity and 13.2 cmHg oxygen partial pressure, and 80 °C with 70% humidity in a climate chamber. The data at 80 °C for all three conditions superimposed to determine the time-temperature shift factor based on the humidity. Data

collected from oven aging superimposed to determine the time-temperature shift factor based on the temperature. Results show humidity dominated the degradation rate in a hydrolysis environment. Method could be turned into a model to predict degradation at other temperatures.

Fabre et.al. [44] developed a three-parameter model based on the WLF theory. Temperature, dynamic mechanical analysis frequency, and moisture content for PA66 could be reduced as a function of each parameter alone. A new relationship developed to tie together relaxation time at a specific temperature and moisture content to a reference temperature at the corresponding reference moisture content. Validation applied for the individual parameters and combined relationship. Method is unique but appears complex due to several unknown parameters and assumptions the calculations require.

El-Mazry et. al. [45] developed a general kinetic model for reversible hydrolysis in PA66. Resin samples dried for 72 hours at 80 °C under vacuum. Film samples for analysis produced by compression molding then stored in a desiccator until ready for testing. A portion of the film samples exposed to various water vapors at 40 °C, 50 °C, 60 °C, and 70 °C between 0% and 90% relative humidity for water absorption. Other film samples immersed in distilled water maintained at 60 °C, 70 °C, 80 °C, and 90 °C for several hours for hydrolytic aging. Differential scanning calorimetry, used to monitor morphological changes, showed the appearance and growth of secondary melt peaks just before the primary melt peak. This indicated a secondary crystallization during hydrolytic aging. This suspected to be a direct consequence of hydrolytic chain scission in the PA66 amorphous phase plasticized by water. Chain scission destroys entanglement network in the amorphous phase. This frees small macromolecular

segments which self-diffuse to the crystals' surface and initiate crystallization. Tensile testing, conducted at 23°C and 50% relative humidity, evaluated the embrittlement on the mechanical behavior. Main changes take place in the early periods of the distilled water exposure. The PA66 changed from ductile to brittle failure.

Ferreño et. al. [46] studied mechanical and fracture properties at 0 %, 1 %, 3 %, and 6 % water content for PA6. Test specimens prepared by injection molding, dried in an oven at 100°C, immersed in 40°C water until desired weight percent, then stored in hermetically sealed bags until ready for testing. Material softening increased with moisture. This resulted in decrease in Young's modulus, yield stress, and ultimate strength with an increase in strain. Finite element model developed to characterize the fracture behavior. Results show material's resistance to fracture increased with increasing moisture. The polymer matrix undergoes great deformation prior to fracture accompanied by debonding between the matrix and reinforcing fibers.

Reis et. al. [47] studied the influence of temperature and aging on mechanical behavior and fracture of aliphatic PA11. Corrected inherent viscosity (CIV) monitored the molecular weight decrease from hydrolysis of the polymer chain. ASTM D5045 fatigue and ASTM D638 tensile specimens cut from an unused flexible subsea pipe with an inner polymeric pressure sheath. Specimens aged in water at 140°C for some number of days. Unaged samples yielded CIV values of 1.8 dl/g. Aged samples at different durations yielded values of 1.04 dl/g and 1.18 dl/g. Tensile tests performed on the aged samples at -5 °C, 23 °C, 50 °C, and 90 °C at different crosshead speeds of 0.5 mm/min, 5 mm/min, and 50 mm/min. Temperatures based on real average operating conditions of deep-sea oil exploration. Rapid depressurization of fluid-gas mixture causes the

temperature to drop below 0°C. Temperatures in reservoirs at the bottom of a well influenced by the proximity to the earth's mantle and can be quite high. A razor cut, for fracture testing, administered to the samples after aging and tested at -5 °C, 23 °C, and 90 °C at a crosshead speed of 10 mm/min. Tensile values did not change much between the test speeds. The CIV of the aged samples evaluated are 1.02 dl/g, 1.3 dl/g, and 1.05 dl/g. Superplastic behavior observed at high temperatures and high CIV. Brittle behavior observed at temperatures below 25 °C and CIV less than 1.1 dl/g.

Taktak et. al. [3] presented experimental and numerical approaches to assess the hydrolysis aging effect on PA6 mechanical properties and ductile tearing. Samples dried until constant dry weight reached. Moisture conditioning completed by immersing samples in distilled water at 24 °C, 70 °C, and 90 °C. Samples removed from water and weighed at regular intervals to monitor water uptake. Moisture sorption process continued until the maximum saturation. The mass gain increased gradually with the exposure time indicating water diffuses into the bulk polymer. The equilibrium water uptake reached. The sorption behavior in distilled water seemed similar at higher temperature. Saturation was not reached for samples immersed at 24 °C during the study. The experimental results considered for samples exposed to distilled water at 70 °C and 90 °C. Tensile and fracture properties of the conditioned samples were investigated. Tensile strength and yield stress decreased with increasing water content. The elongation at break increases with increasing water content. The strain drops down at the equilibrium moisture content 8%. The polymer showed affects from long exposure time in distilled water at high temperature. Plasticization effects demonstrated initially. Hydrolysis of the polymer dominated as exposure time increased. PA6 polymer exhibited

a ductile fracture behavior. It develops a localization of plastic flow during tension necking then crazing followed by rupture of the remaining ligament.

Material in the melt state show rheological sensitivity explaining degradation occurs during injection molding. Melt processing steps can modify polymer structure such as chain scission or cross linking. All affected by how much water and air are introduced into the melt during processing. As previously discussed, moisture and heat can lead to hydrolysis processes. Over time viscosity slacken due to scission events from post condensation lowering molecular weight. Melt flow index decreases as a result of crosslink products hindering flow. Low molecular weight products include NH_2/COOH oligomers from hydrolysis and compounds from amide terminal groups from thermal oxidation. Low molecular weight products widen the molar mass distribution [48].

2.3.3 Thermal Oxidation

Thermal oxidation occurs with high temperature exposure. Effects of this mechanism resemble hydrolysis degradation. Several studies on these effects on polyamide behavior come to the same results and summarized in this section. Polyamide oxidation results from weak bonds in methylene resulting in hydrogen abstraction and the decomposition of hydroperoxides induced by nitrogen. The main stable oxidation products from disproportionation processes are imides which are more prevalent in aromatic polyamides than in aliphatic polyamides. Chain scission is the primary cause for embrittlement. Discoloration seen in polyamides is possibly due to methylene attack during oxidation [49]. Small increase in molar mass at the initial stage of heat exposure can be attributed to a slow post polycondensation process. Over time the molar mass decrease occurs from thickening of the crystalline lamella. Crystallinity increases with

exposure. Initial increase is due to annealing. As the exposure time continues, the crystallinity increases due to crystallization process, where broken chains in the amorphous region make their way into the crystalline region. Tensile behavior encounters ductile-brittle transition [50]. Thermal oxidation begins at the surface. Oxidation on the polymer surface occurs faster than in the bulk of the material. Increasing temperature leads to more pronounced degradation outcome. Oxygen induced chain scission decreases molar mass. Crystallization leads to increase in crystallinity and crystal thickness. Degree of oxidation increases over time [51]. Oxygen permeability and reaction rate does not change over time [52].

2.3.4 Degradation Prevention

The damaging effects of hydrolysis and thermal oxidation compromise material and part integrity. Filler content and additives reduce or eliminate degradation effects. Additives serve a role in preventing damaging effects in polyamides. Heat stabilizers reduce the effects of thermal oxidative degradation. Sterically hindered phenolic stabilizers prevent autooxidation by converting peroxyl radicals to hydroperoxides. Phenolic antioxidants and copper salts trap radicals and stop the propagation process. Iodide salts decompose hydroperoxides [52]. Phosphorous based antioxidants provide preventive measures against degradation by decomposing hydroperoxides into nonreactive products before they decompose into hydroxy radicals [6]. Combining glass fiber and rubber particles as the filler content can improve strength in hydrolysis processes. The amount of water absorbed correlates to the amount of fillers present. More fillers will have less water uptake. Glass fibers prevent the sharp ductile-brittle transition while the rubber particles increase the break strain [32]. Glass fiber treatments

in reinforced polyamides can be formulated to increase water resistance in a hydrolysis environment. Bergeret et.al. [53] compared glass fiber treatment in composite materials between standard preparation and specific water resistance preparation. The treatment was simplified to two main components, the coupling agent to chemically bind the glass fiber surface with the polymer matrix and the film former agent to protect the glass fiber during processing. The standard preparation utilizes aminosilane coupling agent and polyurethane film former agent. The special preparation utilizes amino silane coupling agent and polyurethane/acrylic film former agent. Tensile and impact properties demonstrated better aging resistance. Material demonstrated lower water uptake for the special treatment compared to standard treatment. In the presence of water, the alkyl bonds are the most stable, ester bonds are least stable while amide and urethane bonds are in between at polymer/glass matrix in the special preparation. The ester present from the acrylic is a pendant function which does not affect the main chain during hydrolysis.

2.4 Drying Studies

Starting with dry material is important in a manufacturing setting. Moisture can have negative effects on finished parts from plasticization to hydrolysis. Part manufacturers receive nylons in the form of pellets. These pellets are received in dried form from the resin manufacturer. There are instances when the damaged packaging begins the absorption process for resin. The pellets reach moisture equilibrium when the vapor pressure inside the pellet increases to equal the vapor pressure surrounding the pellet. This allows the pellets to absorb moisture from the air. Eliminating moisture from resin starts with exposure to high temperatures. The higher the temperature the more excited water molecules get. The more the molecules move the further apart and

the more moisture rises to the surface [31]. Remove moisture from the pellet by surround the pellet with hot dry air to disrupt moisture equilibrium. This imbalance allows the moisture within the pellet to migrate towards the surface. After enough time under hot, dry conditions the pellet reaches equilibrium with its surrounding conditions becomes dry [54]. Another factor in drying resin is air flow. Constant air flow removes heated water vapor and cool condensed water from settling back onto the pellets [31].

There are many types of dryers to take into consideration. Large scale manufacturers tend to use desiccant dryers. Oven dryers are the simplest equipment for drying resin on a small scale but lack enough air flow [55] and can damage material if not closely monitored. Vacuum dryers are a little more versatile than oven dryers. This can be used for pellets and small parts. In a vacuum drying process, the material is subjected to reduced pressure environment that aids evaporation of water without the risk of scaling or oxidation residue [56]. The advantage is no desiccant or dew point to monitor [57].

Oliver Kast and Christian Bonten [58] studied the drying process of PA6 along with polyester (PET), polylactide (PLA), and polyhydroxybutyrate (PHB) to evaluate the influence of material properties and drying parameters on drying speed. Their study takes into consideration additional moisture uptake experienced in real production conditions from long term storage and contact with ambient air. The experiment begins by increasing the moisture content of the resin samples between 0.15 % (PET) to 0.5 % (PA6) using climate chamber set to 23 °C and 86 % humidity. The samples dried to 0.1 % moisture content in a dehumidifying dryer at 50 °C, 80 °C, and 120 °C. All the polymers exhibited different drying behaviors. PA6 dried four times slower at 50 °C compared to 80 °C and 120 °C. This behavior is attributed to the amorphous region

where water accumulates. The amorphous region locks in the moisture below the glass transition point which is approximately 56 °C. The dryer machine design is another factor in the drying process. Dryer capacity is intended for complete filling where the air flow rate and moisture transfer into the air is more efficient. At partial capacity, the pellets are more likely sitting in a dead space outside of the air flow stream. After 25 hours of drying, 2.5-kilogram sample of PA6 resulted in 1.5 % moisture content while 0.5-kilogram sample tested at 1.75 %. Comparison of zero viscosity measurements between the untreated and dried samples determined drying effect. Reduction in viscosity indicates a decrease in average molar mass leading to polymer chain degradation. Viscosity measurements of PA6 untreated sample, 50 °C dried sample, and 120°C dried sample are 2700 Pa·s, 1800 Pa·s, and 2200 Pa·s, respectively. This implies drying PA6 at lower temperature and longer time is more damaging than at higher temperature for a shorter time. The overall recommendations are to measure the actual moisture content to estimate drying time, use the glass transition temperature as the minimum temperature limit, and select higher temperatures for faster drying with less degradation. Selection of the upper temperature limit must be chosen carefully to avoid side effects such as post-crystallization.

Pedroso et. al. [59] studied drying effects on recycled glass fiber reinforced PA6. Note the glass fiber content before and after recycling is not specified in the research. The ground material was dried at 120 °C and evaluated after 3 hours, 6 hours, and 9 hours using TGA. The moisture content was determined by weight loss at 150°C, where 3-hour sample lost 35.4% of initial moisture, 6-hour sample lost 50%, and 9-hour sample lost 68.8%. Crystallinity of the virgin to the ground material after drying was measured

by DSC, where the virgin is 58%, 3-hour sample is 46%, 6-hour sample is 55%, and 9-hour sample is 54%. The reduction in the crystallinity affects the packing capability of the polymer chain. The ground material was extruded, formed into pellets, then injection molded into test specimens for tensile and flexural testing. Prior to mechanical testing, specimens conditioned 48 hours at 23°C and 50% relative humidity. Compared to the virgin sample, the tensile strength dropped approximately 18% and flexural strength by 16% for the dried samples. The differences between the three drying times are small. The differences are attributed to hydrolytic and thermal degradation. Considering only the drying process of this research, the time period of drying shows some influence over the mechanical properties.

The water profile through a sample differs between water absorption and drying. When water is removed during the drying process, tensile stiffness and strength are close to unaged samples. This indicates plasticization effect is reversible. Recovery of mechanical properties is much longer than reducing with water saturation. There is a relationship between water content, glass transition, and yield stress. Yield stress is related to chain mobility characterized by the glass transition temperature. Chain mobility increases with increasing water content. Increase in water content decreases glass transition temperature. This leads to decreasing yield stress. Chain mobility can increase with increasing test temperature. This results in the same effect on glass transition temperature and yield stress.

2.5 Water Diffusivity

Water diffusivity studies on PA6 and PA66 give insight into the moisture absorption rate from the atmosphere or water immersion. Diffusion is dependent on

temperature and water concentration as well as whether the amorphous region is in the glassy or rubbery state. It is not a linear relationship with time. At high water activities, higher water absorption occurs. This is attributed to water clustering in the polymer. Diffusion rates increase at higher temperatures. Another factor that should be taken in the diffusion behavior is the glass transition. Diffusion rates are lower in the glassy state, or temperatures below the glass transition temperature, than in the rubbery state, or temperatures above the glass transition temperature. In the rubbery state, the water activity in the external environment affects absorption which follows the free volume theory. In this case, volume increases due to creation of holes in the polymer above the glass transition temperature. This amplifies polymer-water interaction and leads to an increase in water diffusion rate.

CHAPTER 3: Experiment

3.1 Materials

Several polyamide materials selected to evaluate behavior across various nylon compositions. Grilon BS Black 9832 [22] is an unreinforced PA6. Grilon BG-50S Black 9697 [60] is a 50% glass reinforced PA6. Grilon TSG-50/4 Black 9832 [61] is a 50% glass reinforced PA66+PA6 polymer blend. Grilamid TR 90 Natural [62] is an amorphous, unreinforced PA MACM12 containing aliphatic and cycloaliphatic chains. Grilamid LV-5H Black 9733 [63] is a 50% glass reinforced PA12. Grivory G21 Natural [64] is an amorphous, aromatic, and unreinforced PA6I/6T. Grivory GV-5H Black 9915 [65] is 50% glass reinforced PA66+PA6I/X blend of semicrystalline and partially aromatic copolyamides. All black materials are heat stable grades.

Resin manufactured and provided by EMS-GRIVORY. Resin received in 20-kg poly-lined bags. Material used directly from packaging without pre-drying. Each material resin injection molded into 4 mm thick ISO Multipurpose Type 1A tensile specimens on Arburg® 320KS Allrounder 700-250. Specimens stored in moisture-proof aluminum bags until ready to test.

3.2 Differential Scanning Calorimetry

The glass transition temperatures measured by differential scanning calorimetry (DSC) on Mettler-Toledo 1/700, equipped with an automatic sampler, in accordance with ISO 11357 ([66], [67]). Heat rate set to 20 K/min. Test conducted on resin and specimens after molding to determine drying operating range. Detection of glass transition shifts after moisture absorption proved difficult due to dampening effects. Vicat softening temperature monitored as an alternative thermal profile.

3.3 Absorption and Desorption Treatment

3.3.1 Weight Change

Weight (g) obtained for specimens before immersion, intervals during immersion, after immersion, and intervals during drying. The mass of water absorbed (%) determined by calculating $\frac{m_{after\ immersion} - m_{initial}}{m_{initial}} \times 100\%$. The mass of water desorbed (%) determined by calculating $\frac{m_{after\ immersion} - m_{after\ drying}}{m_{initial}} \times 100\%$. The difference between absorbed and desorbed is amount retained in the specimen.

3.3.2 100°C Water Saturation

Specimens immersed in boiling distilled water until saturation to confirm data sheet value and observe samples for adverse effects. Saturation treatment conducted individually by product. Apparatus consisted of 3-liter glass condensation reaction vessel with heating mantle. Weight measurements taken at different intervals to monitor absorption. Samples removed from boiling water, placed in ambient water bath for five minutes, and excess water wiped off before weighing.

3.3.3 23°C Water Conditioned

Specimens immersed 720 hours in 23°C deionized water for partial absorption without heat effects. Containers kept closed and stored in standard laboratory conditions during the absorption process. Weight measurements taken at different intervals to monitor absorption.

3.3.4 Other Absorption Methods for Comparison

Three additional absorption methods included for comparison to the boiling water method. One group of specimens placed in standard laboratory environment of 23°C ± 2°C and 50% ± 10% relative humidity. Second group of specimens placed in

conditioning chamber set to 70°C ± 2°C and 62% ± 5% relative humidity. Third group of specimens placed in 23°C ± 2°C circulating water bath. All groups received 2000 hours of exposure time.

3.3.5 Drying

Specimens from 3.3.2 and 3.3.3 divided into four groups for drying at 80°C, 100°C, 120°C, and 140°C. Ovens selected for desorption is Binder® FED Heat/Drying Oven with Forced Convection Model FD53UL. Air changes set to 60/hour. All product specimens dried together.

3.4 Mechanical Testing

3.4.1 Karl Fisher (KF) Moisture Analysis

Moisture content determined analytically in accordance with ISO 15512 [29]. Vaporization method utilized for samples with low weight change, less than or equal to 0.5%, and conducted on Mettler Stromboli C30 with LabX software. Methanol extraction method utilized for samples with higher weight change, greater than 0.5%, and conducted on Mettler V20 Volumetric Titrator. Baseline measurements obtained from the material resin directly from the packaging and specimens after molding. Moisture level of the resin referred to as “dry as packaged”. Moisture level of unconditioned specimens referred to as “dry as molded” or DAM. Additional measurements collected during water saturation, water conditioning, and drying cycle.

3.4.2 Tensile Stress and Strain

Tensile testing is a widely chosen method for studying moisture and heat age effects in materials. Literature documents the expected behavior pattern in a stress-strain test under various conditions. Tensile stress, strain, and Young’s Modulus measured by

Instron Universal Tester 5967 with Advanced Video Extensometer and Bluehill 3 software in accordance with ISO 527 [68]. Crosshead speed for unreinforced materials set to 50 mm/min and reinforced materials, 5 mm/min.

3.4.3 Charpy Impact Strength

Impact testing serves as another method for studying the moisture and heat age effects. The notch presence increases the sensitivity of the material. Decline in strength from degradation effects expected to occur in impact testing before tensile testing. Charpy impact strength measured by CEAST Resil Impactor in accordance with ISO 179 [69]. Specimens cut from ISO multipurpose tensile bars following injection molding. 45° notch applied to specimens on CEAST Automatic Notchvis Plus before absorption treatment.

3.4.4 Vicat Softening Temperature

Monitoring the change in glass transition for water absorbed samples is not easily achievable with DSC methodology. Softening temperature selected as an alternative to glass transition temperature to detect moisture affects. Vicat softening temperature measured by Instron Ceast HV500 HDT and Vicat Unit with Instron CeastVIEW software in accordance with ISO 306 [70]. Method A120 utilized 10 N force and 120 K/h heat rate.

3.4.5 Relative Viscosity

Degradation monitored by measuring relative viscosity before and after immersion in addition to after drying. Relative viscosity measured by Rheotek RPV-2 Polymer Viscometer in accordance with ISO 307 [71]. Bath temperature set to 20°C.

Solvent is m-cresol. Viscosity number (VN) calculated from relative viscosity (η_R) using the formula, $VN = (\eta_R - 1) * 200$.

3.4.6 Yellowness Index and CIE b Value

Monitoring the discoloration for the amorphous grades during drying achieved by measuring the yellowness index and CIE b-value. Yellowness index and CIE b value measured by Datacolor 600 Spectrophotometer with Datacolor Tools Plus software in accordance with ASTM E313 [72] and ASTM D2244 [73]. Instrument utilizes 1964 CIE standard 10° observer, standard illuminant D_{65}, standard white tile (L* = 96.33, a* = −0.61, b* = 0.10, C* = 0.62, h = 170.63), and 9mm aperture.

CHAPTER 4: Results and Discussion

4.1 Preliminary Profile

Table 4.1 displays the Karl Fisher moisture content, glass transition temperature, and viscosity number of both resin and molded specimen. Increase in moisture content for specimens indicates moisture absorption during the injection molding process. The increased moisture reduced both the glass transition temperature and viscosity number for all materials, except PA6I/6T, indicating some plasticization occurred. Increased moisture in PA6I/6T resulted in the opposite effect. Increased glass transition and viscosity number may indicate minor cross-linking occurred.

4.2 Adverse Effects on Amorphous Grades

PA6I/6T and PA MACM12 exhibit extreme physical change after certain treatment conditions. PA6I/6T transparency shifted to opaque after exposure to 100°C water (see Figure 4.1). Conditioned PA6I/6T specimens in 120°C oven blistered after 10 minutes of exposure. Blistering and opacity increased after 90 minutes exposure (see Figure 4.2). Conditioned PA6I/6T specimens in 140°C oven displayed large blisters after 10 minutes of exposure. Blistering, softening, and opacity increased after 90 minutes exposure (see Figure 4.3). Saturated PA MACM12 specimens in 80°C oven hazed after 377 hours of exposure (see Figure 4.4). Saturated PA MACM12 specimens in 140°C oven swelled with large bubbles after 15 minutes of exposure (see Figure 4.5).

Crystallinity and voiding are possible reasons for the adverse effects seen in the amorphous grades. Increasing crystallinity lessens transparency [74]. Buckley et. al. [75] observed voiding below the surface affects transparency in boiling water samples. The absorbed water vaporizes at elevated temperatures. Voids occur when the polymer

matrix cannot restrain the expansion. Continued treatment increases the presence and size of voids. The glass transition lowers which allows the rubbery matrix to absorb more water. Softening and distortion gradually follows. Voids expand progressively to produce blisters which eventually rupture causing surface pitting and disintegration. Embrittlement from hydrolytic scission of in-chain amide bonds results in reduction in mechanical properties.

4.3 Weight Change vs Karl Fisher Moisture

Weight change does not correlate with moisture content by Karl Fisher instrumental analysis. Figure 4.6 displays measurements by both methods. Values scatter on both sides of the trendline. Most samples with weight change above 5% shows a lower moisture content while most samples with weight change below 5% shows a higher moisture content.

4.4 Unreinforced PA6

4.4.1 Absorption Behavior

Water absorption curves for PA6 (see Figure 4.7) shows a peak, drop, then increase for 100°C water and 70°C + 62% RH methods. The other two conditions do not exhibit the same peak in the absorption curve. Samples reach maximum saturation in 23°C water, 50% of the water content at 70°C + 62% RH, and 11% of the water content after 2000 hours. 100°C water saturated samples yield a weight change of 9.2% after 81 hours and KF moisture content of 7.2%. 23°C water conditioned samples yield a weight change of 5.9% and KF moisture content of 3.9%.

4.4.2 Desorption Behavior

Figures 4.8 and 4.9 are desorption curves for saturated samples and conditioned samples, respectively. All samples dried below 0% weight change except for saturated samples dried at 120°C, which reached 0.31% weight change. KF moisture content for dried from conditioned samples is 0.2%.

4.4.3 Tensile and Impact Property

Figure 4.10 displays engineering tensile stress-strain curves between DAM, 100°C water saturated, and 23°C water conditioned. Water curves show significant decrease in yield and increase in strain. Figure 4.11 displays engineering stress-strain curves between DAM, 100°C water saturated, and dried samples. Figure 4.12 displays engineering stress-strain curves between DAM, 23°C water conditioned, and dried samples. Dried curves in both cases do not have the defined strain softening peak as the DAM curve. Figure 4.13 displays the change in yield stress over the course of drying 23°C water conditioned samples. Figure 4.14 displays the change in yield strain over the course of drying 23°C water conditioned samples. Figure 4.15 displays the change in Young's modulus over the course of drying 23°C water conditioned samples. Yield values of dried samples are close DAM values. Young's modulus values of dried samples lower than DAM. Figure 4.16 displays the change in notched Charpy impact strength over the course of drying 23°C water conditioned samples. Significant increase in impact strength after conditioning but reaches DAM value after drying quicker than tensile testing.

4.4.4 Degradation Analysis

Figure 4.17 compares viscosity and Vicat softening temperature across different sample states. Both values decrease with water exposure and increase after drying. Dried values equivalent to DAM values.

4.5 50% GF Reinforced PA6

4.5.1 Absorption Behavior

Water absorption curves for 50% GF PA6 (see Figure 4.18) demonstrate the same behavior as unreinforced PA6. 100°C water saturated samples yield a weight change of 4.2% after 33 hours and KF moisture content of 5.1%. 23°C water conditioned samples yield a weight change of 2.5% and KF moisture content of 1.5%.

4.5.2 Desorption Behavior

Figures 4.19 and 4.20 are desorption curves for saturated samples and conditioned samples, respectively. All samples dried below 0% weight change.

4.5.3 Tensile and Impact Property

Figure 4.21 displays engineering tensile stress-strain curves between DAM, 100°C water saturated, and 23°C water conditioned. Water curves show significant decrease in break strength and increase in strain. Figure 4.22 displays engineering stress-strain curves between DAM, 100°C water saturated, and dried samples. Figure 4.23 displays engineering stress-strain curves between DAM, 23°C water conditioned, and dried samples. Dried curves in both cases occur above the DAM curve. Figure 4.24 displays the change in break stress over the course of drying 23°C water conditioned samples. Figure 4.25 displays the change in strain over the course of drying 23°C water conditioned samples. Figure 4.26 displays the change in Young's modulus over the course of drying 23°C water conditioned samples. Break and Young's modulus values of

dried samples exceed DAM values. Figure 4.27 displays the change in notched Charpy impact strength over the course of drying 23°C water conditioned samples. Significant increase in impact strength after conditioning. Dried values occur just below DAM value.

4.5.4 Degradation Analysis

Figure 4.28 compares viscosity and Vicat softening temperature across different sample states. Both values decrease with water exposure and increase after drying. Dried values equivalent to DAM values.

4.6 Reinforced PA66 + PA6

4.6.1 Absorption Behavior

Water absorption curves for 50% GF PA66 + PA6 (see Figure 4.29) demonstrate the same behavior as unreinforced PA6 and 50% GF PA6. 100°C water saturated samples yield a weight change of 4.1% after 33 hours and KF moisture content of 4.4%. 23°C water conditioned samples yield a weight change of 2.0% and KF moisture content of 1.8%.

4.6.2 Desorption Behavior

Figures 4.30 and 4.31 are desorption curves for saturated samples and conditioned samples, respectively. All samples dried below 0% weight change except for saturated samples dried at 140°C, which reached 0.089% weight change.

4.6.3 Tensile and Impact Property

Figure 4.32 displays engineering tensile stress-strain curves between DAM, 100°C water saturated, and 23°C water conditioned. Behavior is similar to 50% GF PA6. Figure 4.33 displays engineering stress-strain curves between DAM, 100°C water

saturated, and dried samples. Figure 4.34 displays engineering stress-strain curves between DAM, 23°C water conditioned, and dried samples. Dried curves in both cases overlap the DAM curve. Figure 4.35 displays the change in break stress over the course of drying 23°C water conditioned samples. Figure 4.36 displays the change in strain over the course of drying 23°C water conditioned samples. Figure 4.37 displays the change in Young's modulus over the course of drying 23°C water conditioned samples. Break values of dried samples are equivalent to DAM. Young's modulus values of dried samples exceed DAM values. The trend at each drying temperature is erratic compared to PA6 and 50% GF PA6. Figure 4.38 displays the change in notched Charpy impact strength over the course of drying 23°C water conditioned samples. Significant increase in impact strength after conditioning. Dried values occur just above DAM value.

4.6.4 Degradation Analysis

Figure 4.39 compares viscosity and Vicat softening temperature across different sample states. Viscosity decreases with water exposure and increase after drying. Vicat softening temperature decreased in the 23°C water conditioned samples. Vicat softening temperature remained unchanged in 100°C water saturated samples.

4.7 Unreinforced PA MACM12

4.7.1 Absorption Behavior

Water absorption curves for PA MACM12 (see Figure 4.40) show a smooth increase in water content over time for 23°C water, 100°C water, and 23°C + 50% RH methods. 70°C + 62% RH method presents a peak at the beginning of the curve, drop, gradual increase, then decline just before 2000-hour mark. Samples reached 83% of the water content in 23°C water, 67% of the water content at 70°C + 62% RH, and 33% of

the water content after 2000 hours. 100°C water saturated samples yield a weight change of 3.0% after 79 hours and KF moisture content of 3.0%. 23°C water conditioned samples yield a weight change of 2.0% and KF moisture content of 1.7%.

4.7.2 Desorption Behavior

Figures 4.41 and 4.42 are desorption curves for saturated samples and conditioned samples, respectively. Drying of 100°C water saturated samples at 140°C discontinued due to bubbling and deformation. The remaining saturated samples did not reach 0% weight change after drying. Conditioned samples dried below 0%. KF moisture content for dried from conditioned samples is 0.1%.

4.7.3 Tensile and Impact Property

Figure 4.43 displays engineering tensile stress-strain curves between DAM, 100°C water saturated, and 23°C water conditioned. Saturated curve shows a reduction in strain compared to DAM. Conditioned curve shows a reduction in yield point, but retains the strain compared to DAM. Figure 4.44 displays engineering stress-strain curves between DAM, 100°C water saturated, and dried samples. Figure 4.45 displays engineering stress-strain curves between DAM, 23°C water conditioned, and dried samples. Dried curves show a higher yield point and stress along the strain hardening region compared to DAM. Figure 4.46 displays the change in yield stress over the course of drying 23°C water conditioned samples. All drying samples exceed DAM value. Figure 4.47 displays the change in yield strain over the course of drying 23°C water conditioned samples. 120°C and 140°C dryings show an immediate increase then gradually decrease over time. 80°C and 100°C dryings show an immediate increase then plateaus for the remaining drying time. Figure 4.48 displays the change in Young's

modulus over the course of drying 23°C water conditioned samples. Values gradually increase over time but trend lower than DAM. Figure 4.49 displays the change in notched Charpy impact strength over the course of drying 23°C water conditioned samples. Significant increase in impact strength after conditioning but drops to DAM value at initial part of drying then continues to decrease below DAM over time.

4.7.4 Degradation Analysis

Figure 4.50 compares viscosity and Vicat softening temperature across different sample states. Both values decrease with water exposure and increase after drying. Dried values trends slightly higher than DAM values. Figures 4.51 and 4.52 displays the change in yellowness index and CIE b-value curves, respectively, over the course of drying 23°C water conditioned samples. 120°C and 140°C dry samples show significantly steep increase in yellowing over time. 80°C and 100°C samples show gradual increase in yellowing over time.

4.8 Reinforced PA12

4.8.1 Absorption Behavior

Water absorption curves for 50% GF PA12 (see Figure 4.53) demonstrate the same behavior as unreinforced PA MACM12. 100°C water saturated samples yield a weight change of 0.87% after 81 hours and KF moisture content of 0.99%. 23°C water conditioned samples yield a weight change of 0.39% and KF moisture content of 0.32%.

4.8.2 Desorption Behavior

Figures 4.54 and 4.55 are desorption curves for saturated samples and conditioned samples, respectively. 140°C, 100°C, and 80°C samples dried below 0% weight change except for saturated samples dried at 120°C, which reached 0.099% weight change.

4.8.3 Tensile and Impact Property

Figure 4.56 displays engineering tensile stress-strain curves between DAM, 100°C water saturated, and 23°C water conditioned. Water samples show decrease in stress and increase in strain. Figure 4.57 displays engineering stress-strain curves between DAM, 100°C water saturated, and dried samples. Dried curves overlap DAM curve. Figure 4.58 displays engineering stress-strain curves between DAM, 23°C water conditioned, and dried samples. Dried curves trend above DAM curve. Figure 4.59 displays the change in break stress over the course of drying 23°C water conditioned samples. Values increase above DAM over time. Figure 4.60 displays the change in strain over the course of drying 23°C water conditioned samples. Values decrease below DAM over time. Figure 4.61 displays the change in Young's modulus over the course of drying 23°C water conditioned samples. Values increase above DAM over time. 80°C shows some decrease towards the end of drying. Figure 4.62 displays the change in notched Charpy impact strength over the course of drying 23°C water conditioned samples. Dried values occur just below DAM value.

4.8.4 Degradation Analysis

Figure 4.63 compares viscosity and Vicat softening temperature across different sample states. Both values decrease with water exposure and increase after drying.

4.9 Unreinforced PA6I/6T

4.9.1 Absorption Behavior

Water absorption curves for PA6I/6T (see Figure 4.64) show a smooth increase in water content over time for 23°C water, 100°C water, and 23°C + 50% RH methods. method presents absorption in stepwise manner. Samples reached maximum saturation in

70°C + 62% RH, 62% of the water content in 23°C water, and 15% of the water content in 23°C + 50% RH after 2000 hours. 100°C water saturated samples yield a weight change of 6.5% after 79 hours and KF moisture content of 2.9%. 23°C water conditioned samples yield a weight change of 2.6% and KF moisture content of 2.4%.

4.9.2 Desorption Behavior

Figures 4.65 and 4.66 are desorption curves for saturated samples and conditioned samples, respectively. Drying of 23°C water conditioned samples at 120°C and 140°C discontinued due to blistering and deformation. Drying temperature of 60°C included in study. Saturated samples dried below 0% weight change at 140°C. Remaining samples dried just above 0% weight change. KF moisture content for dried from conditioned samples ranges between 0.3% and 0.4%.

4.9.3 Tensile and Impact Property

Figure 4.67 displays engineering tensile stress-strain curves between DAM, 100°C water saturated, and 23°C water conditioned. Saturated curve shows embrittlement by absence of yield and significantly low break point. Conditioned curve shows a reduction in yield point and strain. Figure 4.68 displays engineering stress-strain curves between DAM, 100°C water saturated, and dried samples. Embrittlement continued into the dried samples. Figure 4.69 displays engineering stress-strain curves between DAM, 23°C water conditioned, and dried samples. Dried curves show a higher yield point compared to DAM. 100°C curve breaks just after the yield indicating some embrittlement present. 80°C and 60°C curve presents a lower yield point but missing the strain hardening region compared to DAM. Figure 4.70 displays the change in yield stress over the course of drying 23°C water conditioned samples. All drying samples

exceed DAM value. Figure 4.71 displays the change in yield strain over the course of drying 23°C water conditioned samples. 100°C and 80°C dryings show gradual increase over time above DAM. 60°C gradually increases over time but trends just below DAM. Figure 4.72 displays the change in Young's modulus over the course of drying 23°C water conditioned samples. Values trends lower than DAM. Figure 4.73 displays the change in notched Charpy impact strength over the course of drying 23°C water conditioned samples. Values decline over time.

4.9.4 Degradation Analysis

Figure 4.50 compares viscosity and Vicat softening temperature across different sample states. Both values decrease with water exposure and increase after drying 23°C water conditioned samples. Viscosity decreases and Vicat increases after drying 100°C water saturated samples. Dried values trends slightly higher than DAM values. Figures 4.75 and 4.76 displays the change in yellowness index and CIE b-value curves, respectively, over the course of drying 23°C water conditioned samples. Yellowing reduced after conditioning and gradually increases over drying time. 80°C and 60°C trend below DAM whereas 100°C trend slightly above DAM.

4.10 Reinforced PA66 + PA6I/X

4.10.1 Absorption Behavior

Water absorption curves for 50% GF PA66 + PA6I/X (see Figure 4.77) demonstrate the same behavior as PA6I/6T. 100°C water saturated samples yield a weight change of 3.8% after 81 hours and KF moisture content of 3.9%. 23°C water conditioned samples yield a weight change of 1.1% and KF moisture content of 1.1%.

4.10.2 Desorption Behavior

Figures 4.30 and 4.79 are desorption curves for saturated samples and conditioned samples, respectively. All samples dried below 0% weight change except for saturated samples dried at 80°C and 120°C, which reached 0.26% weight change.

4.10.3 Tensile and Impact Property

Figure 4.80 displays engineering tensile stress-strain curves between DAM, 100°C water saturated, and 23°C water conditioned. Water samples show decrease in stress and increase in strain compared to DAM. Figure 4.81 displays engineering stress-strain curves between DAM, 100°C water saturated, and dried samples. Figure 4.82 displays engineering stress-strain curves between DAM, 23°C water conditioned, and dried samples. Dried samples overlap DAM curve. Figure 4.83 displays the change in break stress over the course of drying 23°C water conditioned samples. Figure 4.84 displays the change in strain over the course of drying 23°C water conditioned samples. Figure 4.85 displays the change in Young's modulus over the course of drying 23°C water conditioned samples. Stress values of dried samples are equivalent to DAM. Strain values trend below DAM. Young's modulus values of dried samples exceed DAM. Figure 4.86 displays the change in notched Charpy impact strength over the course of drying 23°C water conditioned samples. Increase in impact strength after conditioning. Dried values occur just below DAM value.

4.10.4 Degradation Analysis

Figure 4.87 compares viscosity and Vicat softening temperature across different sample states. Viscosity slightly decreases with water exposure and increase after drying. Vicat softening temperature remained unchanged between DAM, water exposed, and dried samples.

CHAPTER 5: Conclusions and Path Forward

Monitoring water content solely by weight change leads to inaccurate assumptions regarding dryness level. Moisture check of dried samples with analytical methods shows some retention of water not detectable by weight change. Residual moisture in the dried samples continues to contribute to mechanical property deviation from the dry-as-molded state.

Polyamide products perform both similarly and differently from each other. Unreinforced PA6 study is consistent with findings from previous research studies where water exposure reduces tensile stress and increases tensile strain. The presence of residual water after drying may contribute to the lack of strain softening. 50% GF reinforced PA6 study behaves similarly to unreinforced PA6. Tensile properties improved after drying. Impact properties slightly lower than DAM. 50% GF PA66 + PA6 behaves close to DAM state after drying. 50% GF PA12 exhibits little change in properties between conditioning and drying from DAM. 50% GF PA66+PA6I/X behaves close to DAM state after drying. Little variation observed in viscosity and softening temperature across all sample states. Materials do not exhibit adverse effects to the absorption and desorption methods. The amorphous grades display different results. PA MACM12 exhibits improved tensile and impact properties over time but tends to increase in yellowing from either high drying temperatures or long drying time. PA6I/6T exhibits higher tensile stress but lower impact strength. Yellowing is slight over time. Both materials exhibit some adverse effects depending on saturation level and temperature.

Article statements encouraging drying above the glass transition and discouraging the use of hot air ovens are unfounded by the experiment. Semicrystalline materials benefit from drying at higher temperatures with short durations. Temperatures range 100°C above the glass transition temperature. PA MACM12 properties benefit from temperatures between 100°C and 120°C but increased yellowing poses a potential for other degradation mechanisms not covered by the experiment. PA6I/6T properties benefit from drying at lower temperatures with longer durations. Yellowing does not pose a problem. Temperatures range 30°C to 50°C below the glass transition temperature. Use of oven dryers requires closer monitoring but presents an alternative option to vacuum and desiccant dryers.

Next step for the data collected could include compilation into a predictive model such as an Arrhenius plot. This may open the possibility of further investigating more effective drying methods for specialty nylons. Low cost and high efficiency are the goal in a manufacturing setting. Proper parts drying contributes to waste elimination. Future studies in drying specialty nylons could include polyphthalamide products which are low absorption, heat stabilized materials replacing high performance, specialty polyamides in various market segments. Additionally, studies could include a closer look into the polymer structure in combination with additives either contributing or inhibiting drying effectiveness.

References

[1] M. Kohan, Nylon Plastics Handbook, Munich/Vienna/New York: Hanser Publishers, 1995.

[2] Y. Chen, O. Modi, A. Mhay, A. Chrysanthou and J. O'Sullivan, "The effect of different metallic counter face materials and different surface treatments on the wear and friction of polyamide 66 and its composite in rolling-sliding contact," *Wear,* vol. 255, pp. 714-721, 2003.

[3] R. Taktak, N. Guermazi, J. Derbeli and N. Haddar, "Effect of hygrothermal aging on the mechanical properties and ductile fracture of polyamide 6: Experimental and numerical approaches," *Engineering Fracture Mechanics,* vol. 148, pp. 122-133, 2015.

[4] T. Bárány, E. Földes and T. Czigány, "Effect of thermal and hygrothermal aging on the plane stress fracture toughness of poly(ethylene terephthalate) sheets," *eXPRESS Polymer Letters,* vol. 1, pp. 180-187, 2007.

[5] S. Alessi, D. Conduruta, G. Pitarresi, C. Dispenza and G. Spadaro, "Accelerated ageing due to moisture absorption of thermally cured epoxy resin/polyethersulphone blends, thermal, mechanical and morphological behavior," *Polymer Degradation and Stability,* vol. 96, pp. 642-648, 2011.

[6] V. Radlmaier, C. Heckel, M. Winnacker, A. Erber and H. Koerber, "Effects of thermal cycling on polyamides during processing," *Thermochimica Acta,* vol. 648, pp. 44-51, 2017.

[7] N. Abacha, M. Kubouchi and T. Sakai, "Diffusion behavior of water in polyamide 6 organoclay nanocomposites," *eXPRESS Polymer Letters,* vol. 3, pp. 245-255, 2009.

[8] R. Seltzer, J. Escudero and F. de la Escalera Cutillas, "Influence of hygrothermal aging on the mechanical properties of Nylon 12 composites processed by selective laser sintering.," in *Innovative Developments in Virtual and Physical Prototyping*, Leiden, CRC Press, 2011, pp. 287-289.

[9] S. Alessi, G. Pitarresi and G. Spadar, "Effect of hydrothermal ageing on the thermal and delamination fracture behaviour of CFRP composites," *Composites Part B: Engineering,* vol. 67, pp. 145-153, 2014.

[10] A. Krzyżak, J. Gąska and B. Duleba, "Water absorption of thermoplastic matrix composites with polyamide 6," *Scientific Journals,* vol. 33, pp. 62-68, 2013.

[11] S. Kulkarni, "Overdrying of Resins & Its Prevention," 2 February 2007. [Online]. Available: https://knowledge.ulprospector.com/1210/pe-overdrying-resins/.

[12] W. Hamm and E. Benjamin, "What You Need to Know About Drying Specialty Nylons," 25 April 2017. [Online]. Available: https://www.ptonline.com/articles/what-you-need-to-know-about-drying-specialty-nylons.

[13] K.-H. Su, J.-H. Lin and C.-C. Lin, "Influence of reprocessing on the mechanical properties and structure of polyamide 6," *Journal of Materials Processing Technology,* Vols. 192-193, pp. 532-538, 2007.

[14] Y. Khanna, P. Han and E. Day, "New developments in the melt rheology of nylons. I: Effect of moisture and molecular weight," *Polymer Engineering and Science,* pp. 1745-1754, 1996.

[15] W. Dong and P. Gijsman, "Influence of temperature on the thermo-oxidative degradation of polyamide 6 films," *Polymer Degradation and Stability,* vol. 95, no. 6, pp. 1054-1062, 2010.

[16] B. Howe, "Dry vs. Conditioned Polyamide Nylon Explained," 29 January 2010. [Online]. Available: https://knowledge.ulprospector.com/1489/pe-dry-vs-conditioned-polyamide-nylon/.

[17] DuPont, "DuPont Zytel 7301 NC010," 16 May 2017. [Online]. Available: https://dupont.materialdatacenter.com/profiler/G7BZ7/standard/main/ds.

[18] BASF, "Ultramid 8202 HS," September 2009. [Online]. Available: https://worldaccount.basf.com/wa/AP~en_GB/Catalog/BASFPlastics/doc4/BASF/PRD/30215379/.pdf?asset_type=pds/pdf&language=EN&urn=urn:documentum:eCommerce_sol_EU:09007bb28005ec68.pdf.

[19] Solvay Engineering Plastics, "Technyl C 206F Natural," June 2017. [Online]. Available: https://catalog.ulprospector.com/Datasheet.aspx?I=89581&FMT=PDF&E=295199&SKEY=89581.1498639.193634881%3A806b2c3a-223a-405e-816e-2228b4a26e2d&CULTURE=en-US&.

[20] DSM, "Recommendations for injection molding Novamid 1011CH5-KR," 29 Septemer 2018. [Online]. Available:

https://plasticsfinder.com/api/document/proc/Novamid%C2%AE%201011CH5-KR/PPCpuBYZQ/en/Novamid1011CH5KRen.pdf.

[21] DSM, "Property Data Novamid® 1011CH5-KR," 3 October 2018. [Online]. Available: https://plasticsfinder.com/api/document/tech/Novamid%C2%AE%201011CH5-KR/jMulu9L1p/en/Novamid1011CH5KRenSI.pdf.

[22] EMS-GRIVORY, "Technical Data Sheet: Grilon BS," February 2013. [Online]. Available: https://ems.materialdatacenter.com/eg/en/main/ds/Grilon+BS. [Accessed 18 October 2018].

[23] M. Sepe, "Why (and What) You Need to Dry," 24 April 2014. [Online]. Available: https://www.ptonline.com/articles/why-and-what-you-need-to-dry.

[24] J. Bozzelli, "Injection Molding: You Must Dry Hygroscopic Resins," 23 December 2010. [Online]. Available: https://www.ptonline.com/columns/you-must-dry-hygroscopic-resins.

[25] M. Sepe, "The Materials Analyst, Part 89: The myth of overdrying—Part 1," 31 August 2007. [Online]. Available: https://www.plasticstoday.com/content/materials-analyst-part-89-myth-overdrying-part-1/6917703313643.

[26] A. Ranowsky, "Karl Fischer vs. Loss-On Drying - Which Method is the Best?," 19 November 2013. [Online]. Available: https://www.cscscientific.com/csc-cientific-blog/karl-fischer-vs-loss-on-drying-which-method-is-the-best.

[27] J. Bogart, "The Difference Between Primary + Secondary Moisture Measurement," 10 April 2013. [Online]. Available: https://blog.kett.com/bid/274676/The-Difference-Between-Primary-Secondary-Moisture-Measurement.

[28] M. Spitzlei, "Choosing a method for measuring your material's moisture content," 30 January 2002. [Online]. Available: ftp://ftp.ufv.br/Dea/Disciplinas/Evandro/Eng671/Atividade%20de%20agua/Choosing_method.pdf.

[29] ISO, *ISO 15512 Plastics - Determination of water content,* Geneva: ISO Copyright Office, 2016.

[30] ISO, *ISO 62 Plastics - Determination of water absorption,* Geneva: ISO Copyright Office, 2008.

[31] PolyClean, "Perfect Plastics: The 4 Factors of Resin Drying," 2018. [Online]. Available: http://polycleanusa.com/perfect-plastics-4-factors-resin-drying/.

[32] P.-Y. Le Gac and B. Fayolle, "Impact of fillers (short glass fibers and rubber) on the hydrolysis-induced embrittlement of polyamide 6.6," *Composites Part B: Engineering,* vol. 153, pp. 256-263, 2018.

[33] P. Gilormini and J. Verdu, "On the role of hydrogen bonding on water absorption in polymers," *Polymer,* vol. 142, pp. 164-169, 2018.

[34] M. Broudin, V. Le Saux, P. Le Gac, C. Champy, G. Robert, P. Charrier and Y. Marco, "Moisture sorption in polyamide 6.6: experimental investigation and comparison to four physical-based models," *Polymer Testing,* vol. 171, pp. 87-95, 2015.

[35] I. Clavería, D. Elduque, J. Santolaria, C. Pina, C. Javierre and A. Fernandez, "The influence of environmental conditions on the dimensional stability of components injected with PA6 and PA66," *Polymer Testing,* vol. 50, pp. 15-25, 2016.

[36] L. Monson, M. Braunwarth and C. Extrand, "Moisture absorption by various polyamides and their associated dimensional changes," *Journal of Applied Polymer Science,* vol. 107, pp. 355-363, 2008.

[37] H. Obeid, A. Clément, S. Fréour, F. Jacquemin and P. Casari, "On the identification of the coefficient of moisture expansion of polyamide-6: Accounting differential swelling strains and plasticization," *Mechanics of Materials,* vol. 118, pp. 1-10, 2018.

[38] V. Miri, O. Persyn, J.-M. Lefebvre and R. Seguela, "Effect of water absorption on the plastic deformation behavior of nylon 6," *European Polymer Journal,* vol. 45, p. 757–762, 2008.

[39] G. Baschek, G. Hartwig and F. Zahradnik, "Effect of water absorption in polymers at low and high temperatures," *Polymer,* vol. 40, p. 3433–3441, 1999.

[40] J. Chaichanawong, C. Thongchuea and S. Areerat, "Effect of moisture on the mechanical properties of glass fiber reinforced polyamide composites," *Advanced Powder Technology,* vol. 27, pp. 898-902, 2016.

[41] B. Arash, B. J. Thijsse, A. Pecenko and A. Simone, "Effect of water content on the thermal degradation of amorphous polyamide 6,6: A collective variable-driven hyperdynamics study," *Polymer Degradation and Stability,* vol. 146, pp. 260-266, 2017.

[42] R. Steffen, G. Wallner, J. Rekstad and B. Röder, "General characteristics of photoluminescence from dry heat aged polymeric materials," *Polymer Degradation and Stability,* vol. 134, pp. 49-59, 2016.

[43] R. Bernstein and K. Gillen, "Nylon 6.6 accelerating aging studies: II. Long-term thermal-oxidative and hydrolysis results," *Polymer Degradation and Stability,* vol. 95, pp. 1471-1479, 2010.

[44] V. Fabre, G. Quandalle, N. Billon and S. Cantournet, "Time-Temperature-Water content equivalence on dynamic mechanical response of polyamide 6,6," *Polymer,* vol. 137, pp. 22-29, 2018.

[45] C. El-Mazry, O. Correc and X. Colin, "A new kinetic model for predicting polyamide 6-6 hydrolysis and its mechanical embrittlement," *Polymer Degradation and Stability,* vol. 97, pp. 1049-1059, 2012.

[46] D. Ferreño, I. Carrascal, E. Ruiz and J. Casado, "Characterisation by means of a finite element model of the influence of moisture content on the mechanical and fracture properties of the polyamide 6 reinforced with short glass fibre," *Polymer Testing,* vol. 30, pp. 420-428, 2011.

[47] J. Reis, T. d. Santanna, P. Coutinho, A. Monteiro, S. Teixeria, E. Chaves and H. da Costa Mattos, "Coupled effect of ageing and temperature in the mechanical behaviour of a polyamide," *Polymer Testing,* vol. 53, pp. 267-275, 2016.

[48] G. Filippone, S. C. Carroccio, R. Mendichi, L. Gioiella, N. Dintcheva and C. Gambarotti, "Time-resolved rheology as a tool to monitor the progress of polymer

degradation in the melt state e Part I: Thermal and thermo-oxidative degradation of polyamide 11," *Polymer,* vol. 72, pp. 134-141, 2015.

[49] E. Richaud, O. O. Diogo, B. Fayolle, J. Verdu, J. Guilment and F. Fernagut, "Review: Auto-oxidation of aliphatic polyamides," *Polymer Degradation and Stability,* vol. 98, pp. 1929-1939, 2013.

[50] O. Okamba-Diogo, E. Richaud, J. Verdu, F. Fernagut, J. Guilment and B. Fayolle, "Investigation of polyamide 11 embrittlement during oxidative degradation," *Polymer,* vol. 82, pp. 49-56, 2016.

[51] X.-F. Wei, K. J. Kallio, S. Bruder, M. Bellander, H.-H. Kausch, U. W. Gedde and M. S. Hedenqvist, "Diffusion-limited oxidation of polyamide: Three stages of fracture behavior," *Polymer Degradation and Stability,* vol. 154, pp. 73-83, 2018.

[52] P. Gijsman, W. Dong, A. Quintana and M. Celina, "Influence of temperature and stabilization on oxygen diffusion limited oxidation profiles of polyamide 6," *Polymer Degradation and Stability,* vol. 130, pp. 83-96, 2016.

[53] A. Bergeret, L. Ferry and P. Ienny, "Influence of the fibre/matrix interface on ageing mechanisms of glass fibre reinforced thermoplastic composites (PA-6,6, PET, PBT) in a hygrothermal environment," *Polymer Degradation and Stability,* vol. 94, pp. 1315-1324, 2009.

[54] M. Haynie, "Knowledge Center Plastics Drying - What are Hygroscopic Resins?," 2018. [Online]. Available: https://www.ptonline.com/knowledgecenter/Plastics-Drying/Resin-Types/Hygroscopic-VS-Non-Hygroscopic-Resins.

[55] M. Haynie, "Knowledge Center Plastics Drying - Oven Dryers," 2018. [Online]. Available: https://www.ptonline.com/knowledgecenter/Plastics-Drying/Dryer-Types/Oven-Dryers.

[56] Binder, "Effective and gentle drying in a vacuum," January 2017. [Online]. Available: https://www.binder-world.com/en/News-Press/News-Updates/Applications-of-vacuum-drying-chambers.

[57] M. Haynie, "Knowledge Center Plastics Drying - Vacuum Dryer," 2018. [Online]. Available: https://www.ptonline.com/knowledgecenter/Plastics-Drying/Dryer-Types/Vacuum-Dryers.

[58] O. Kast and C. Bonten, "Debunking the myths about drying," *Kunststoffe International,* vol. 107, pp. 39-42, 2017.

[59] A. Pedroso, L. Mei, J. Agnelli and D. Rosa, "The influence of the drying process time on the final properties of recycled glass fiber reinforced polyamide 6," *Polymer Testing,* vol. 21, pp. 229-232, 2002.

[60] EMS-GRIVORY, "Technical Data Sheet: Grilon BG-50 S," May 2002. [Online]. Available: https://ems.materialdatacenter.com/eg/en/main/ds/Grilon+BG-50+S. [Accessed 18 October 2018].

[61] EMS-GRIVORY, "Technical Data Sheet: Grilon TSG-50," June 2002. [Online]. Available: https://ems.materialdatacenter.com/eg/standard/main/ds. [Accessed 9 December 2016].

[62] EMS-GRIVORY, "Grilamid TR 90 Natural," January 2015. [Online]. Available: https://ems.materialdatacenter.com/eg/standard/main/ds. [Accessed 18 October 2018].

[63] EMS-GRIVORY, "Grilamid LV-5H," September 2009. [Online]. Available: https://ems.materialdatacenter.com/eg/standard/main/ds. [Accessed 9 December 2018].

[64] EMS-GRIVORY, "Technical Data Sheet: Grivory G 21 Natural," March 2008. [Online]. Available: https://ems.materialdatacenter.com/eg/standard/main/ds. [Accessed 18 October 2018].

[65] EMS-GRIVORY, "Technical Data Sheet: Grivory GV-5H Black 9915," January 2006. [Online]. Available: https://ems.materialdatacenter.com/eg/standard/main/ds. [Accessed 18 October 2018].

[66] ISO, *ISO 11357-1 Plastics - Differential scanning calorimetry (DSC) Part 1: General principles,* Geneva: ISO Copyright Office, 2016.

[67] ISO, *ISO 11357-2 Plastics - Differential scanning calorimetry (DSC) Part 2: Determination of glass transition temperature and glass transition step height,* Geneva: ISO Copyright Office, 2013.

[68] ISO, *ISO 527 Plastics - Determination of tensile properties,* Geneva: ISO Copyright Office, 2012.

[69] ISO, *ISO 179 Plastics - Determination of Charpy impact properties,* Geneva: ISO Copyright Office, 2010.

[70] ISO, *ISO 306 Plastics - Thermoplastic materials - Determination of Vicat softening temperature (VST),* Geneva: ISO Copyright Office, 2013.

[71] ISO, *ISO 307 Plastics - Polyamides - Determination of viscosity number,* Geneva: ISO Copyright Office, 2007.

[72] ASTM, *E313 Standard Practice for Calculating Yellowness and Whiteness Indices from Instrumentally Measured Color Coordinates,* West Conshohocken: ASTM International, 2005.

[73] ASTM, *D2244 Standard Practice for Calculation of Color Tolerances and Color Differences from Instrumentally Measured Color Coordinates,* West Conshohocken: ASTM International, 2016.

[74] Mallard Creek Polymers, "Crystalline vs Amorphous Polymers," 14 July 2017. [Online]. Available: http://www.mcpolymers.com/library/crystalline-vs.-amorphous-polymers. [Accessed 21 April 2018].

[75] A. Buckley , P. A. Curnuck, M. E. B. Jones and I. Thomas, "The effect of boiling water on an amorphous aromatic polyamide," *Polymer International,* vol. 4, no. 2, pp. 173-181, 1972.

Tables

Material	Resin			Molded Specimen		
	KF (%)	T_g (°C)	VN	KF (%)	T_g (°C)	VN
PA6	0.02	65.7	162	0.04	46.6	160
50% GF PA6	0.05	58.7	164	0.12	49.5	152
50% GF PA66+PA6	0.01	61.5, 119	186	0.09	60.0, 122	160
PA MACM12	0.04	157	144	0.02	155	142
50% GF PA12	0.01	49.9	176	0.04	46.7	174
PA6I/6T	0.01	125	104	0.07	130	106
50% PA66+PA6I/X	0.01	39.7, 95.3	156	0.06	33.3, 90.0	150

Table 4.1: Initial Moisture Content, Glass Transition Temperature, and Viscosity Number Profile

Figures

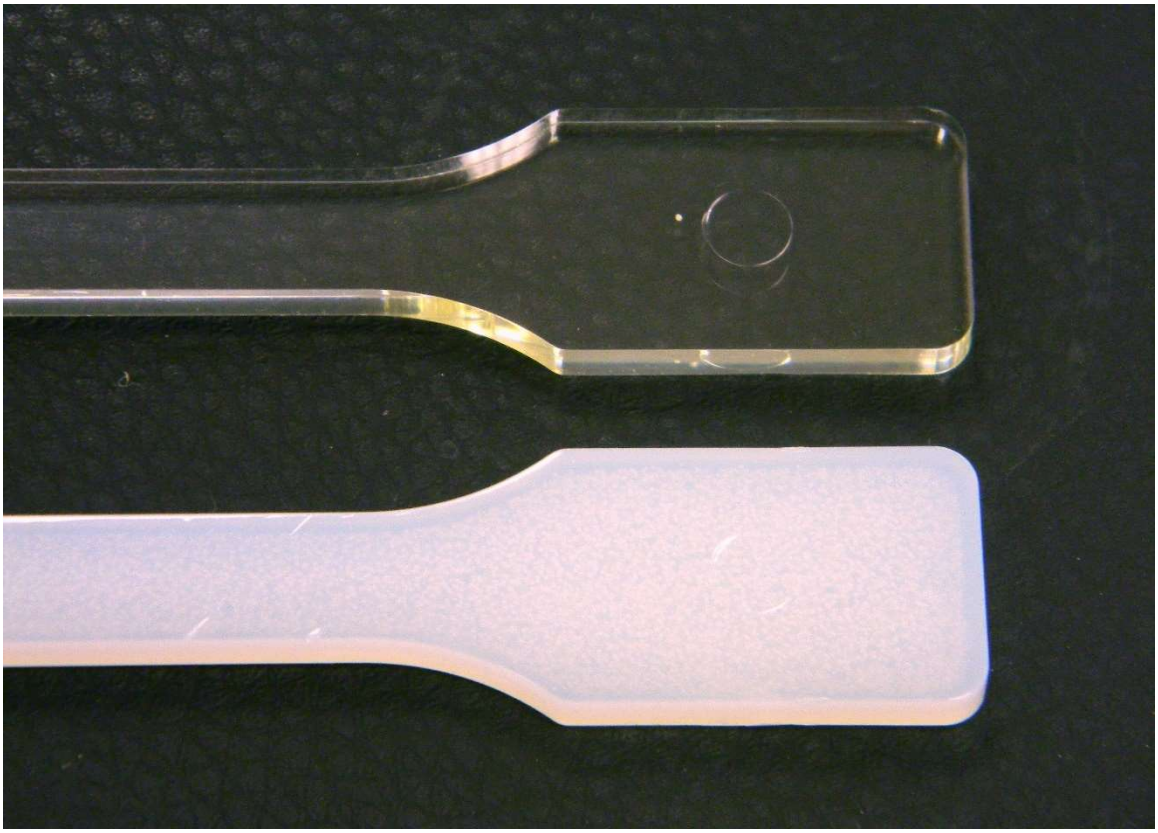

Figure 4.1: PA6I/6T DAM vs After 100°C Water Treatment

Clear specimen (top) becomes opaque after exposure in 100°C water (bottom).

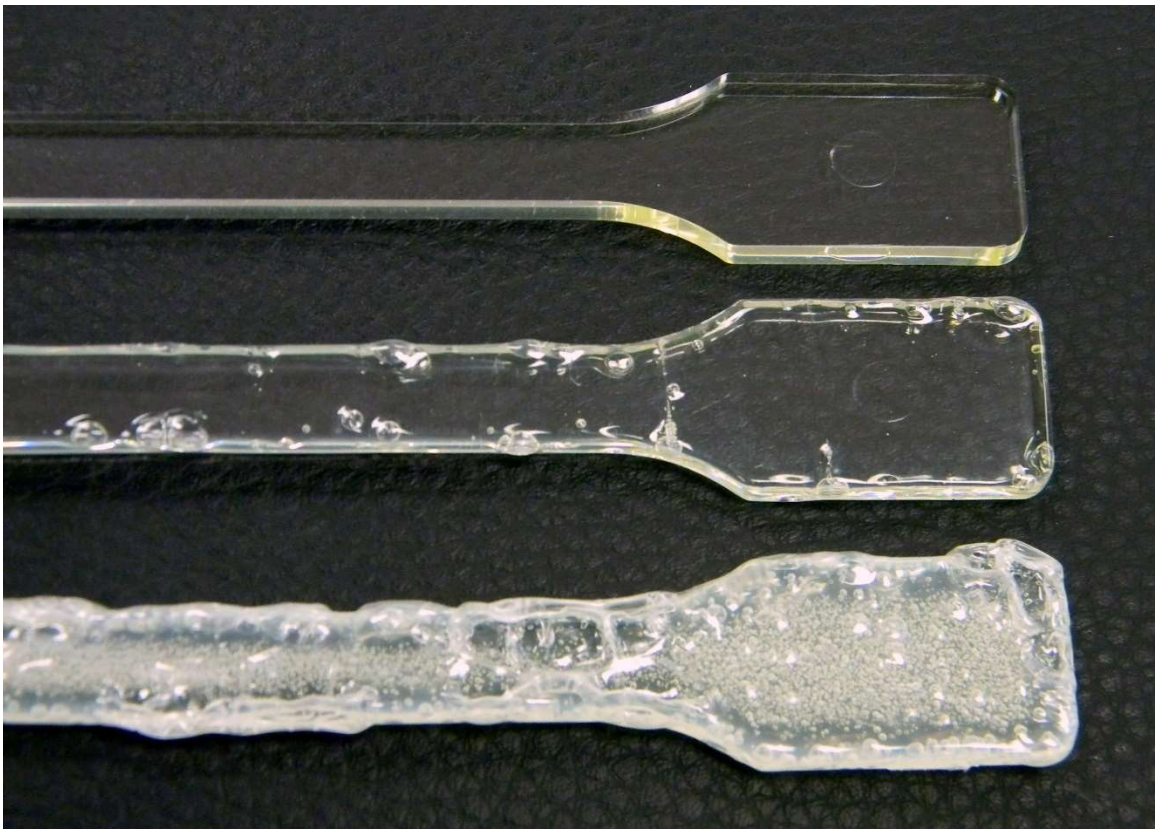

Figure 4.2: Conditioned PA6I/6T After 120°C Oven Drying

Conditioned specimen (top) in 120°C oven displays blisters after 10 minutes (middle) and increased opacity after 90 minutes (bottom).

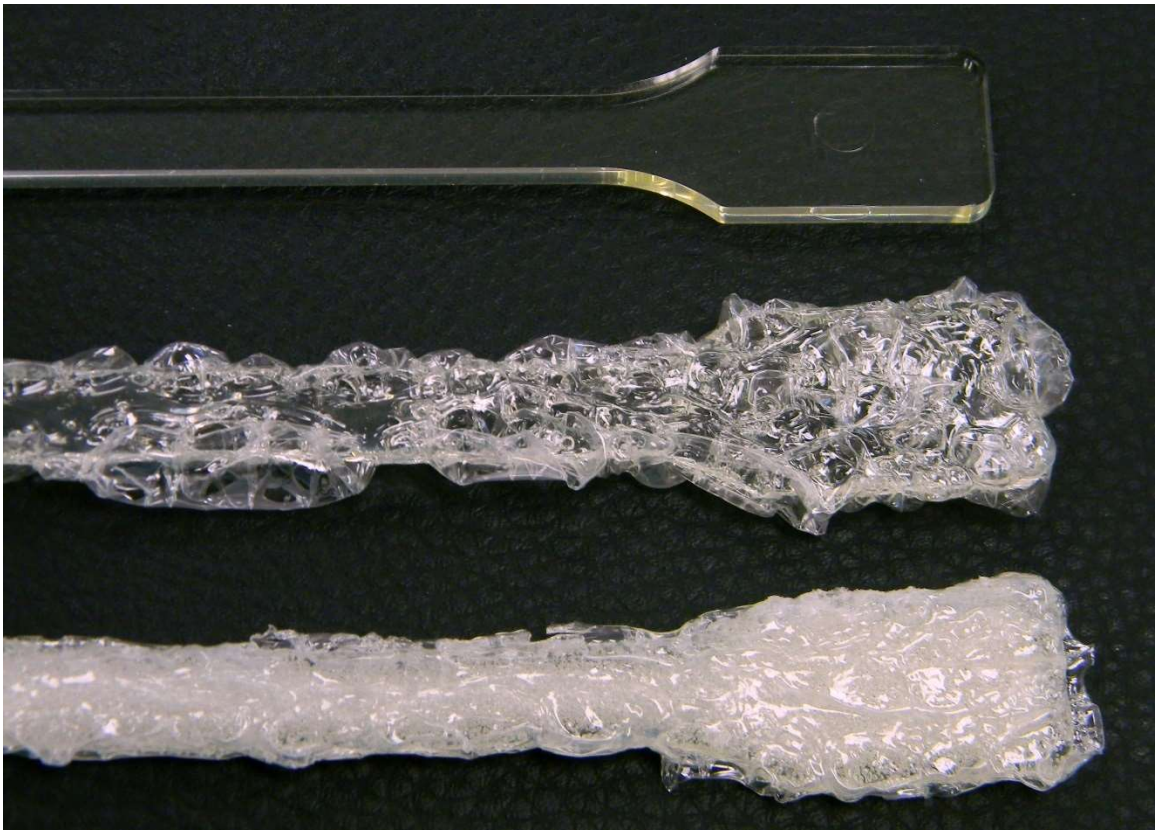

Figure 4.3: Conditioned PA6I/6T After 140°C Oven Drying

Conditioned specimen (top) in 140°C oven displays large blisters after 10 minutes (middle) and increased opacity after 90 minutes (bottom).

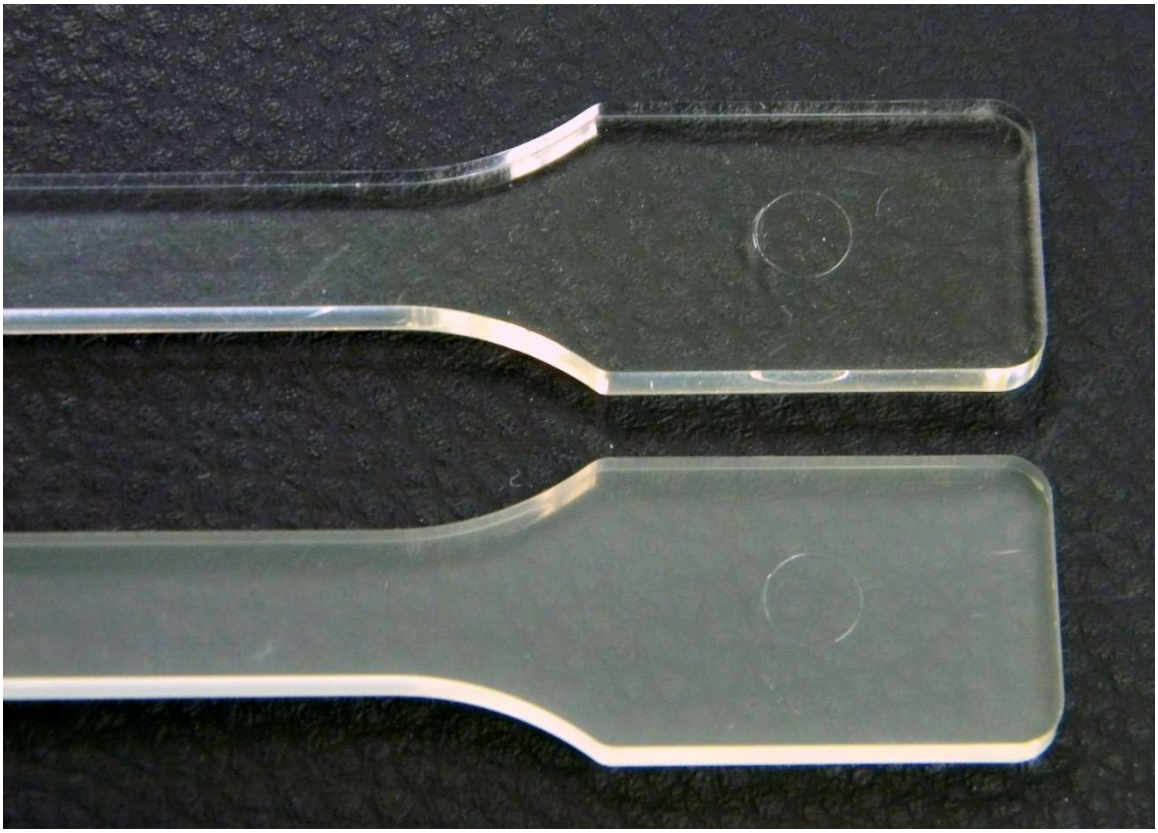

Figure 4.4: Saturated PA MACM12 After 80°C Oven Drying

Saturated PA MACM12 specimen (top) in 80°C oven becomes hazy (bottom) after long drying time.

Figure 4.5: Saturated PA MACM12 After 140°C Oven Drying

Saturated PA MACM12 specimen (top) in 140°C fills with large bubbles (bottom) after 15 minutes exposure.

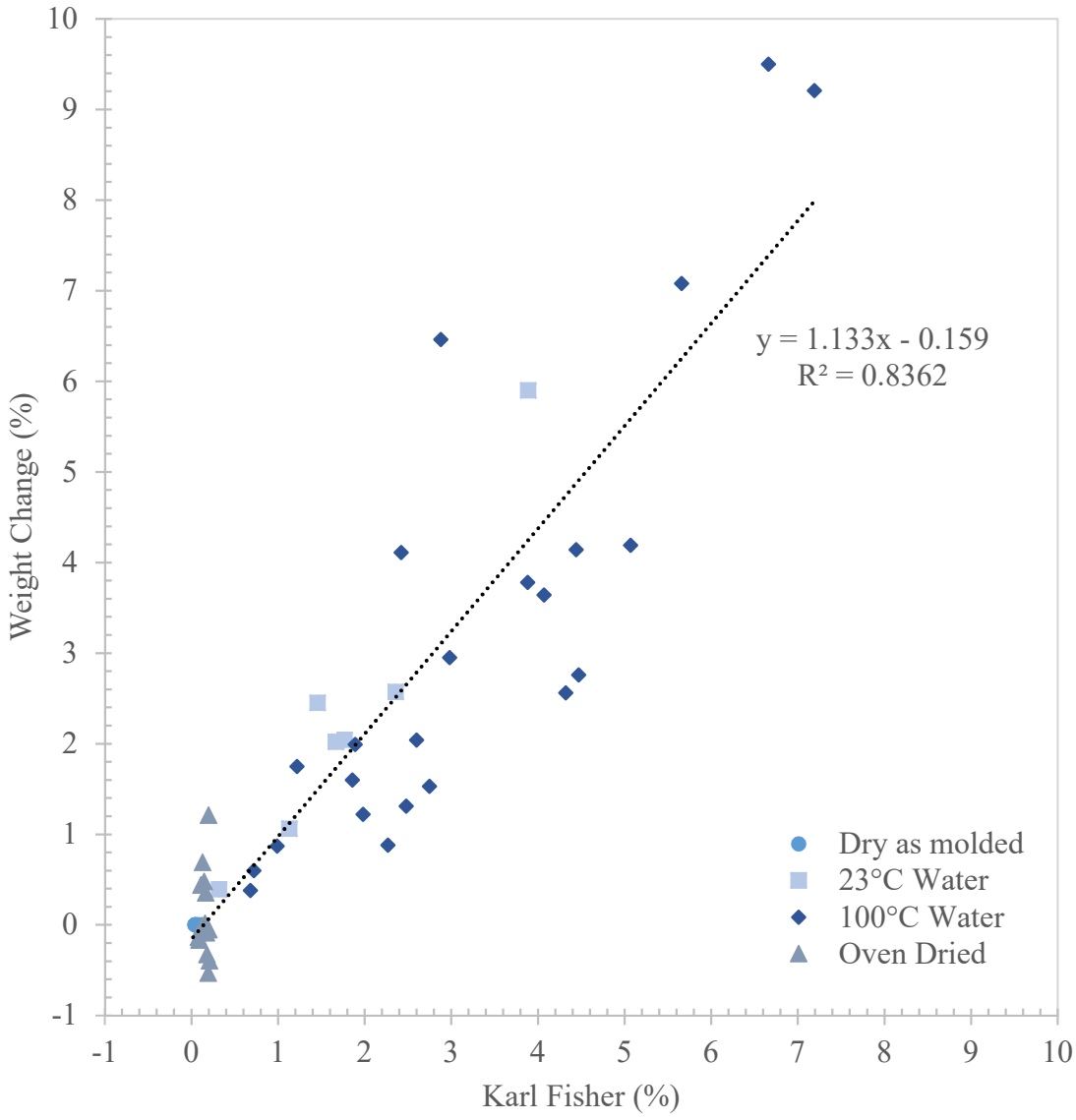

Figure 4.6: Weight Change vs Karl Fisher Moisture Content

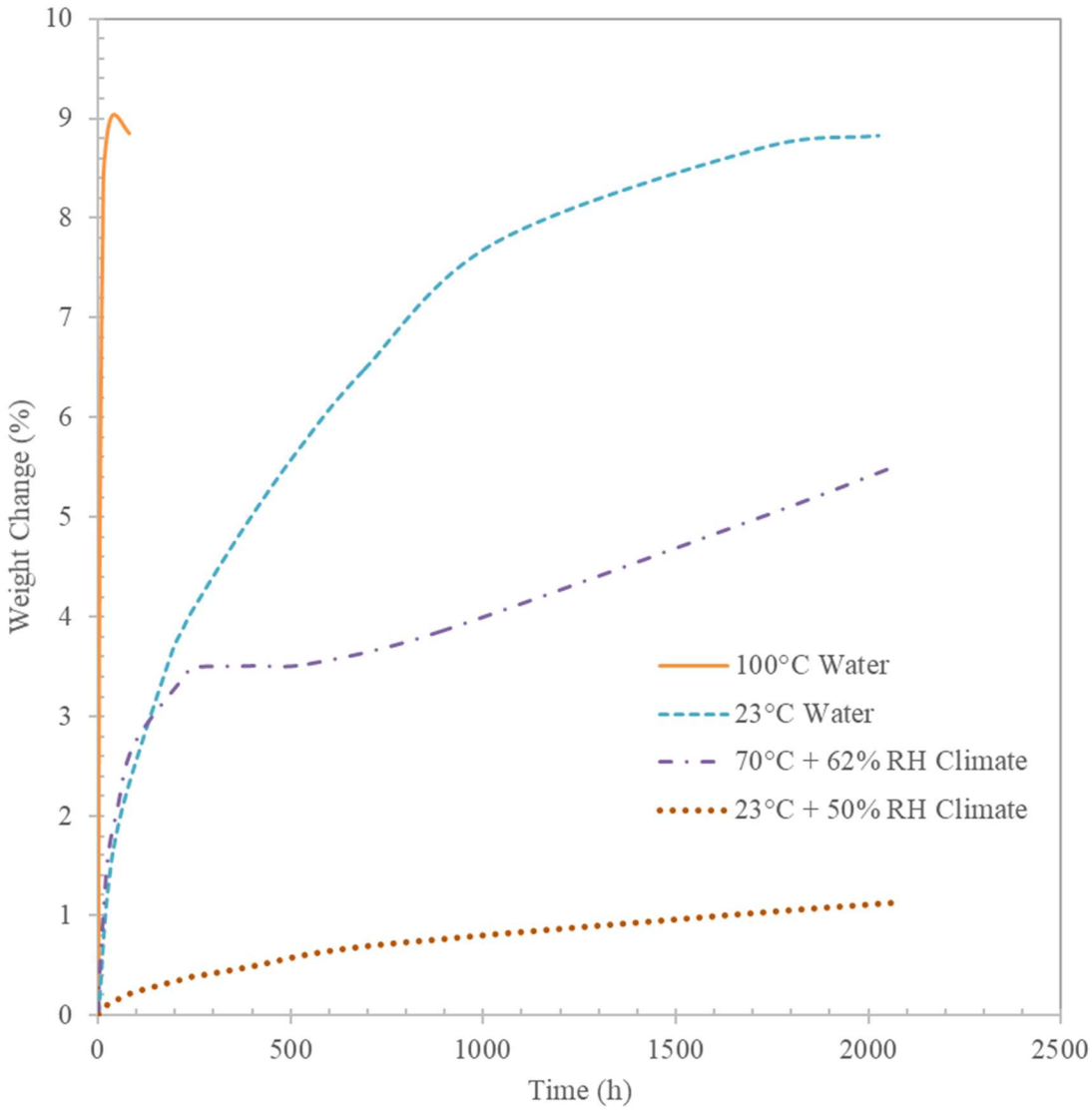

Figure 4.7: Unreinforced PA6 Absorption Comparison

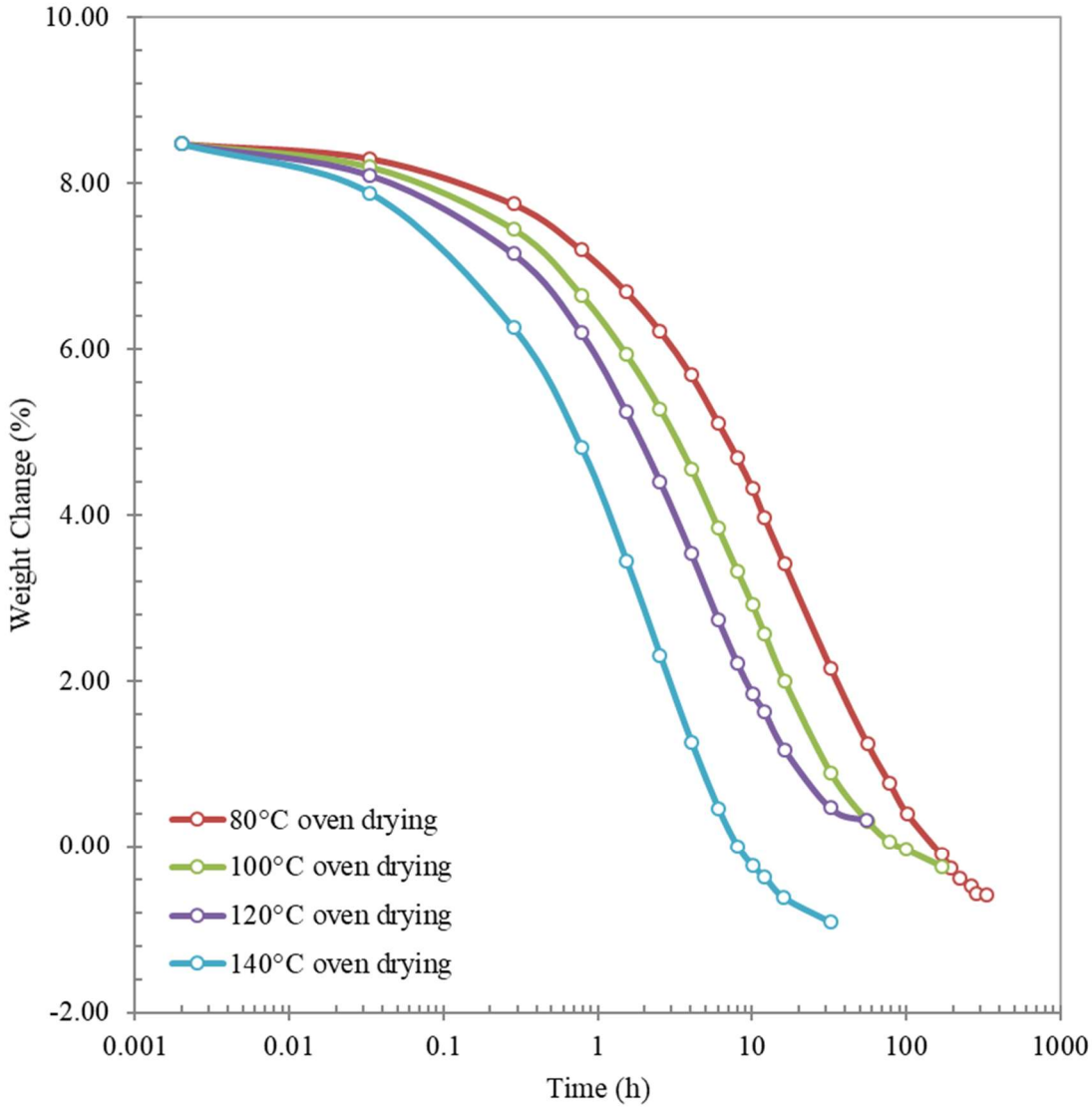

Figure 4.8: Desorption of Saturated PA6 Samples

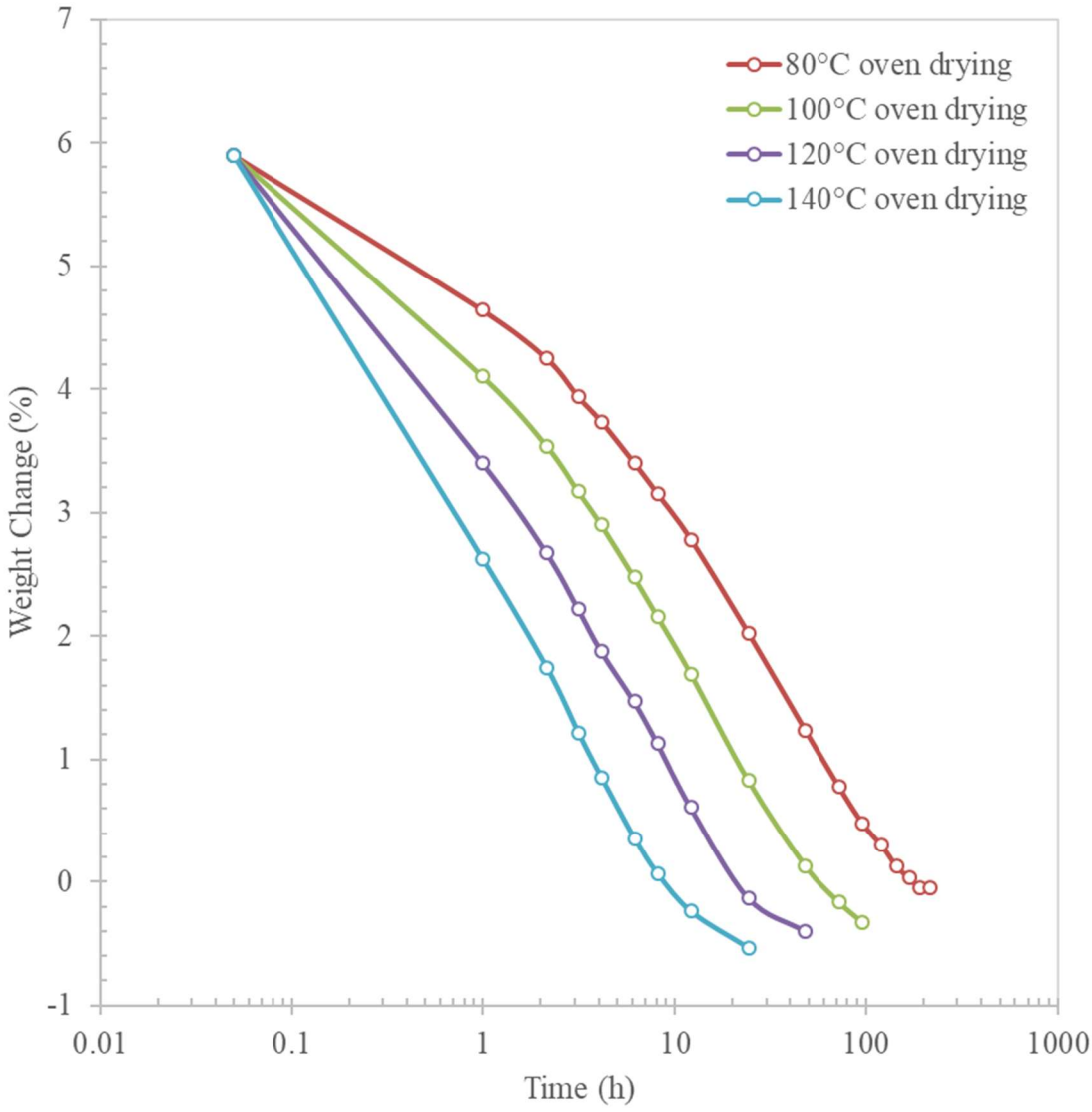

Figure 4.9: Desorption of Conditioned PA6 Samples

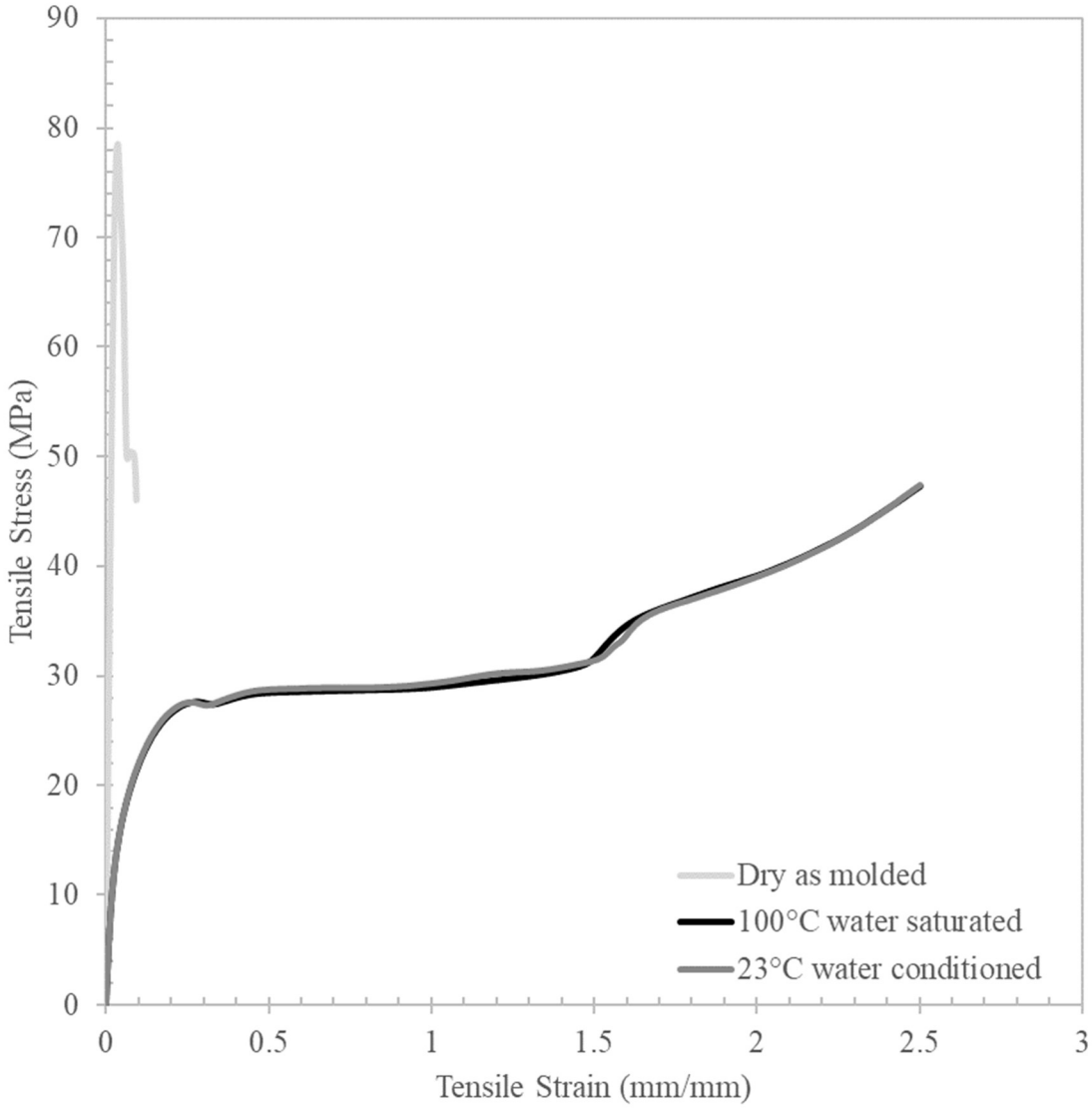

Figure 4.10: PA6 Tensile Stress-Strain DAM vs Water Samples

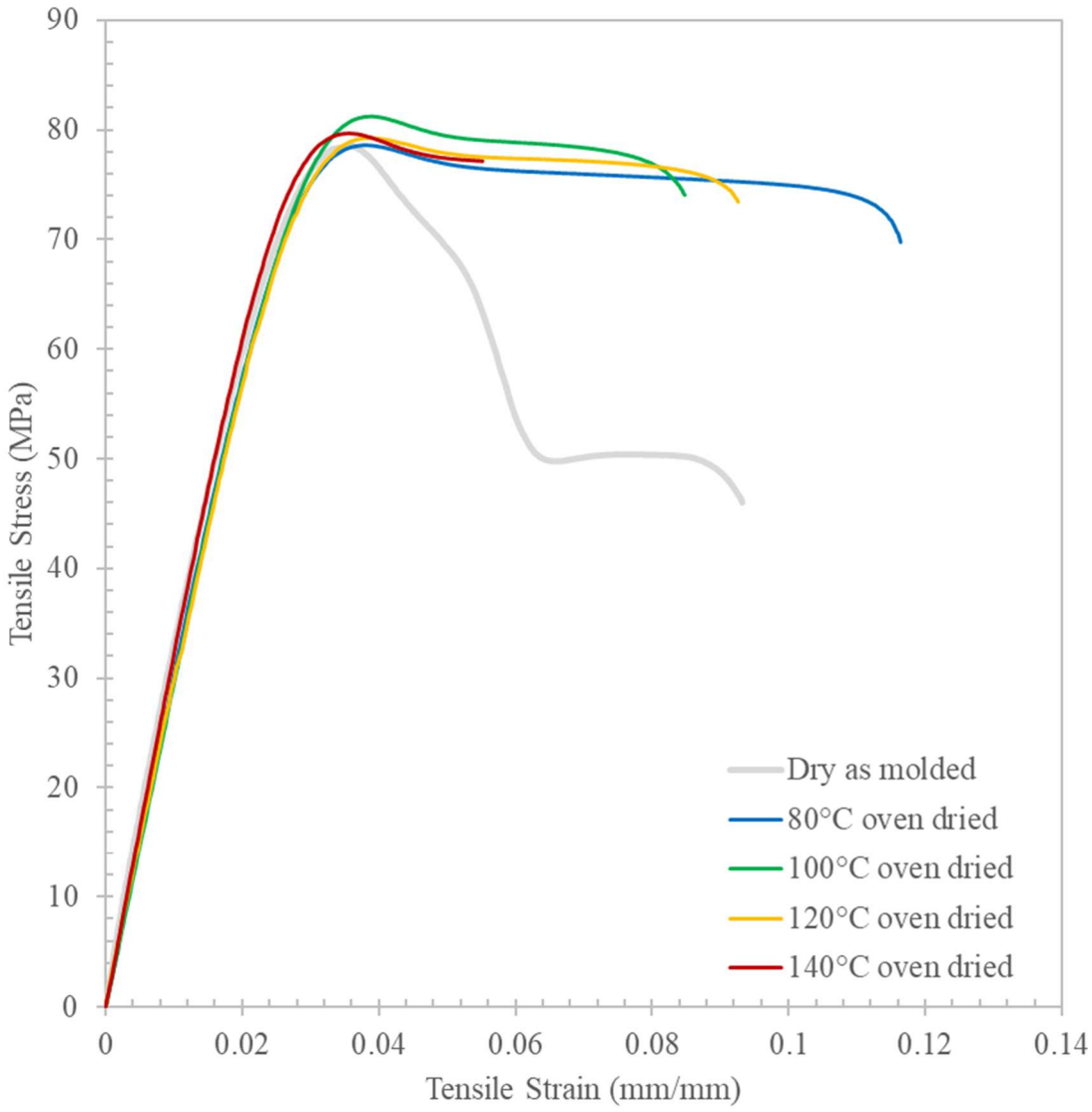

Figure 4.11: PA6 Tensile Stress-Strain DAM vs Dried from Saturated

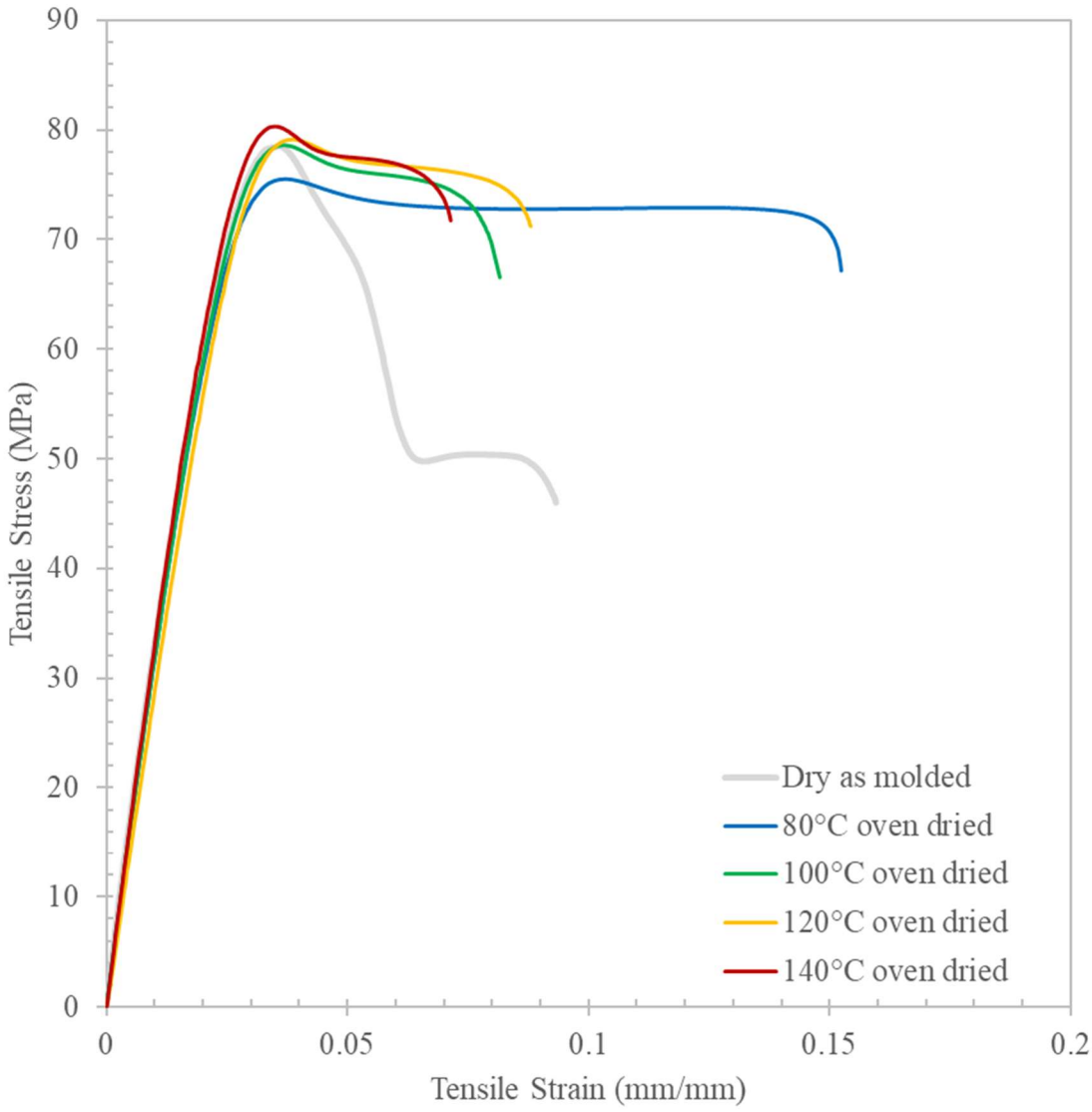

Figure 4.12: PA6 Tensile Stress-Strain DAM vs Dried from Conditioned

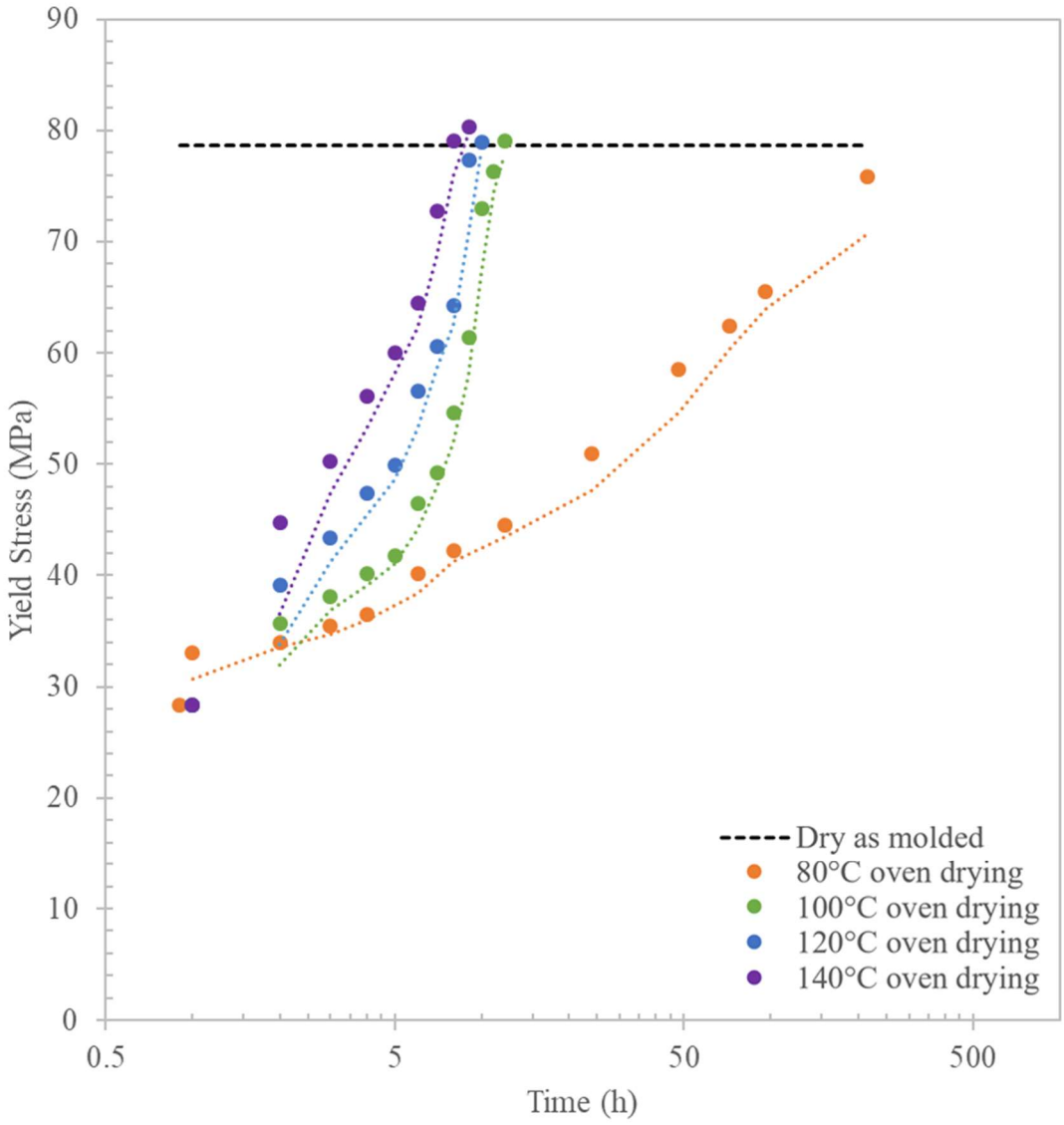

Figure 4.13: PA6 Tensile Yield Stress Dried from Conditioned

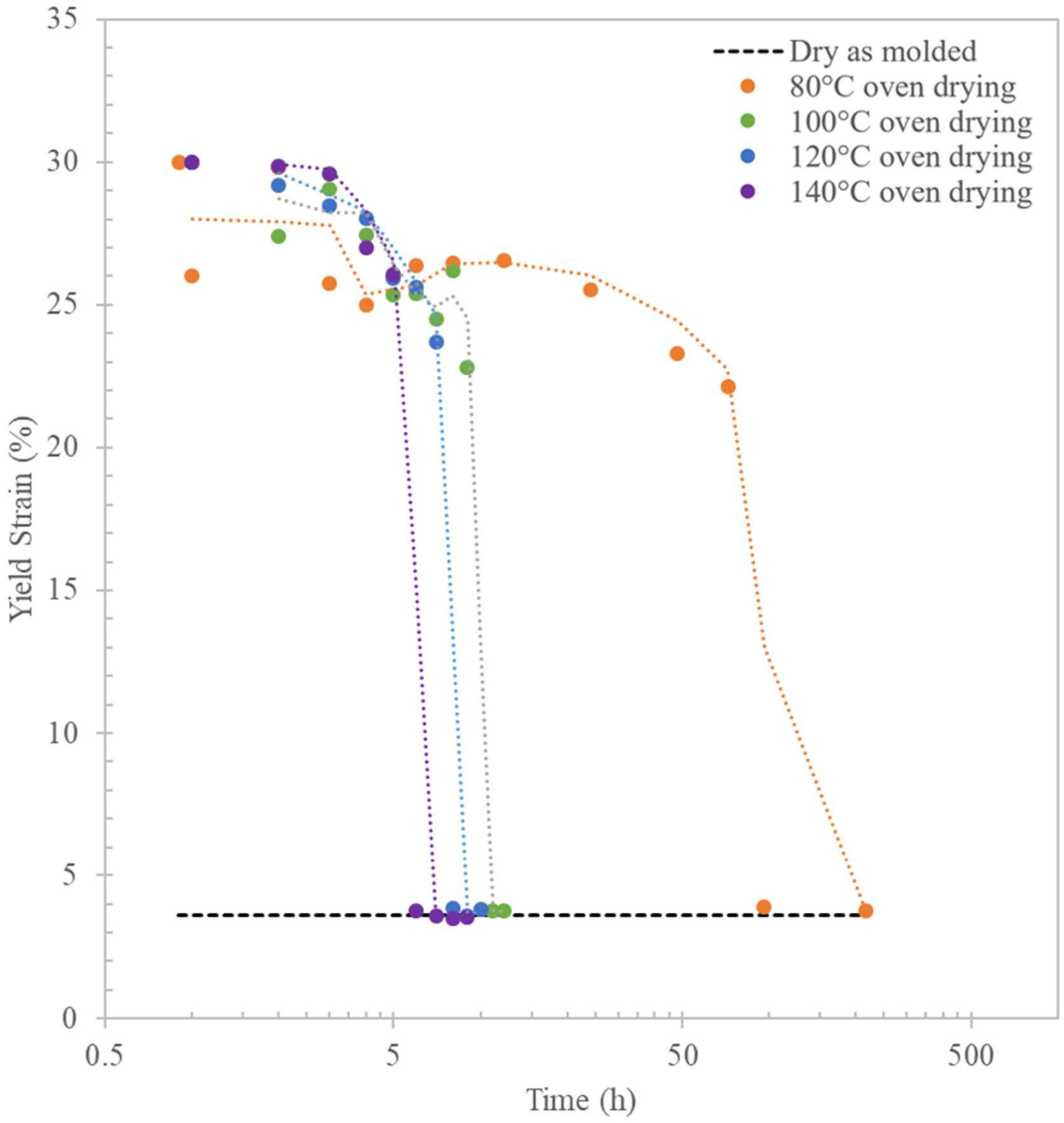

Figure 4.14: PA6 Tensile Yield Strain Dried from Conditioned

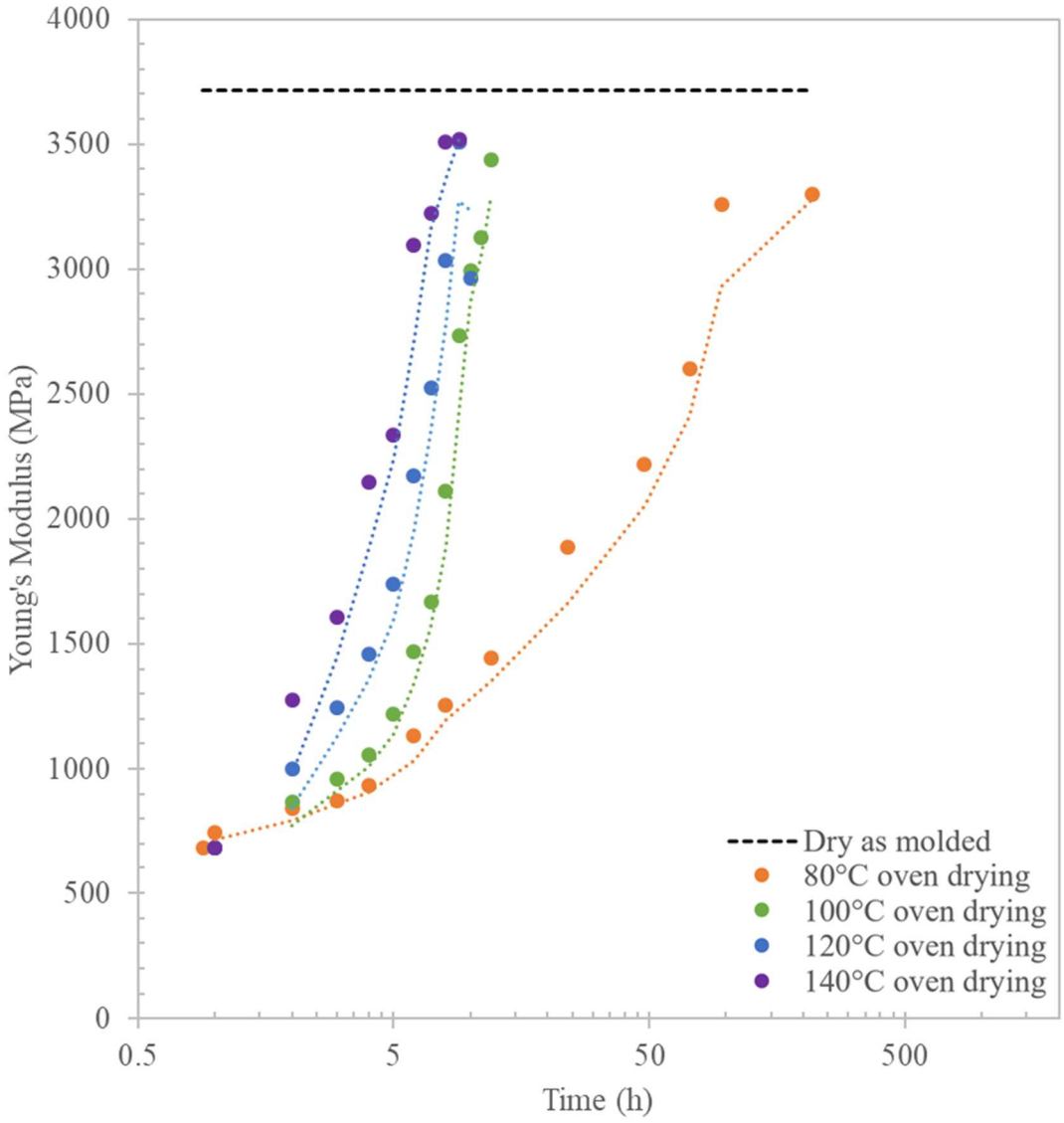

Figure 4.15: PA6 Young's Modulus Dried from Conditioned

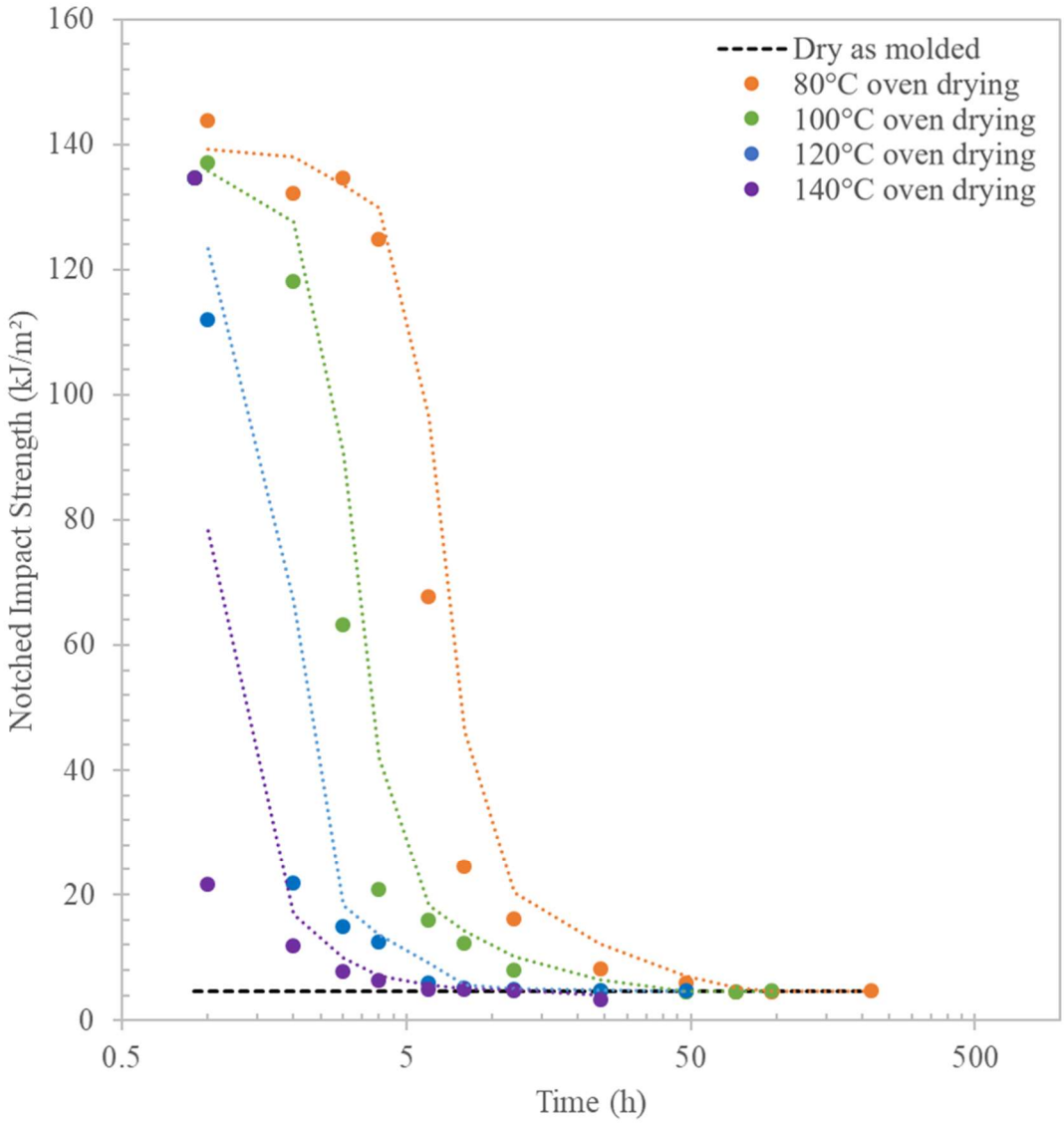

Figure 4.16: PA6 Charpy Impact Dried from Conditioned

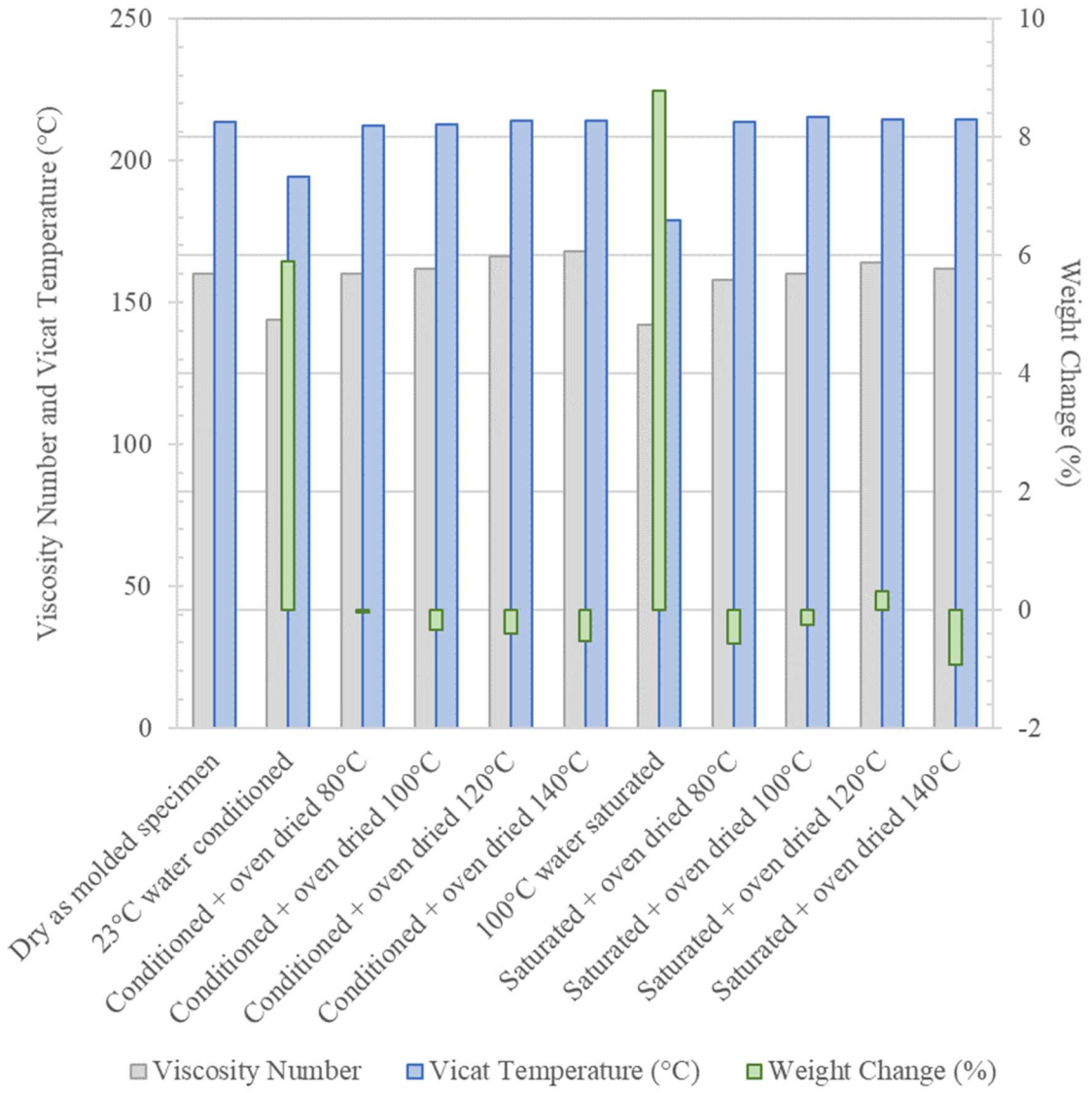

Figure 4.17: PA6 Viscosity Number and Vicat Temperature

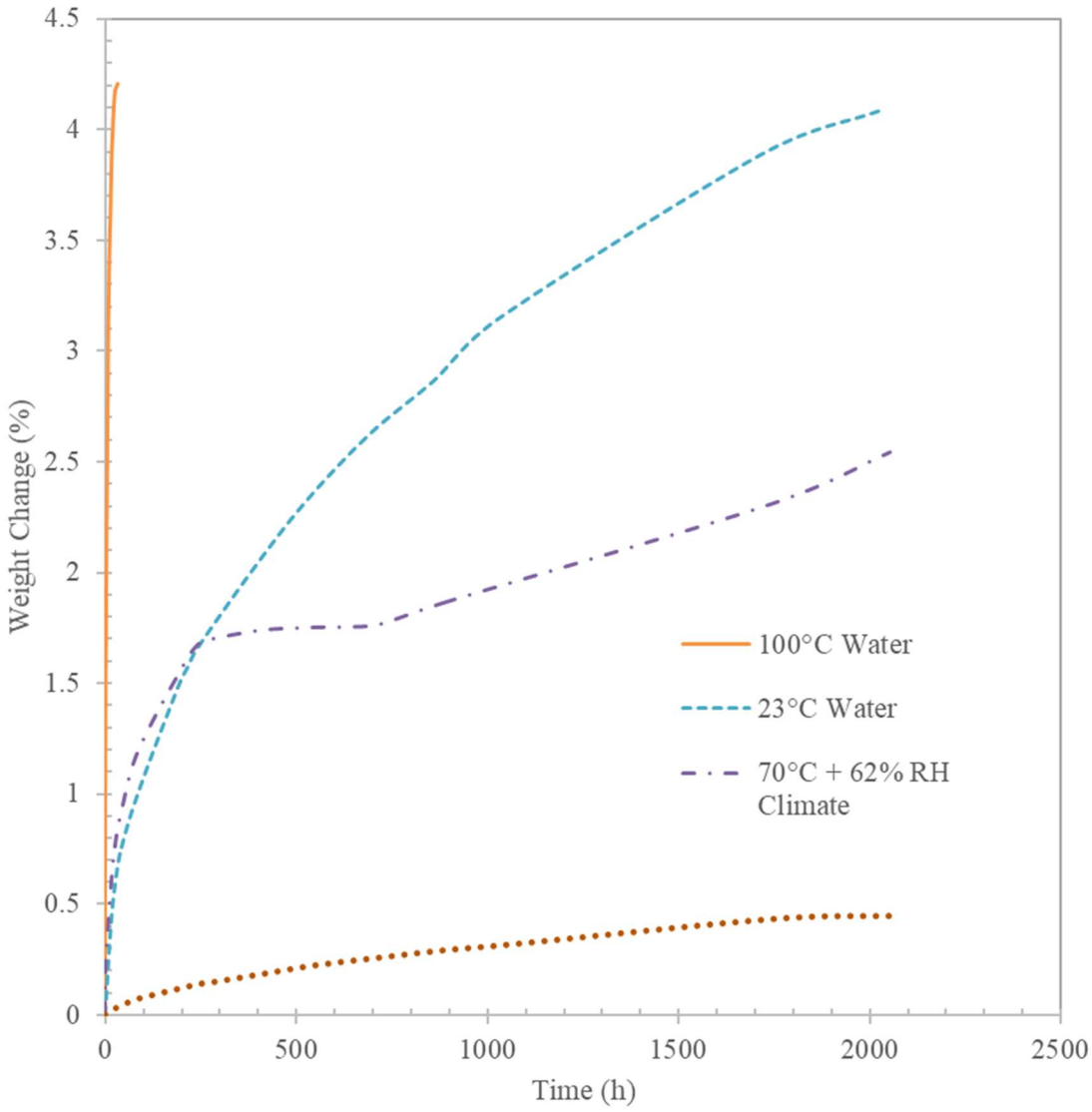

Figure 4.18: 50% GF Reinforced PA6 Absorption Comparison

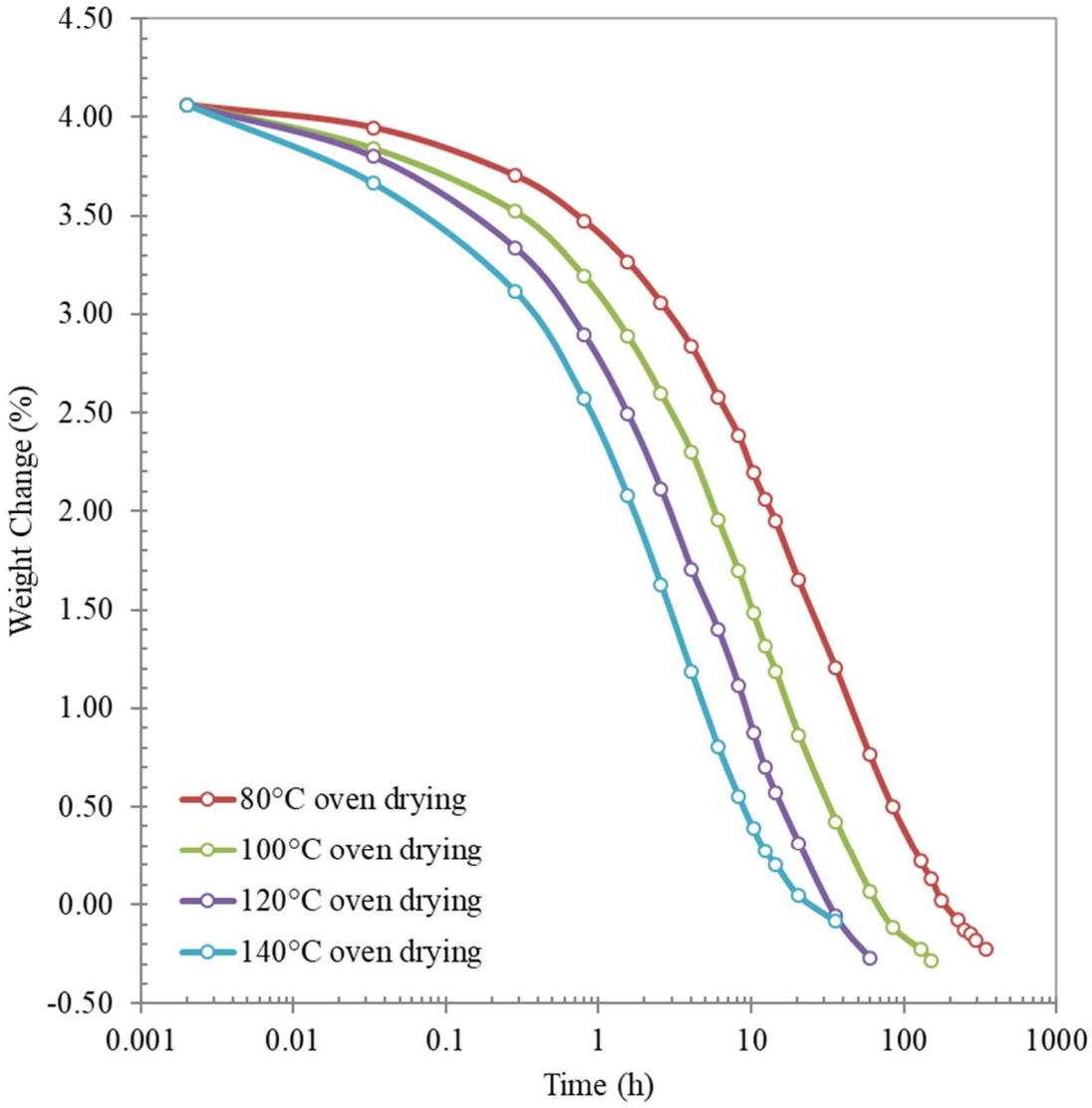

Figure 4.19: Desorption of Saturated 50% GF PA6 Samples

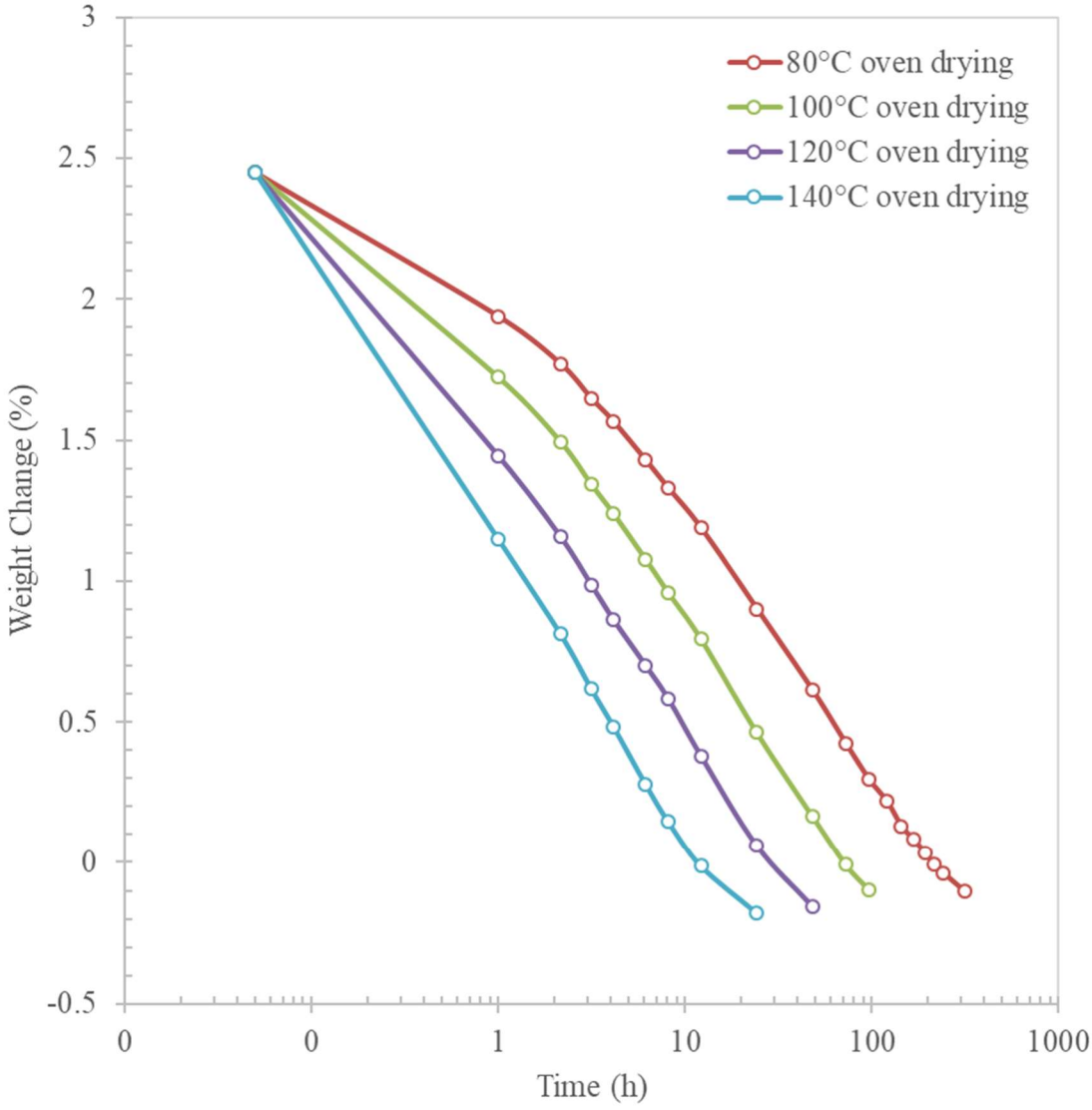

Figure 4.20: Desorption of Conditioned 50% GF PA6 Samples

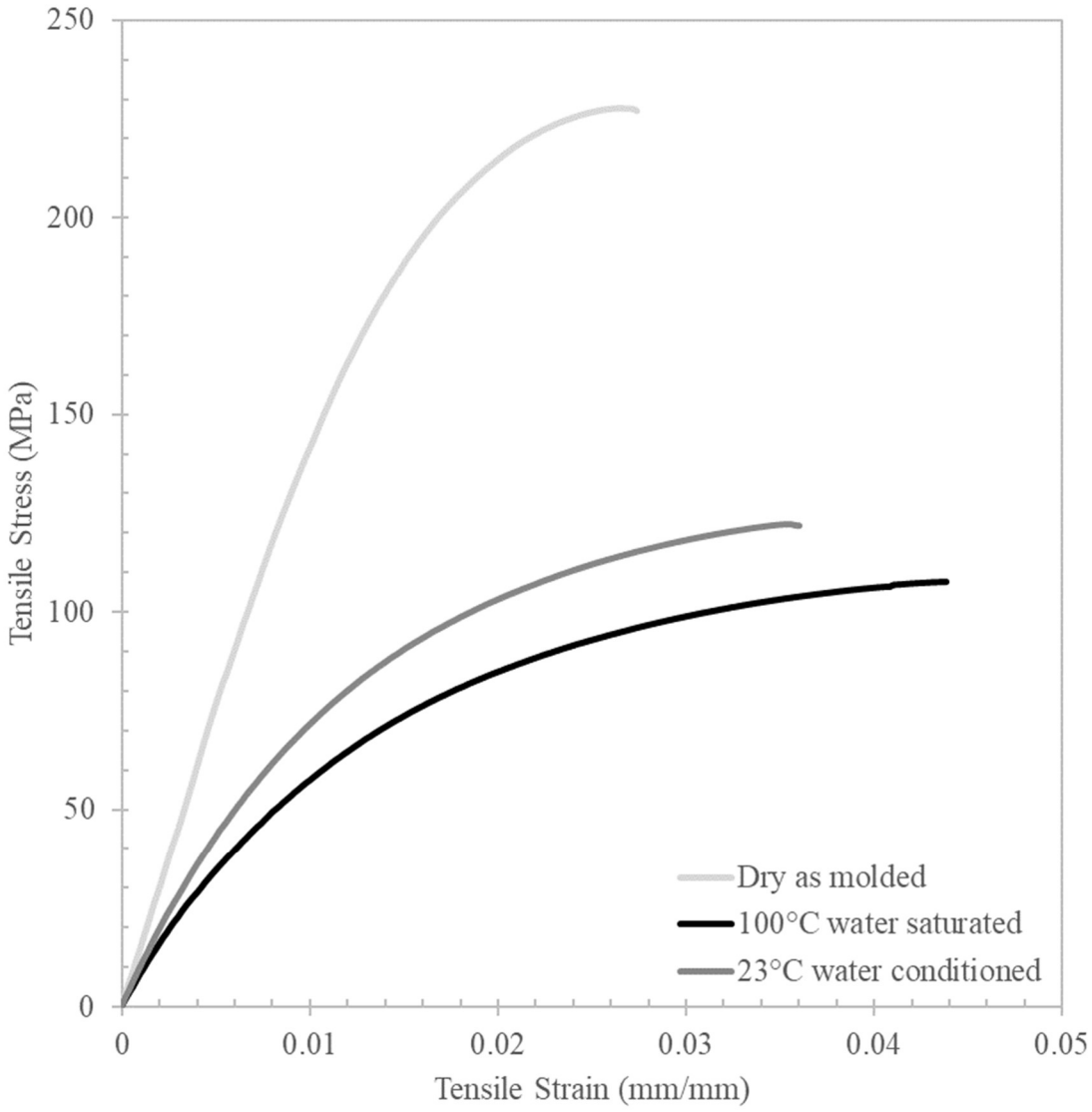

Figure 4.21: 50% GF PA6 Tensile Stress-Strain DAM vs Water Samples

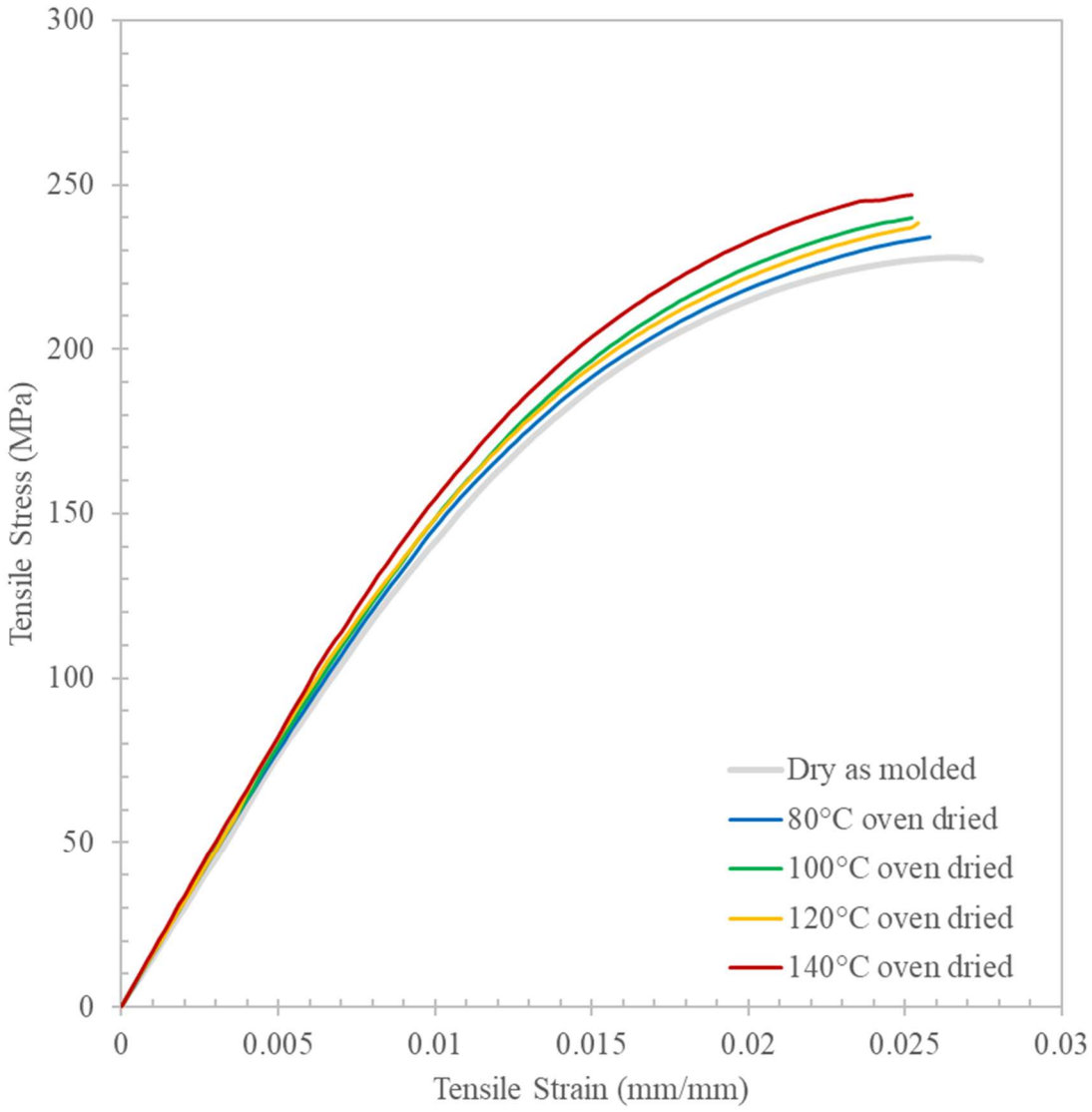

Figure 4.22: 50% GF PA6 Tensile Stress-Strain DAM vs Dried from Saturated

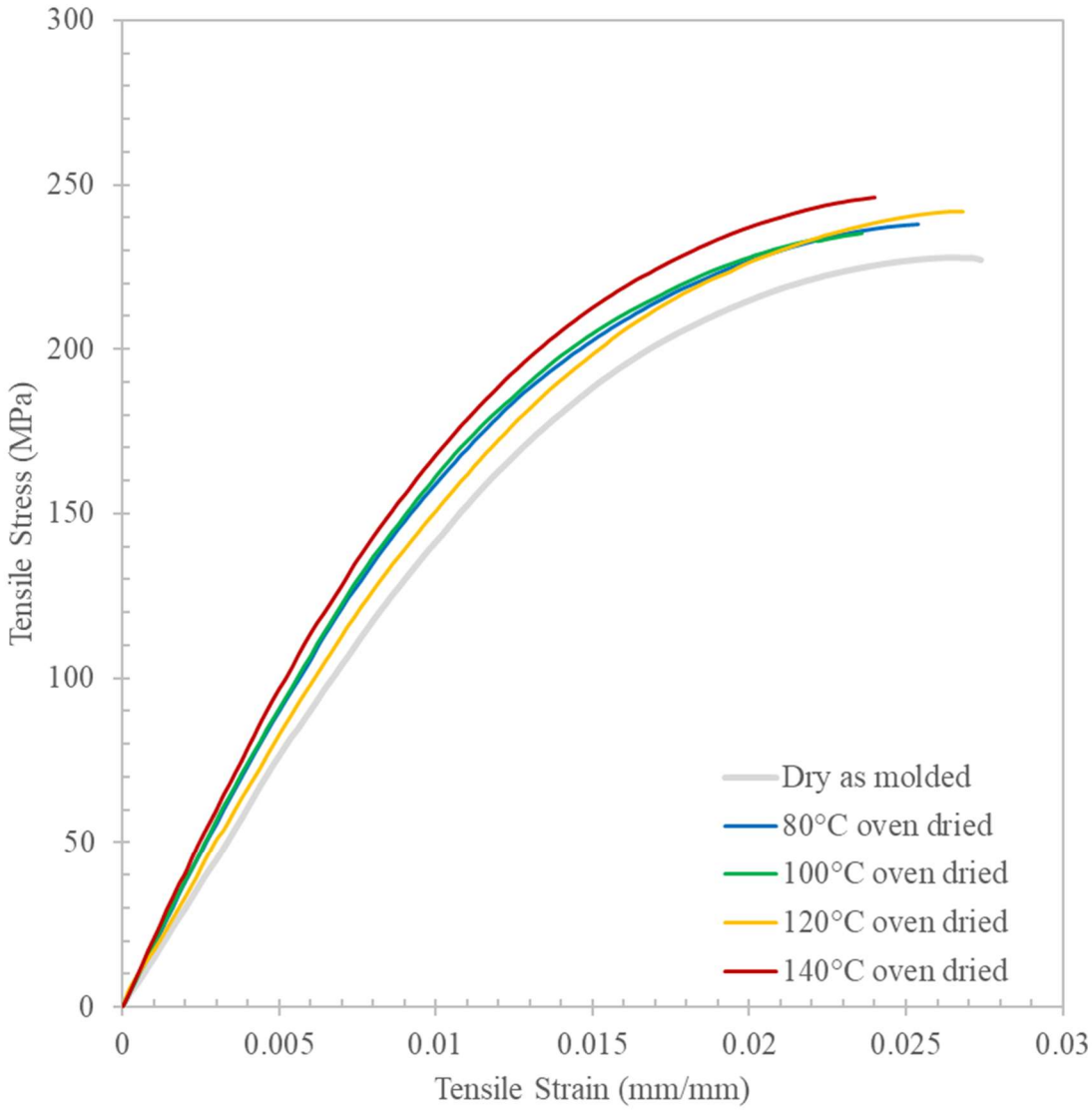

Figure 4.23: 50% GF PA6 Tensile Stress-Strain DAM vs Dried from Conditioned

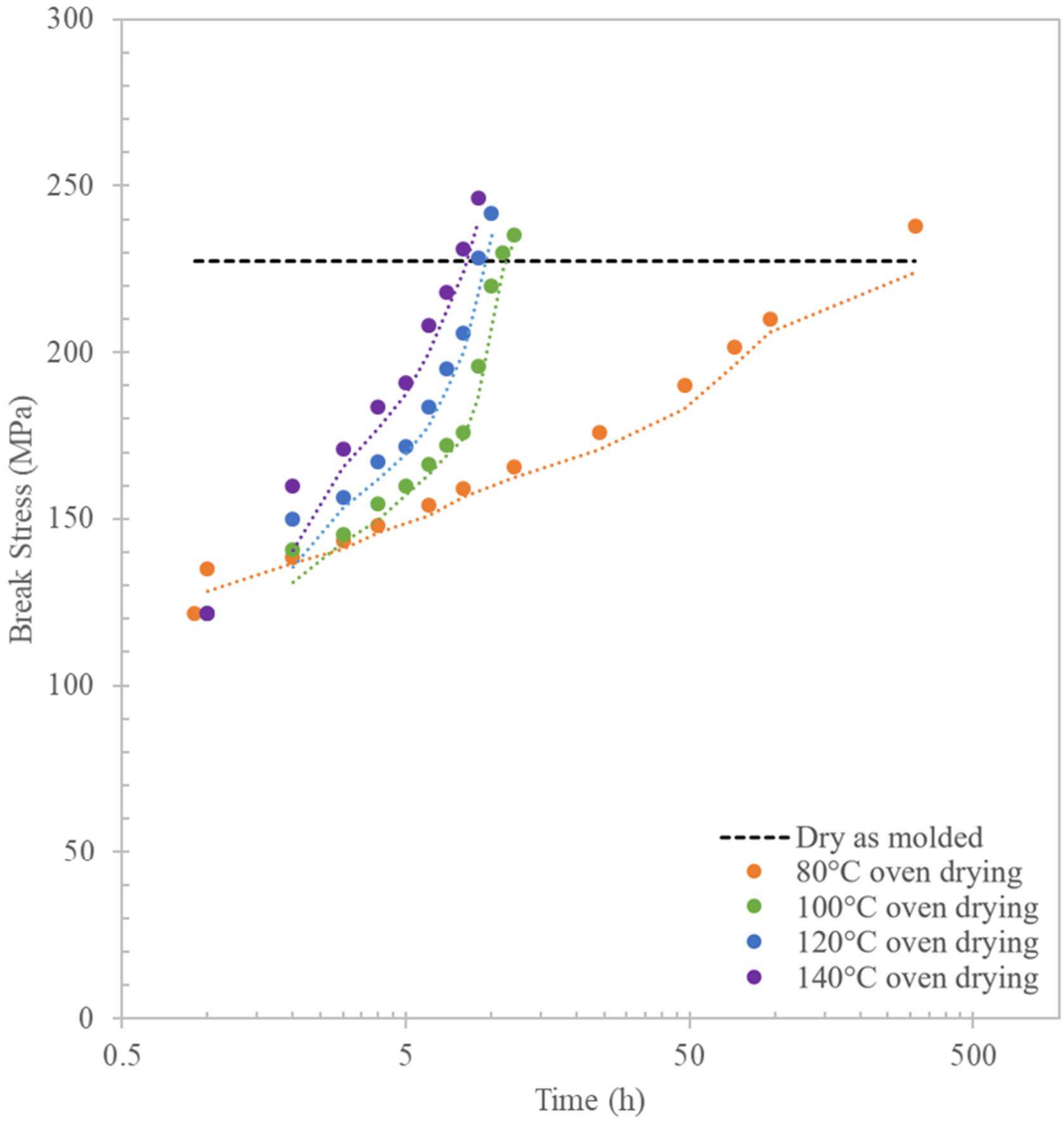

Figure 4.24: 50% GF PA6 Tensile Break Stress Dried from Conditioned

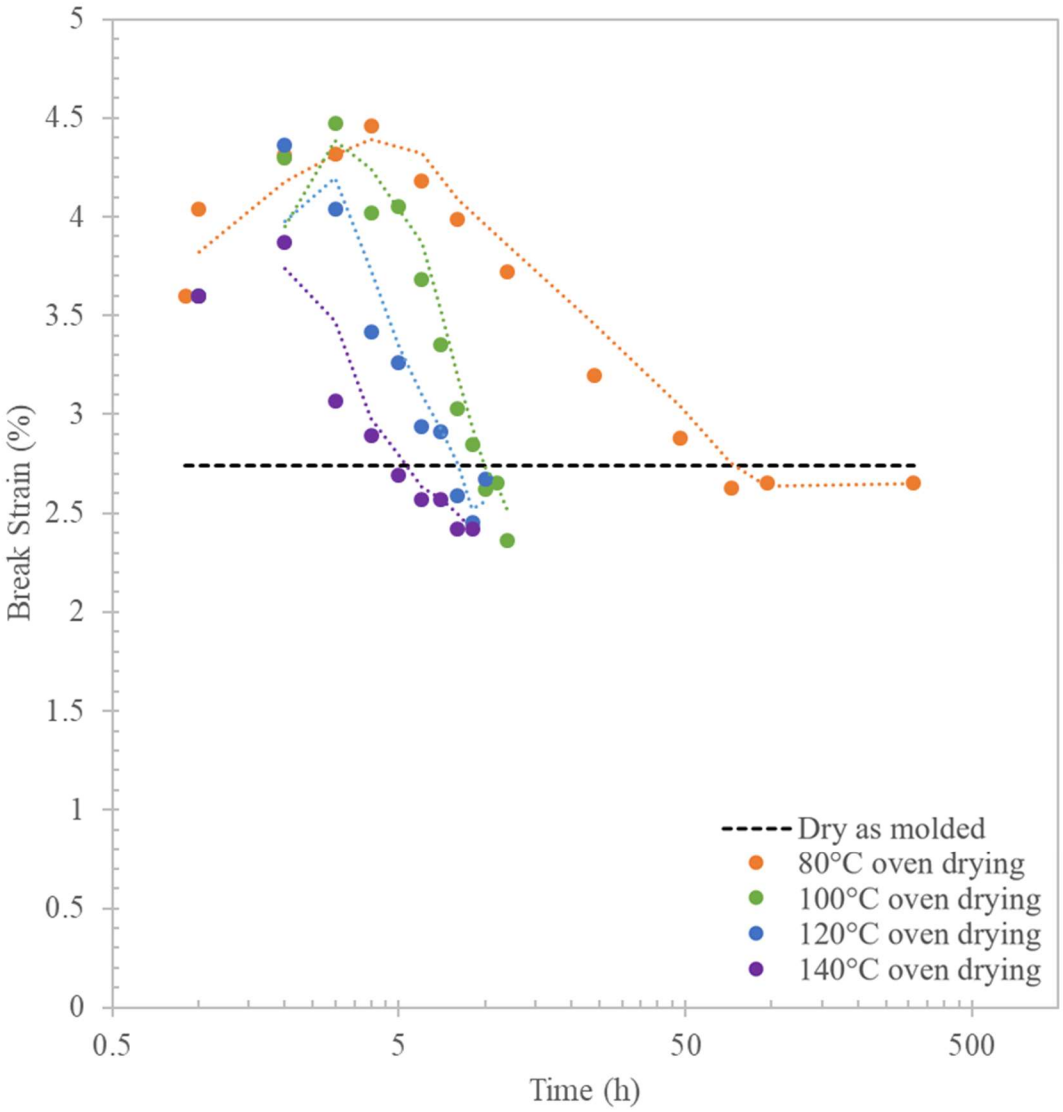

Figure 4.25: 50% GF PA6 Tensile Break Strain Dried from Conditioned

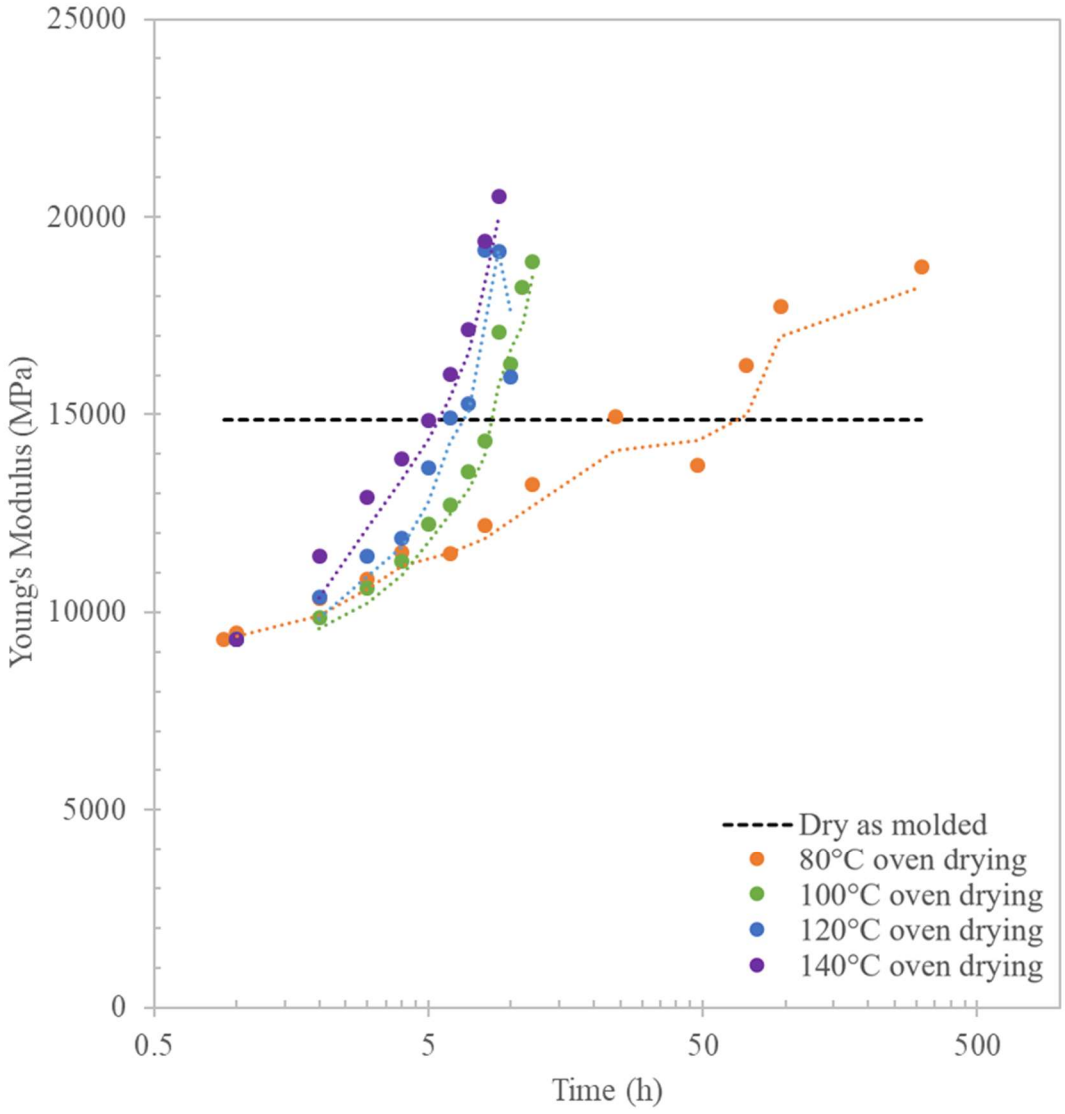

Figure 4.26: 50% GF PA6 Young's Modulus Dried from Conditioned

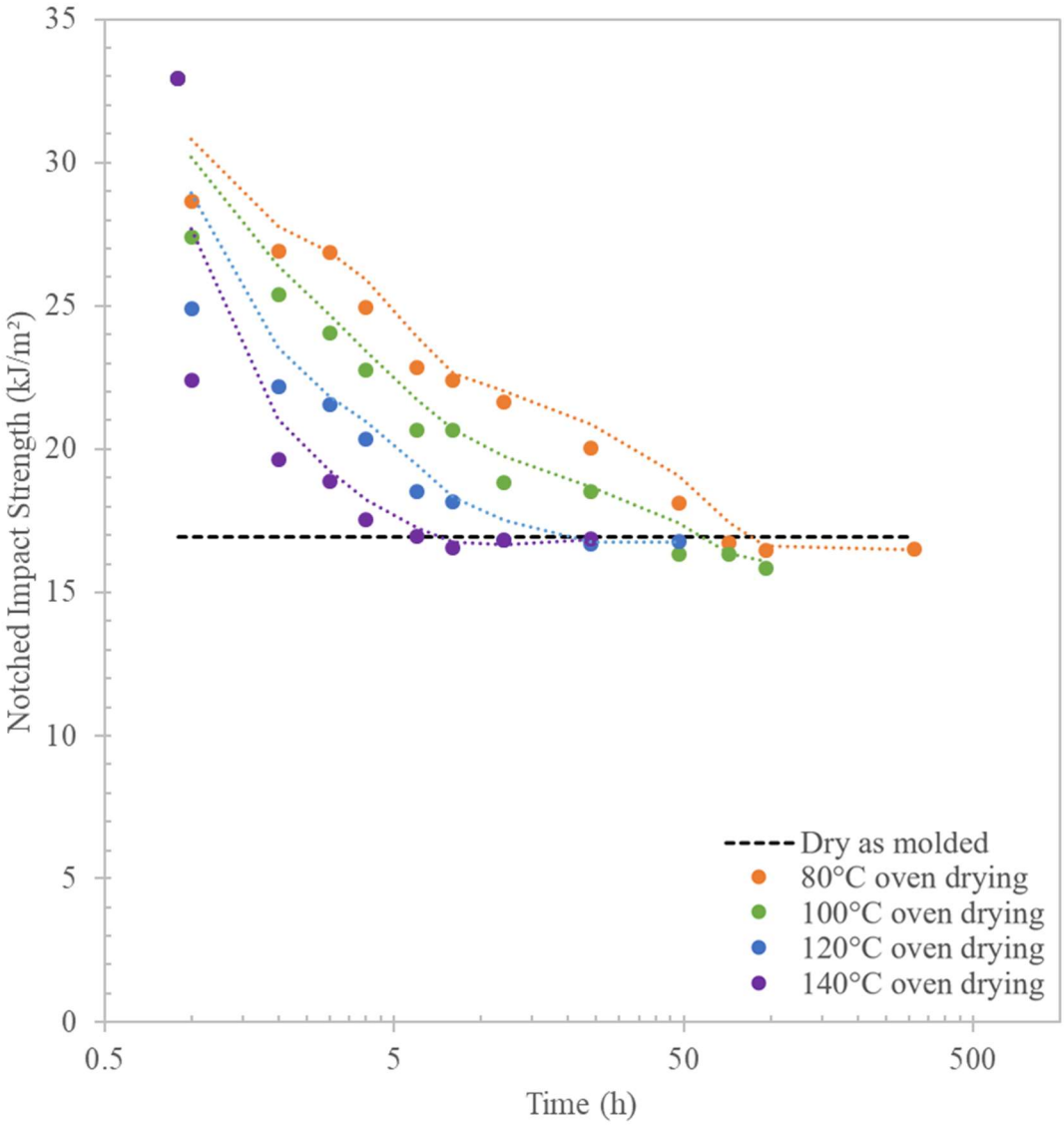

Figure 4.27: 50% GF PA6 Charpy Impact Dried from Conditioned

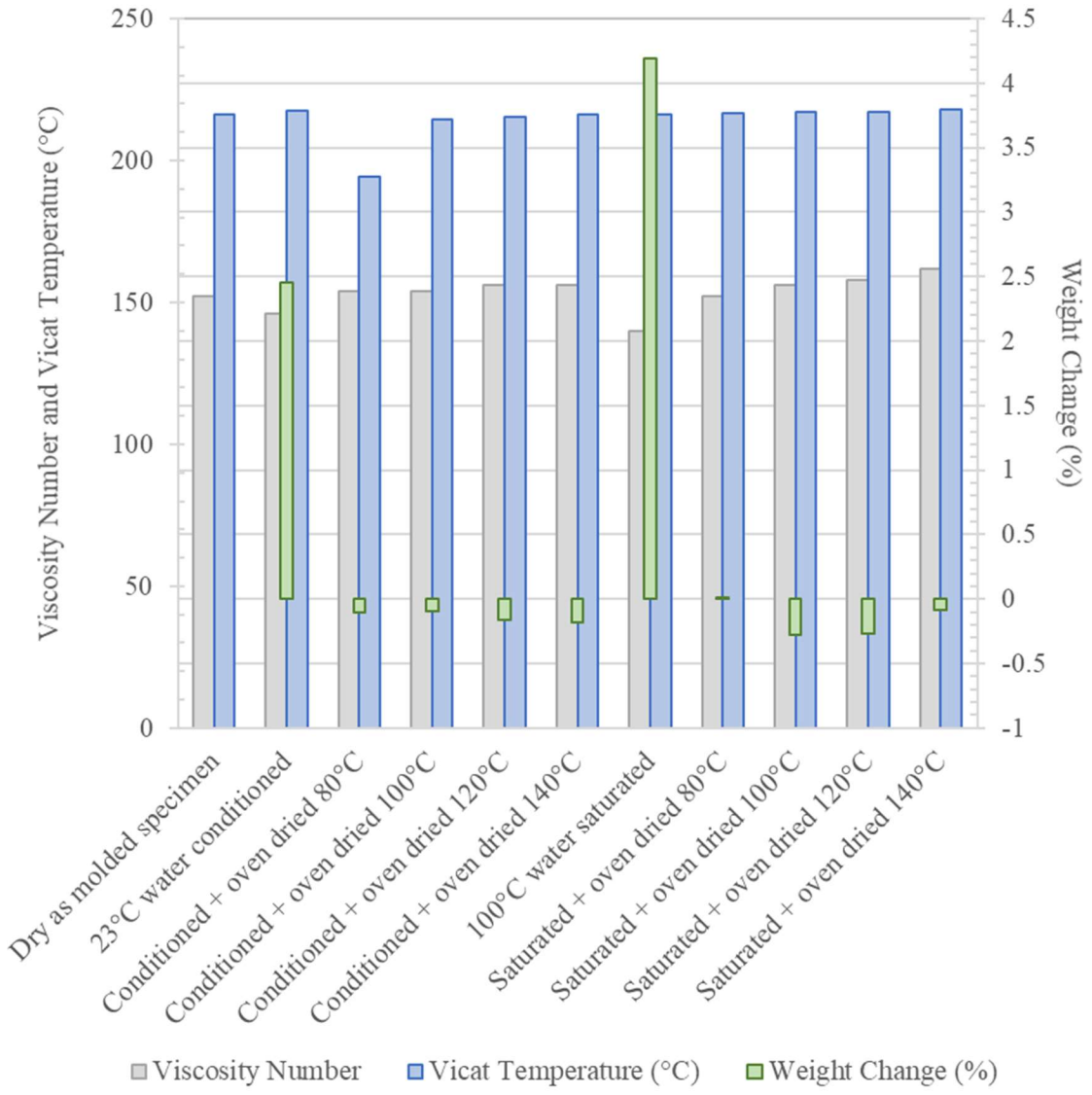

Figure 4.28: 50% GF PA6 Viscosity Number and Vicat Temperature

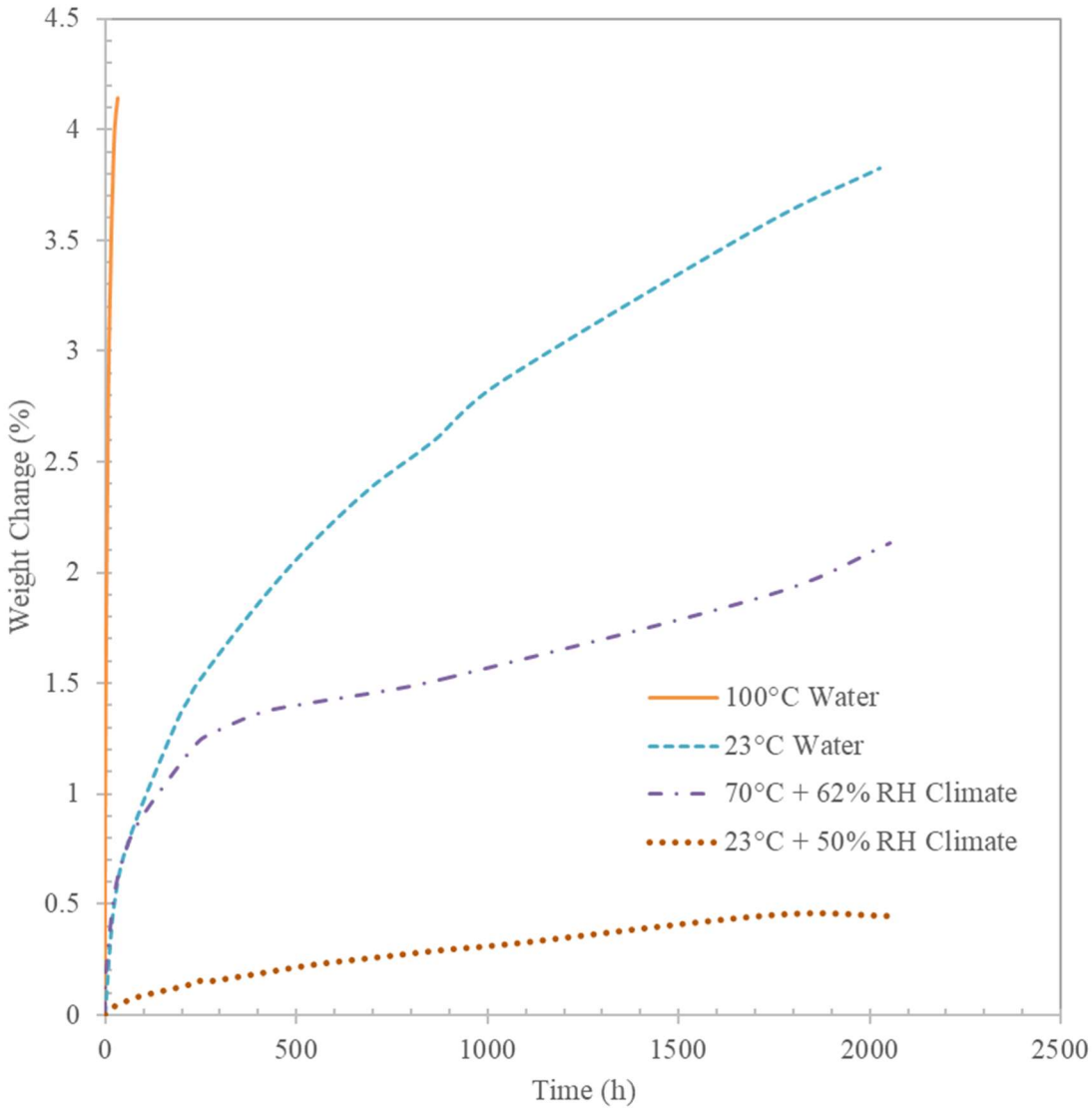

Figure 4.29: 50% GF Reinforced PA66+PA6 Absorption Comparison

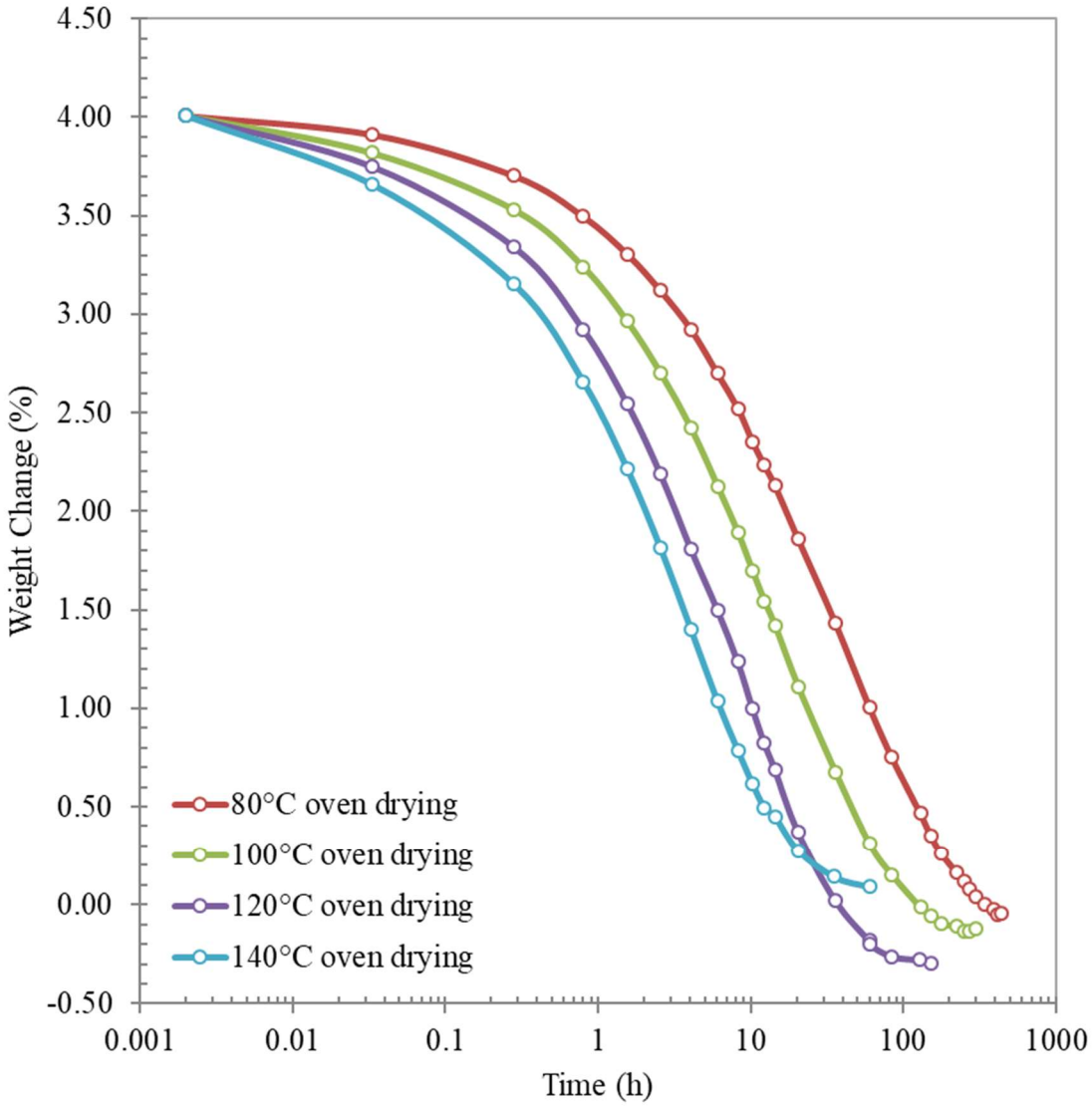

Figure 4.30: Desorption of Saturated 50% GF PA66+PA6 Samples

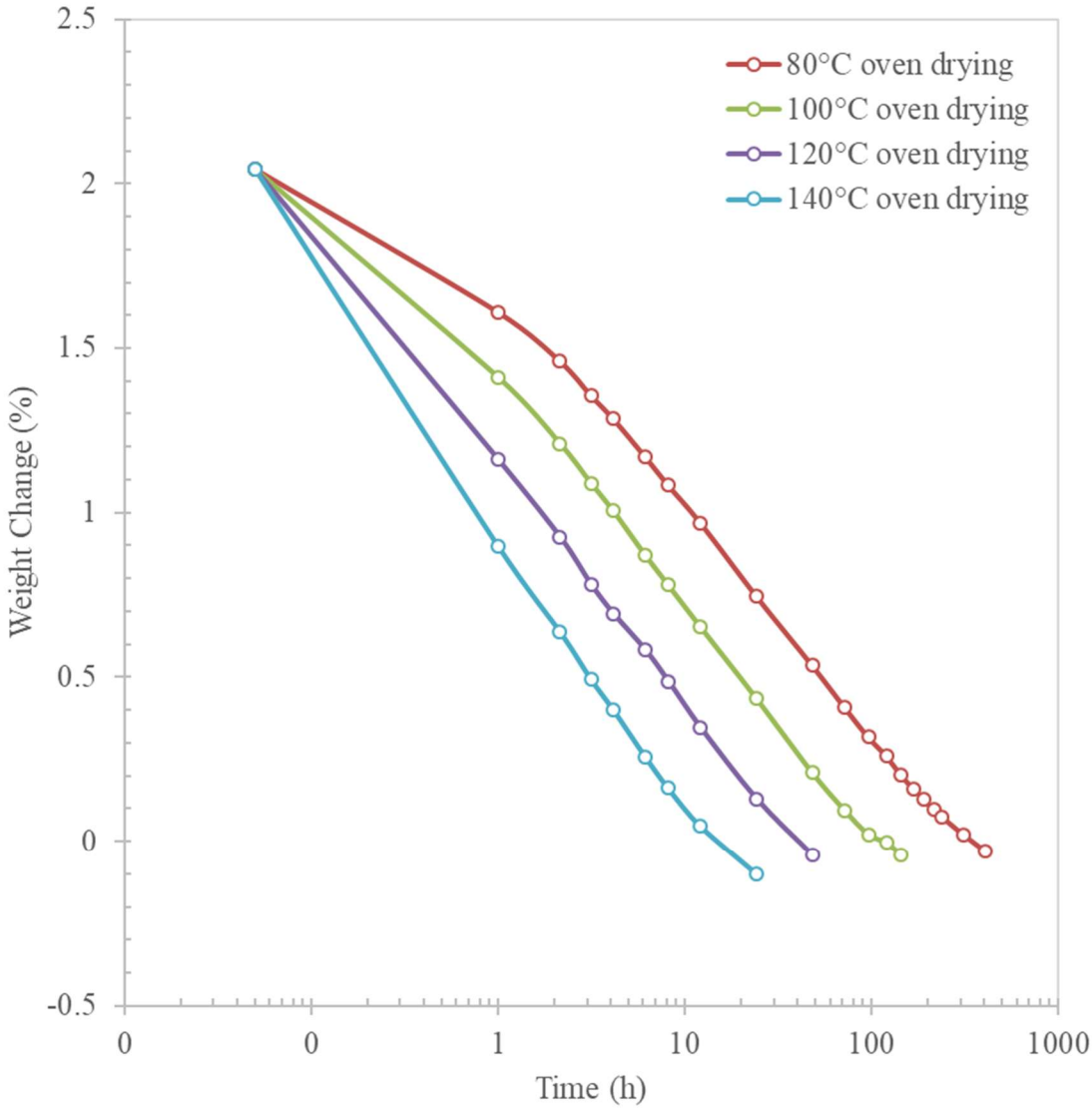

Figure 4.31: Desorption of Conditioned 50% GF PA66+PA6 Samples

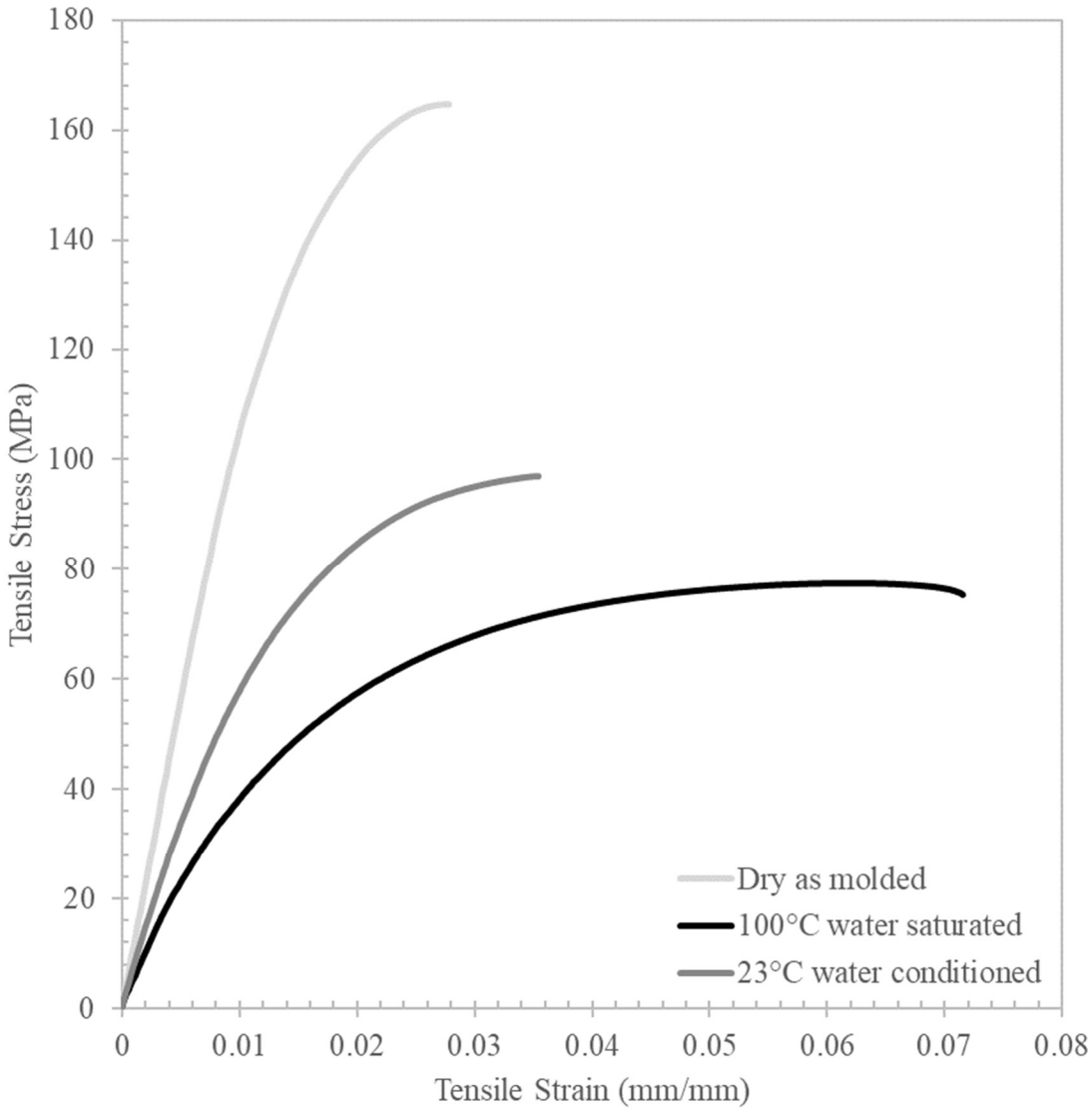

Figure 4.32: 50% GF PA66+PA6 Tensile Stress-Strain DAM vs Water Samples

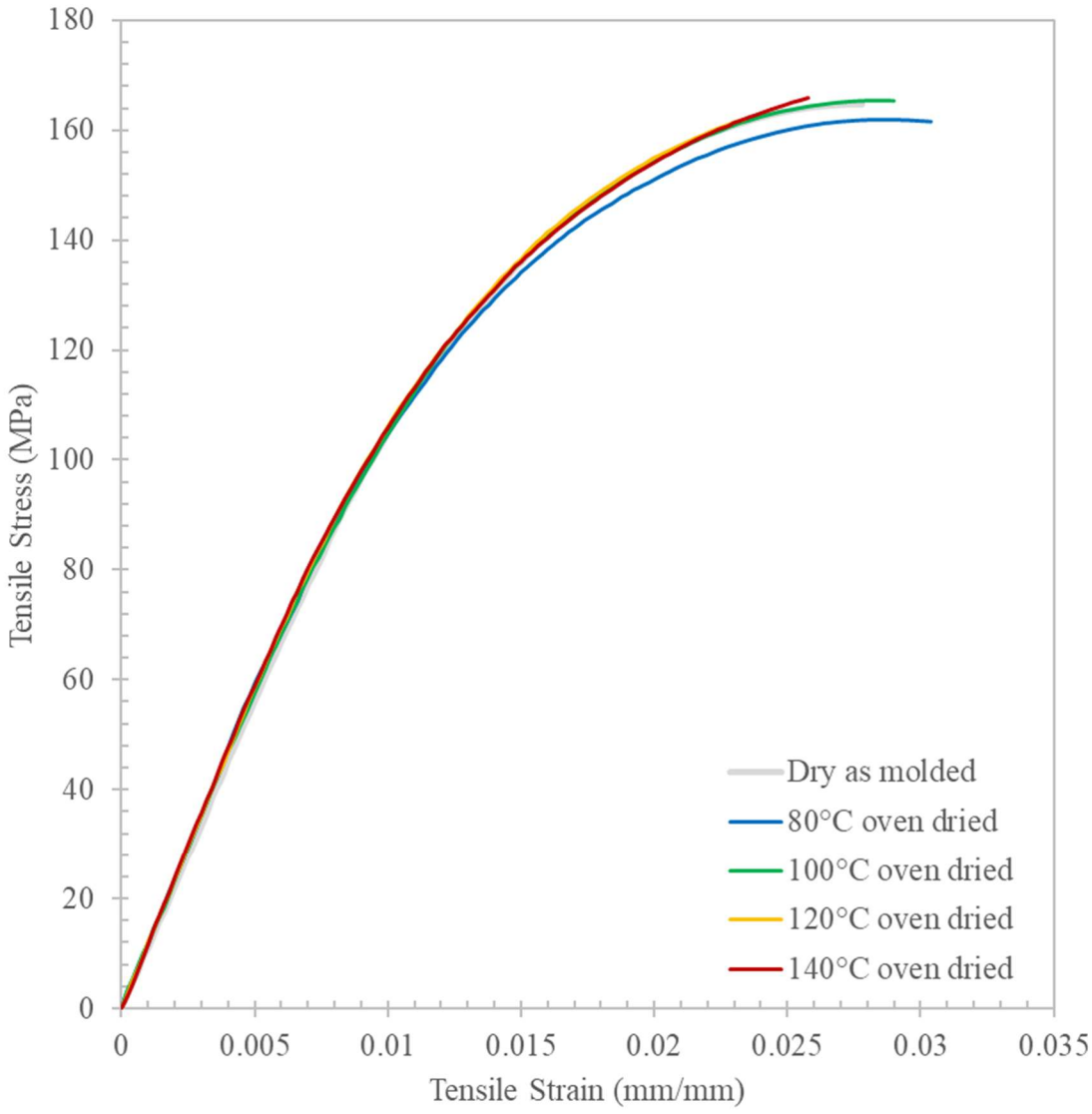

Figure 4.33: 50% GF PA66+PA6 Tensile Stress-Strain DAM vs Dried from Saturated

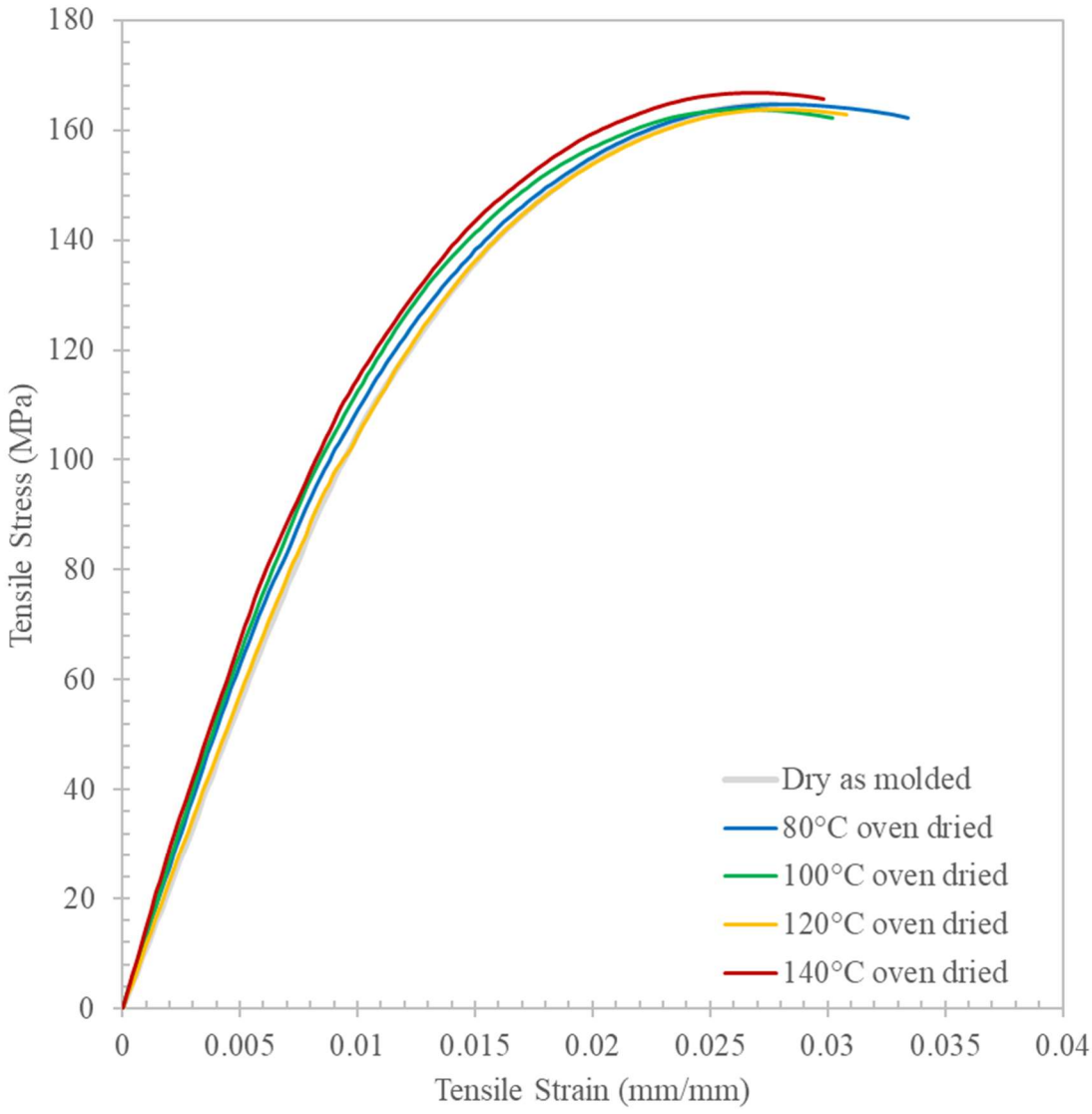

Figure 4.34: 50% GF PA66+PA6 Tensile Stress-Strain DAM vs Dried from Conditioned

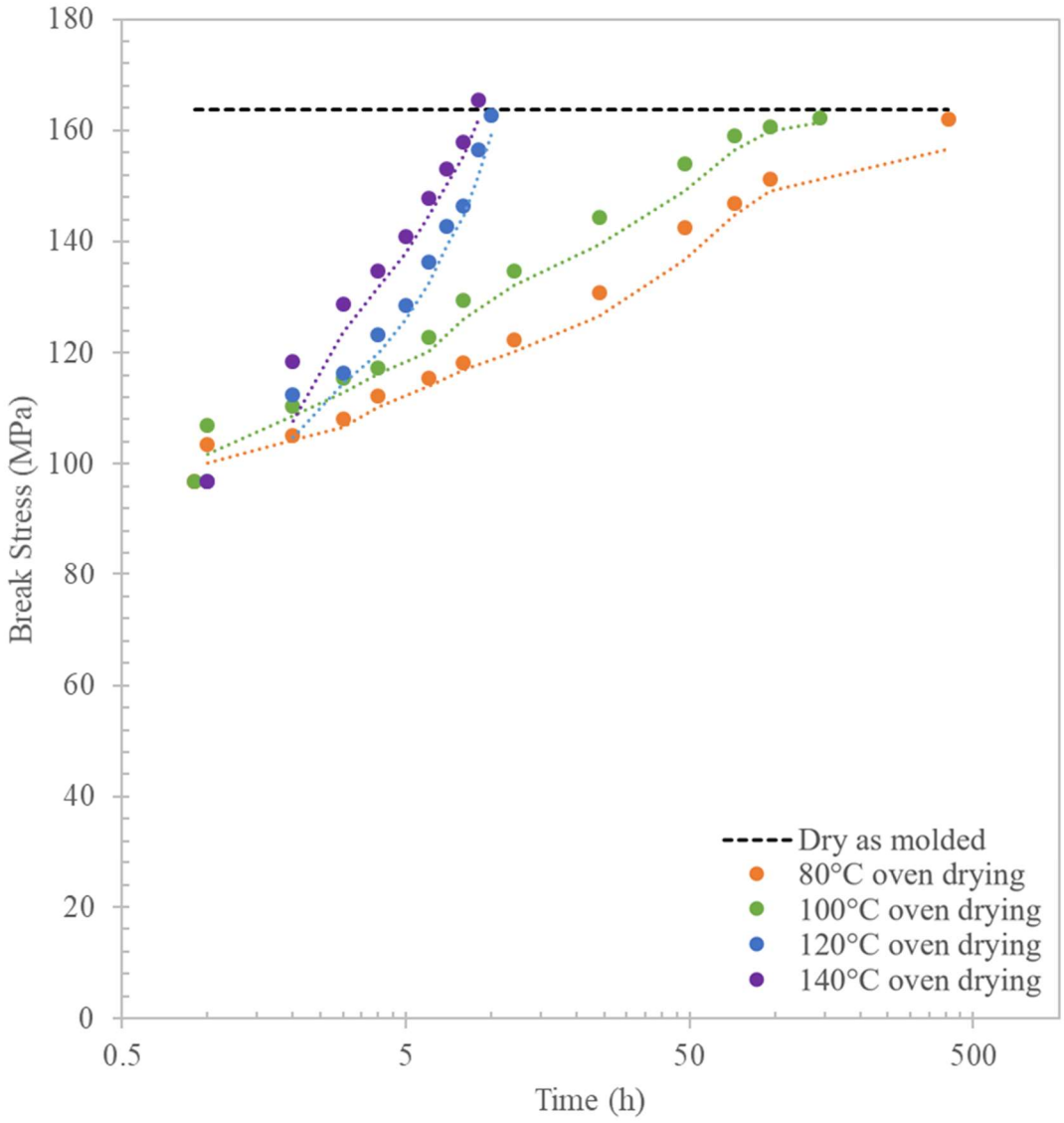

Figure 4.35: 50% GF PA66+PA6 Tensile Break Stress Dried from Conditioned

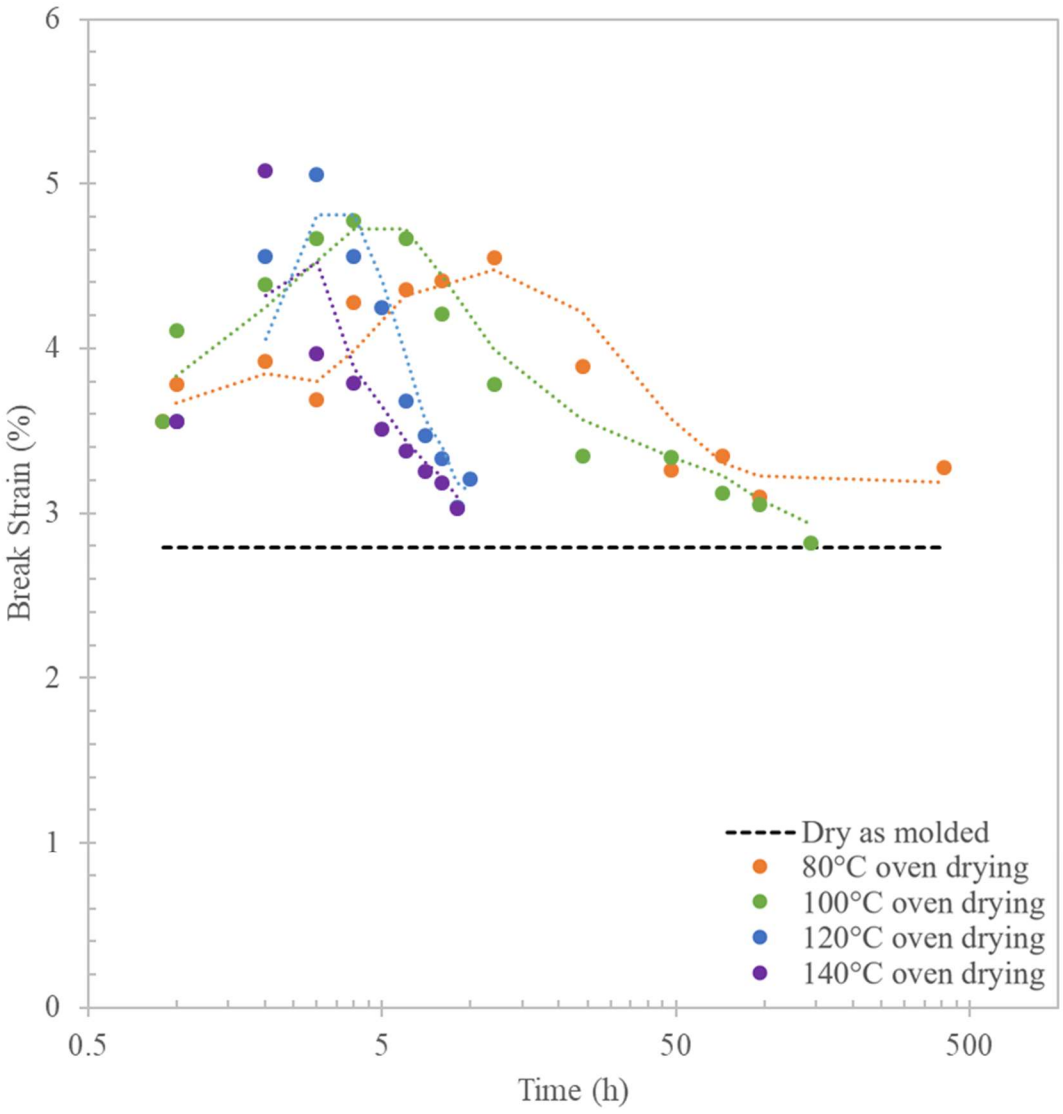

Figure 4.36: 50% GF PA66+PA6 Tensile Break Strain Dried from Conditioned

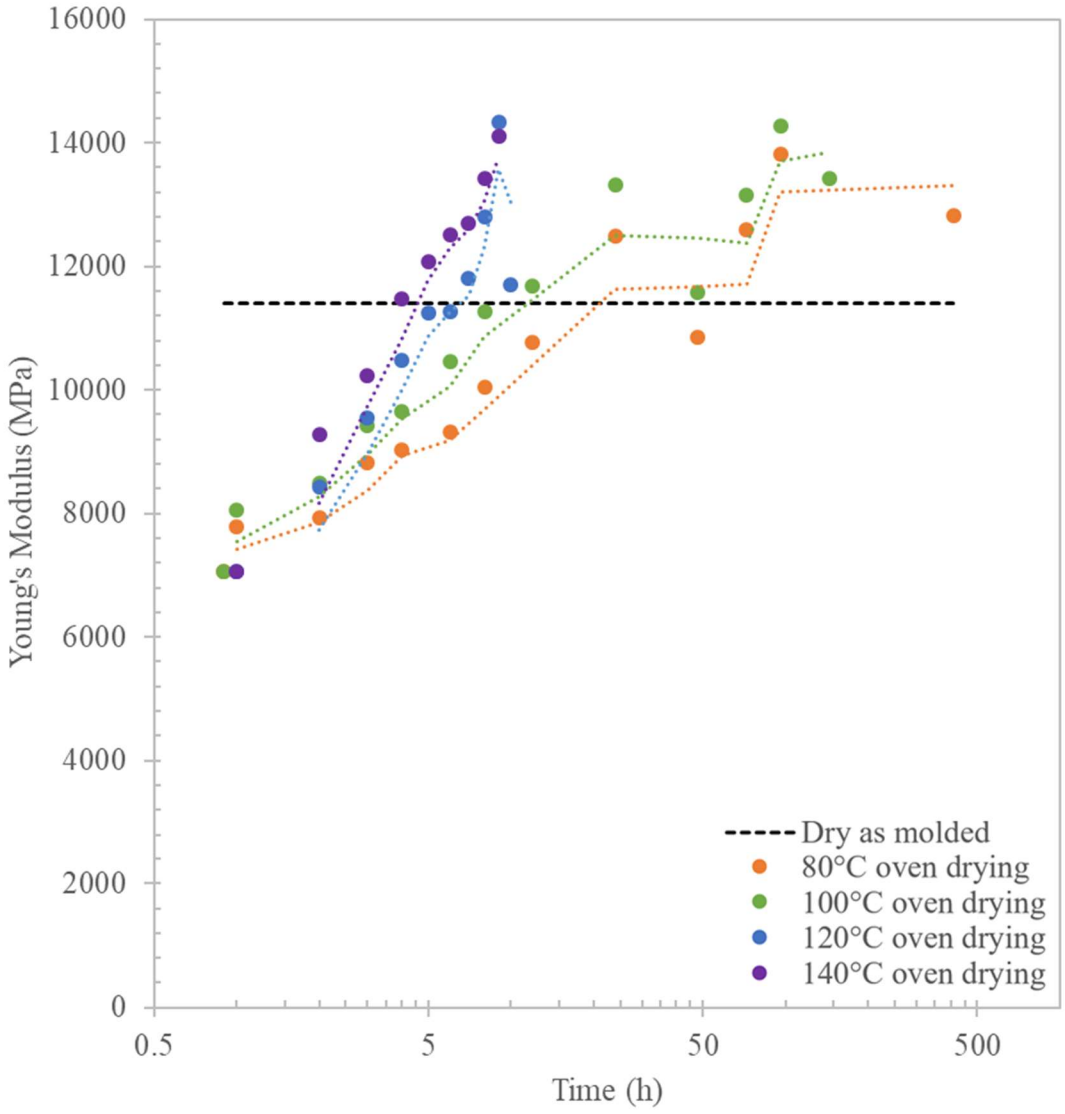

Figure 4.37: 50% GF PA66+PA6 Young's Modulus Dried from Conditioned

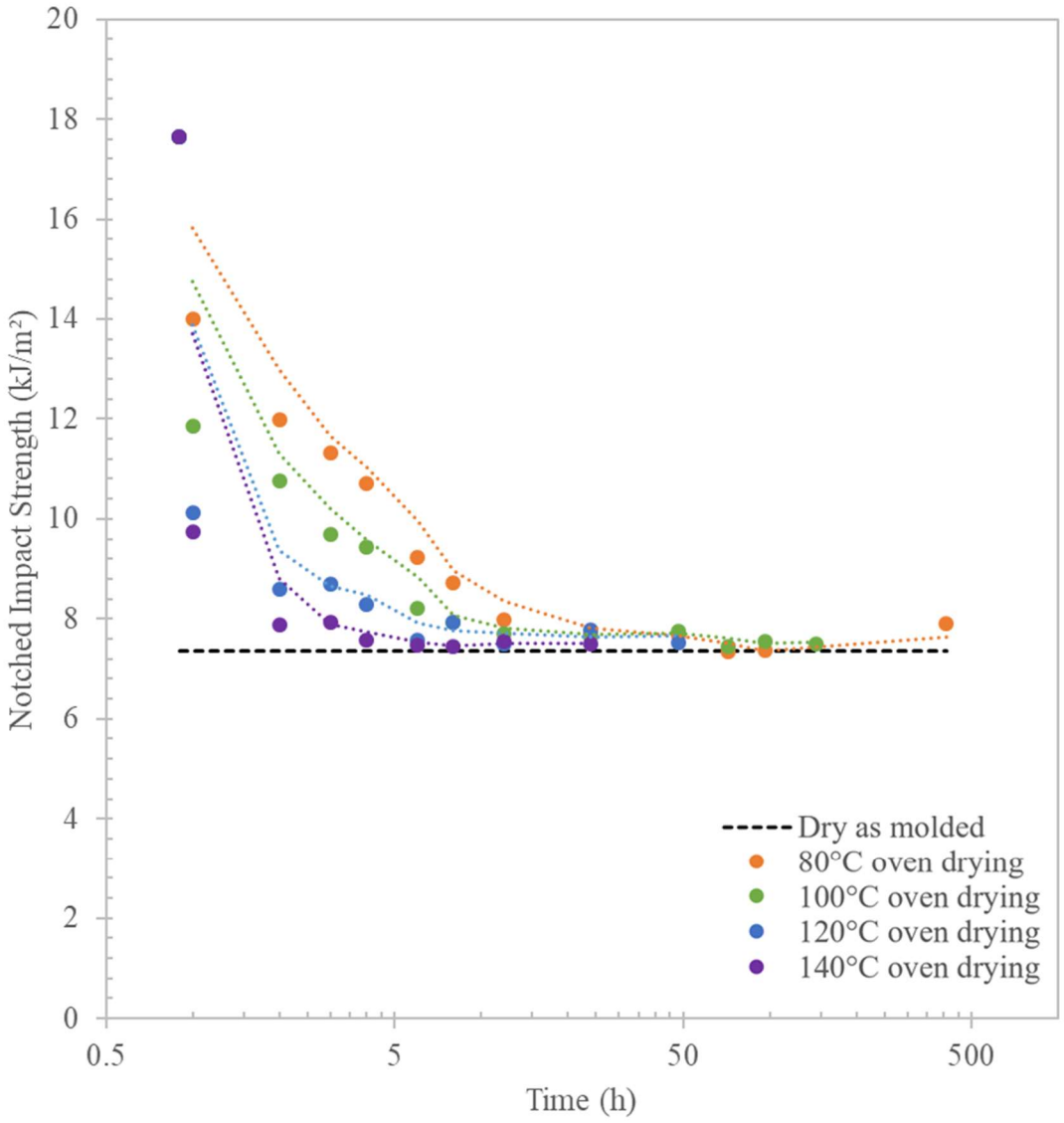

Figure 4.38: 50% GF PA66+PA6 Charpy Impact Dried from Conditioned

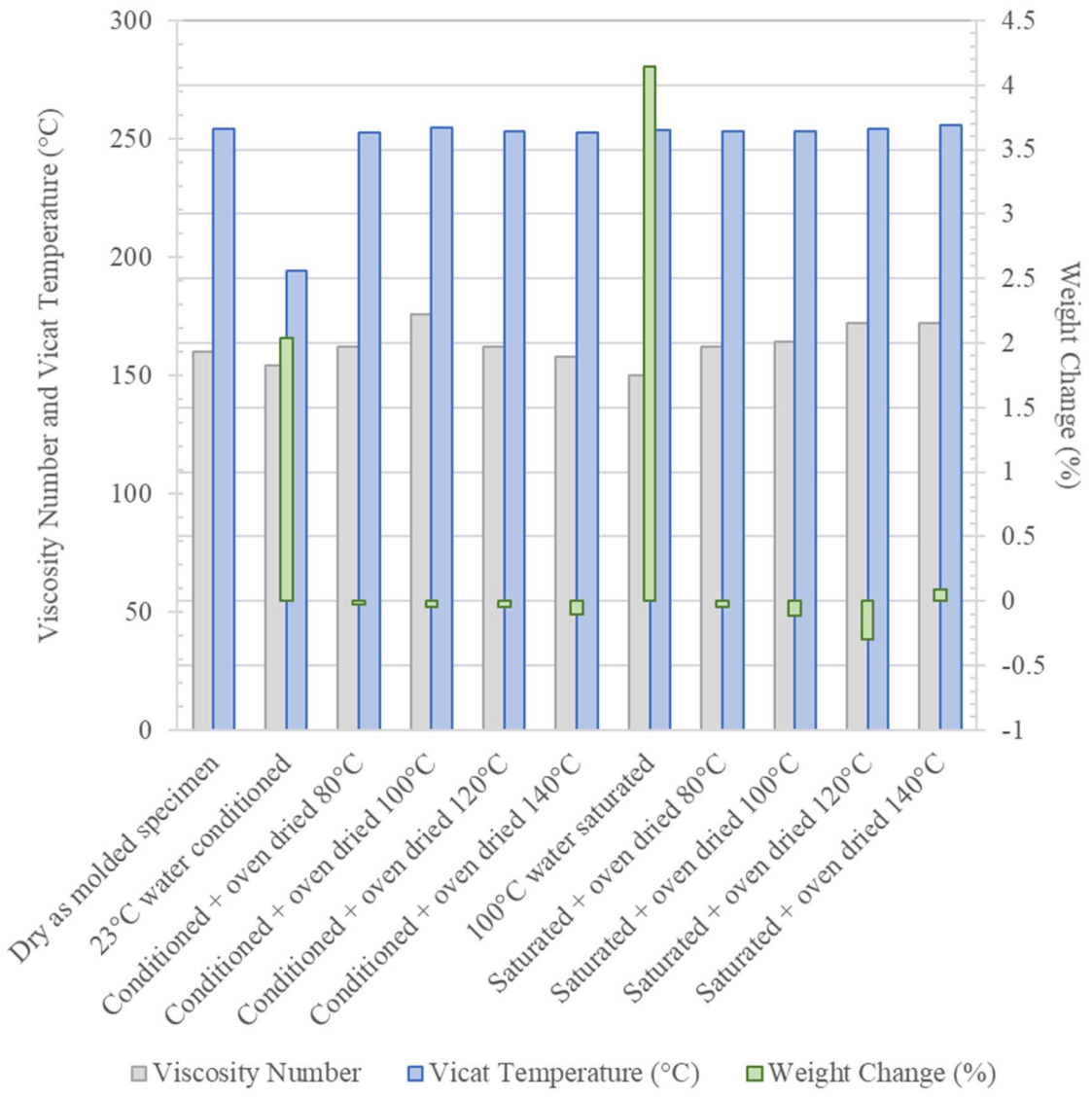

Figure 4.39: 50% GF PA66+PA6 Viscosity Number and Vicat Temperature

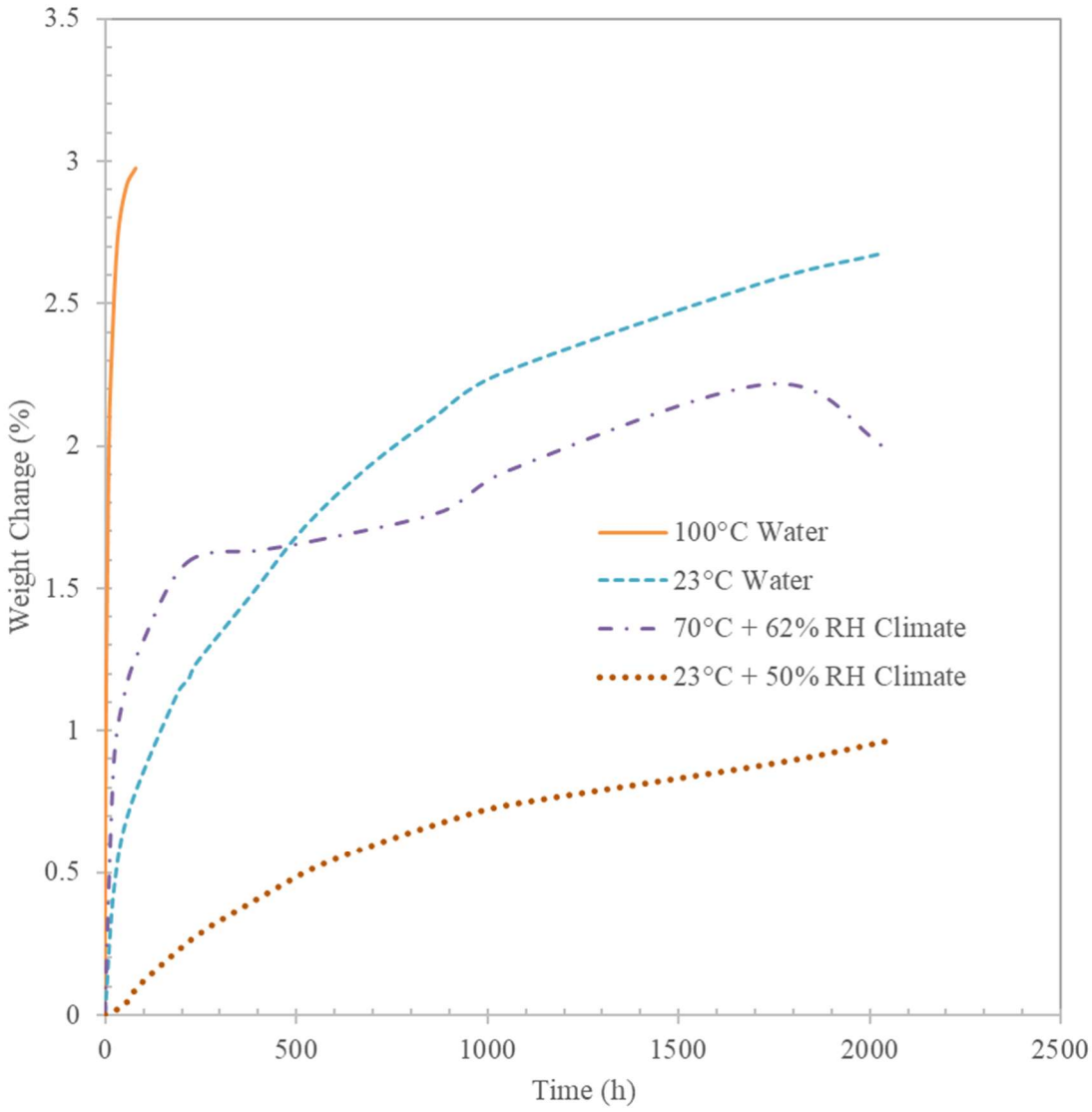

Figure 4.40: Unreinforced PA MACM12 Absorption Comparison

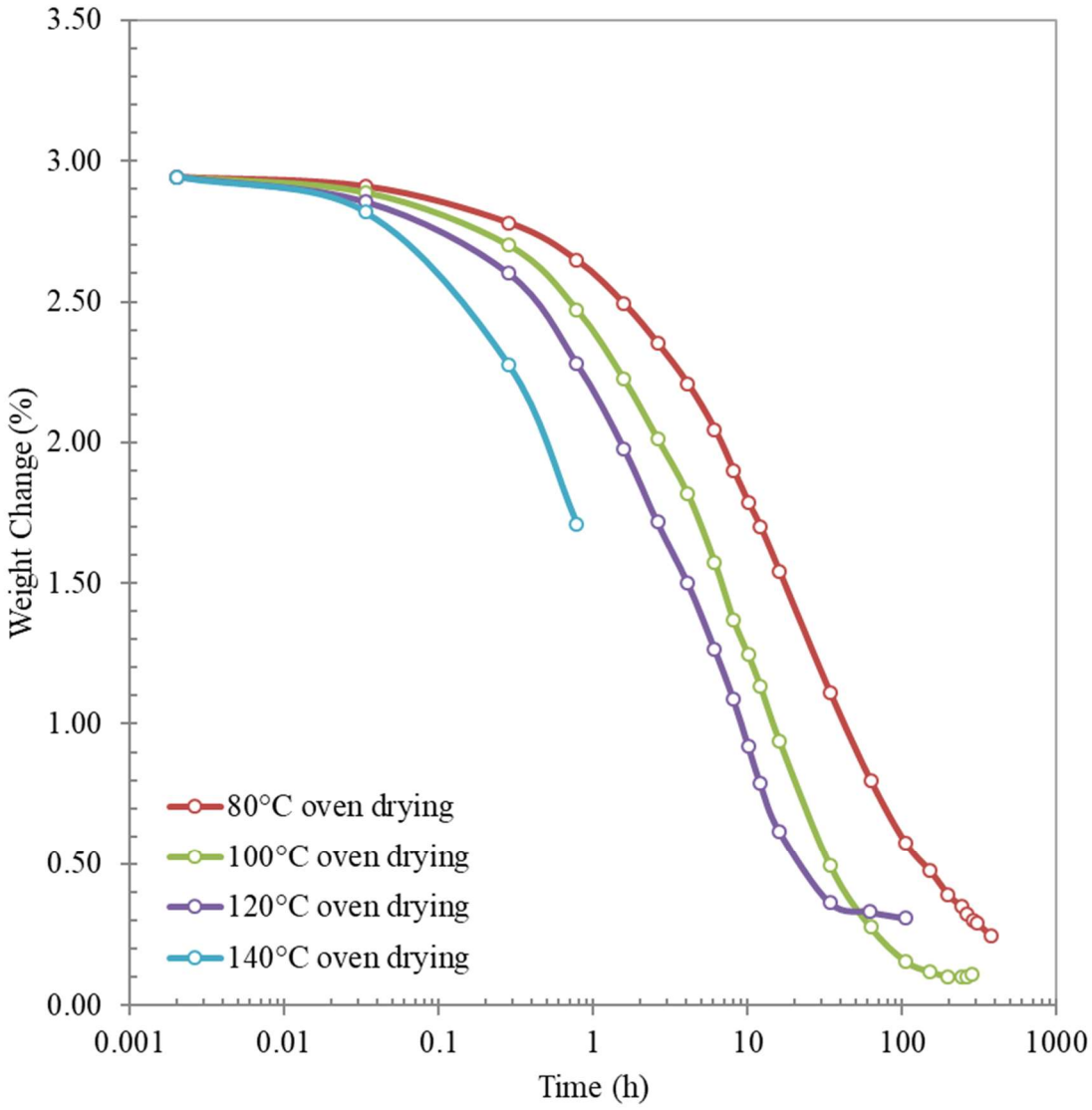

Figure 4.41: Desorption of Saturated PA MACM12 Samples

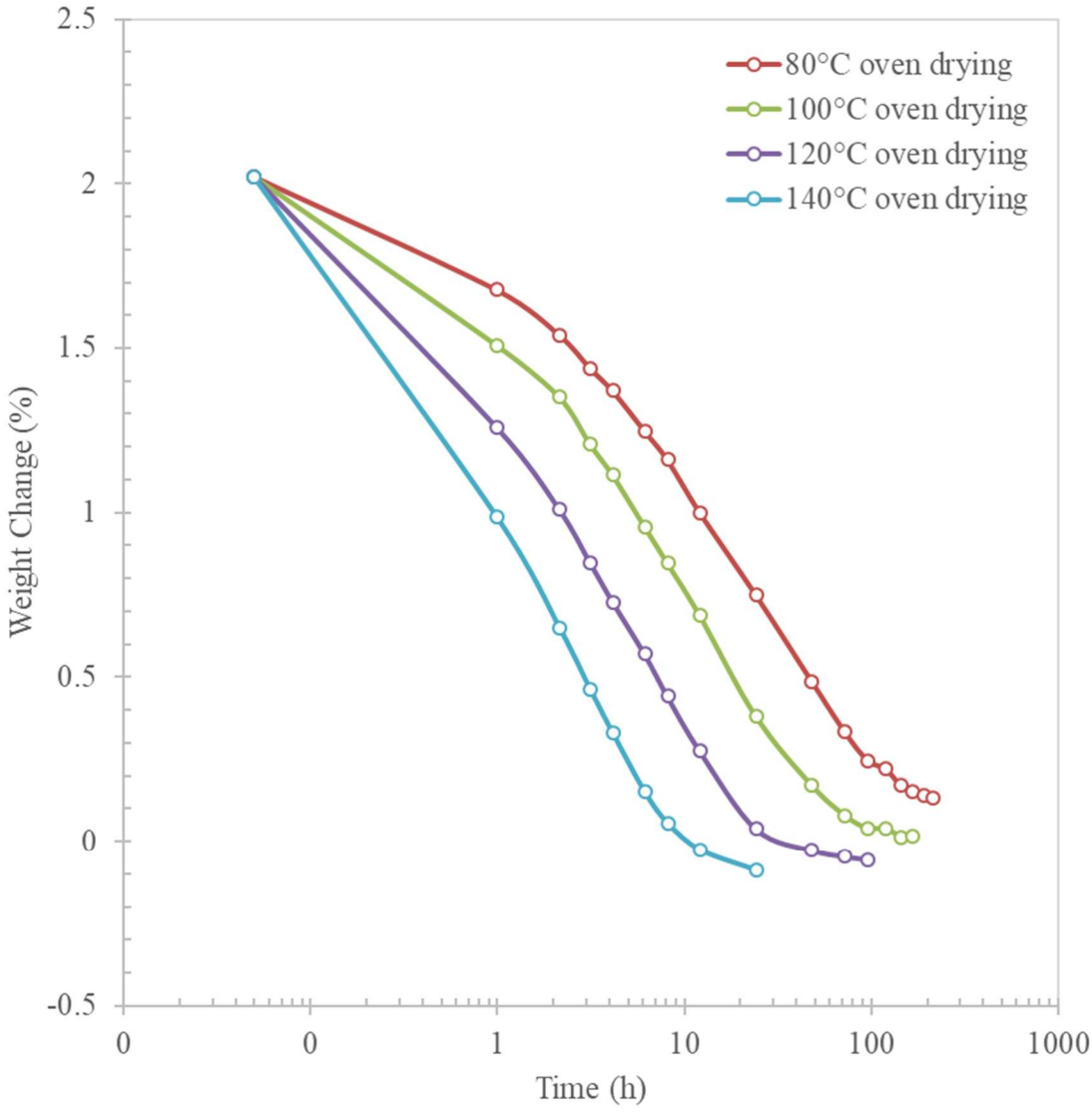

Figure 4.42: Desorption of Conditioned PA MACM12 Samples

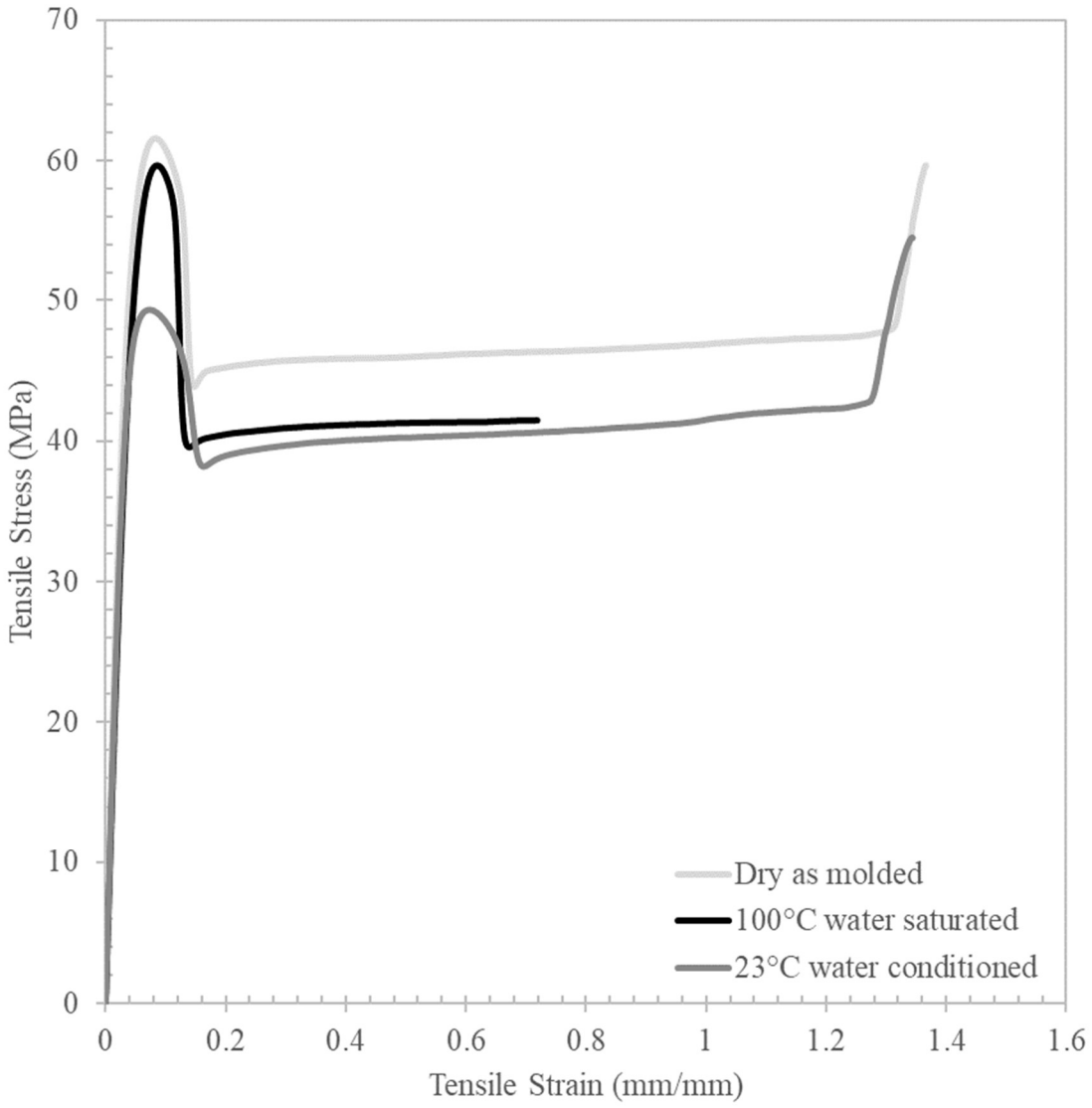

Figure 4.43: PA MACM12 Tensile Stress-Strain DAM vs Water Samples

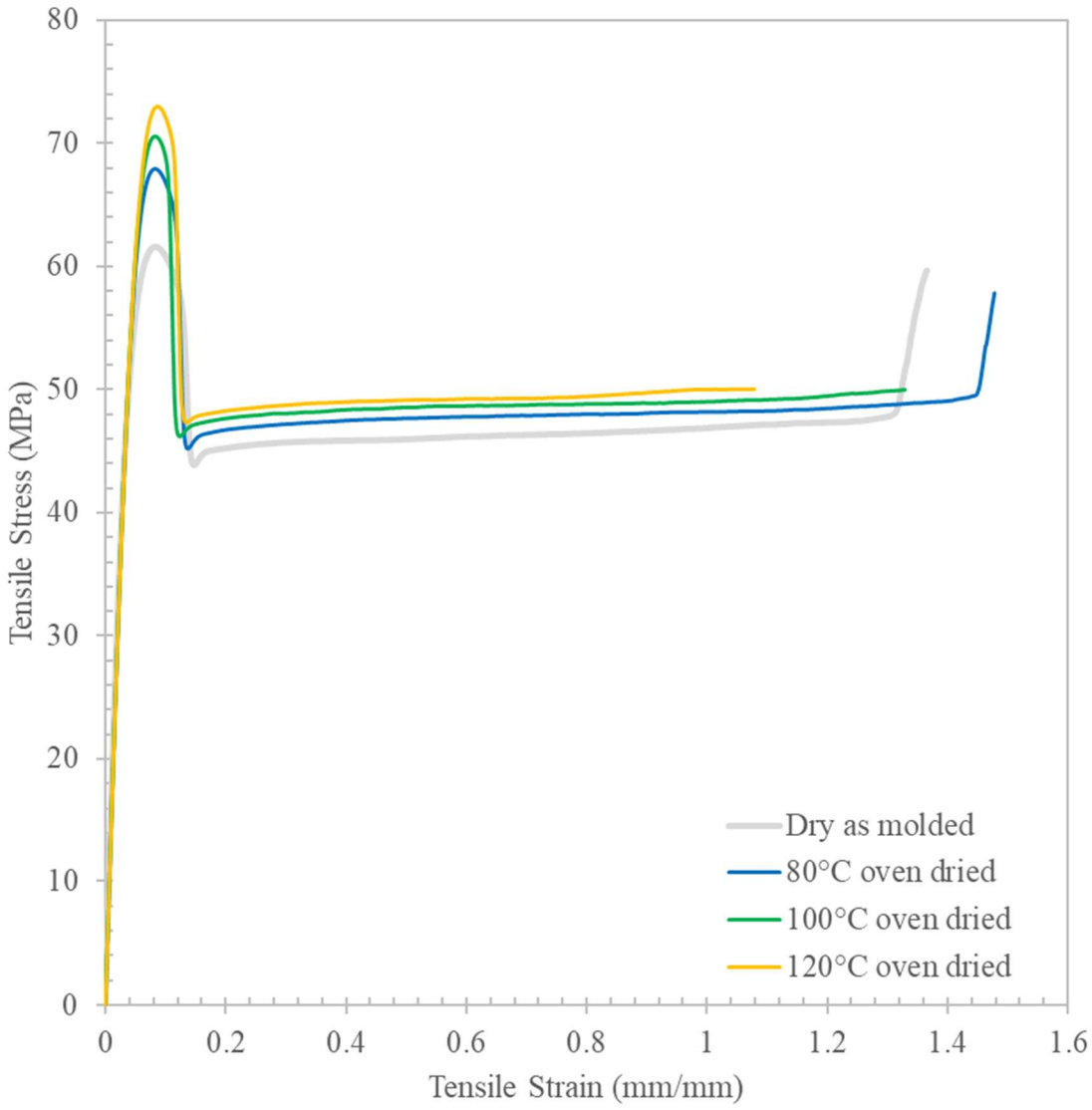

Figure 4.44: PA MACM12 Tensile Stress-Strain DAM vs Dried from Saturated

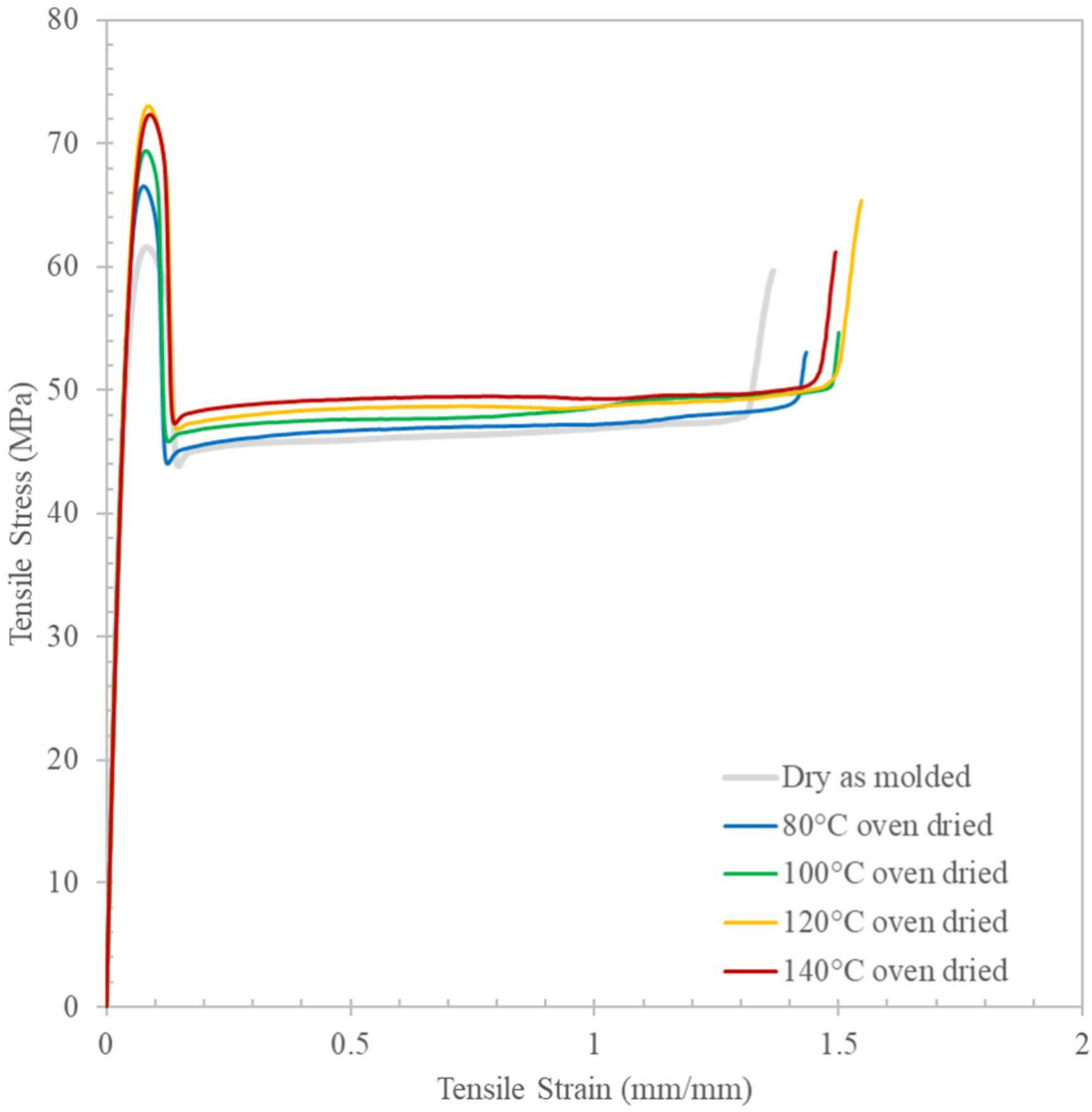

Figure 4.45: PA MACM12 Tensile Stress-Strain DAM vs Dried from Conditioned

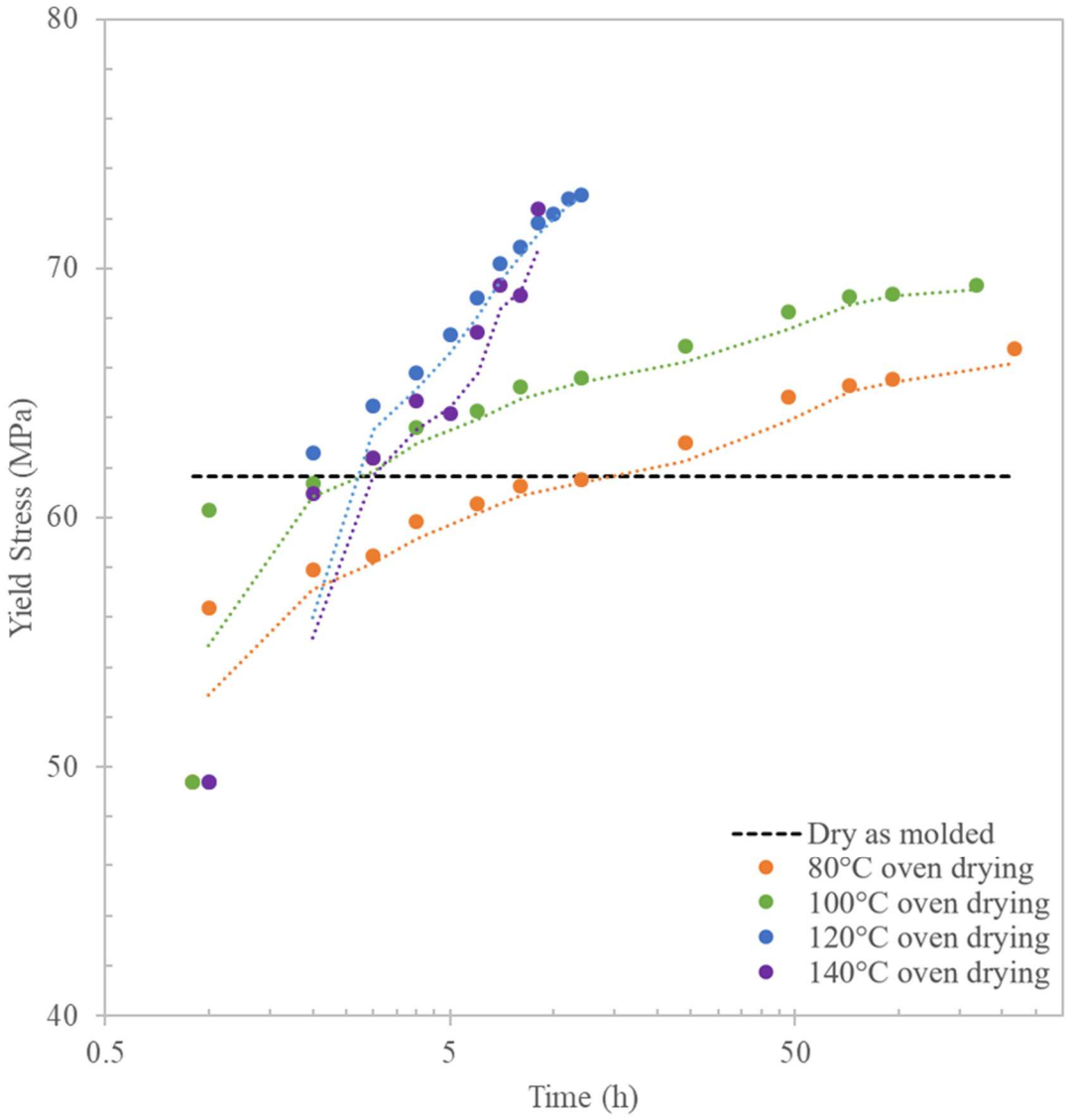

Figure 4.46: PA MACM12 Tensile Yield Stress Dried from Conditioned

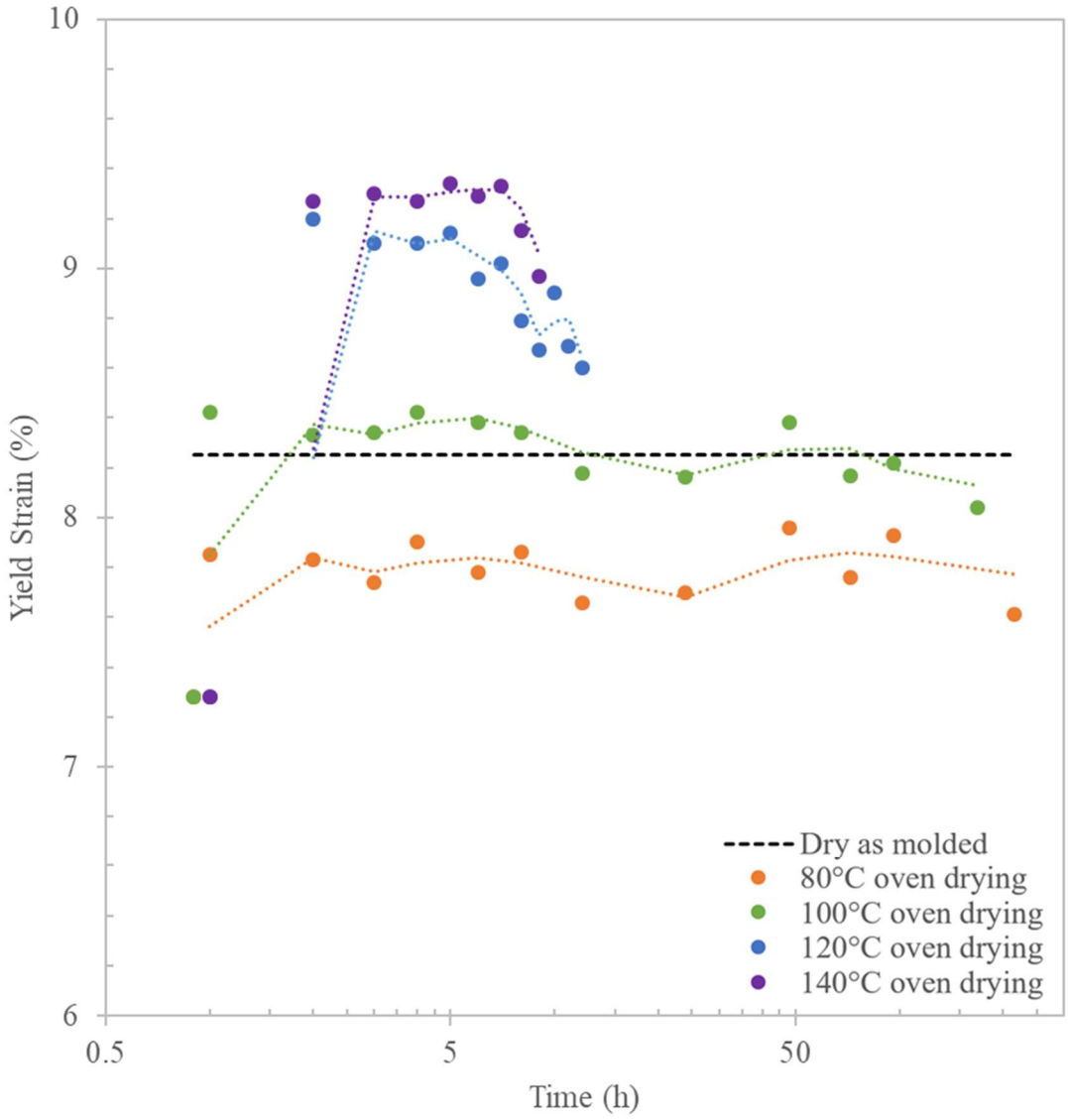

Figure 4.47: PA MACM12 Tensile Yield Strain Dried from Conditioned

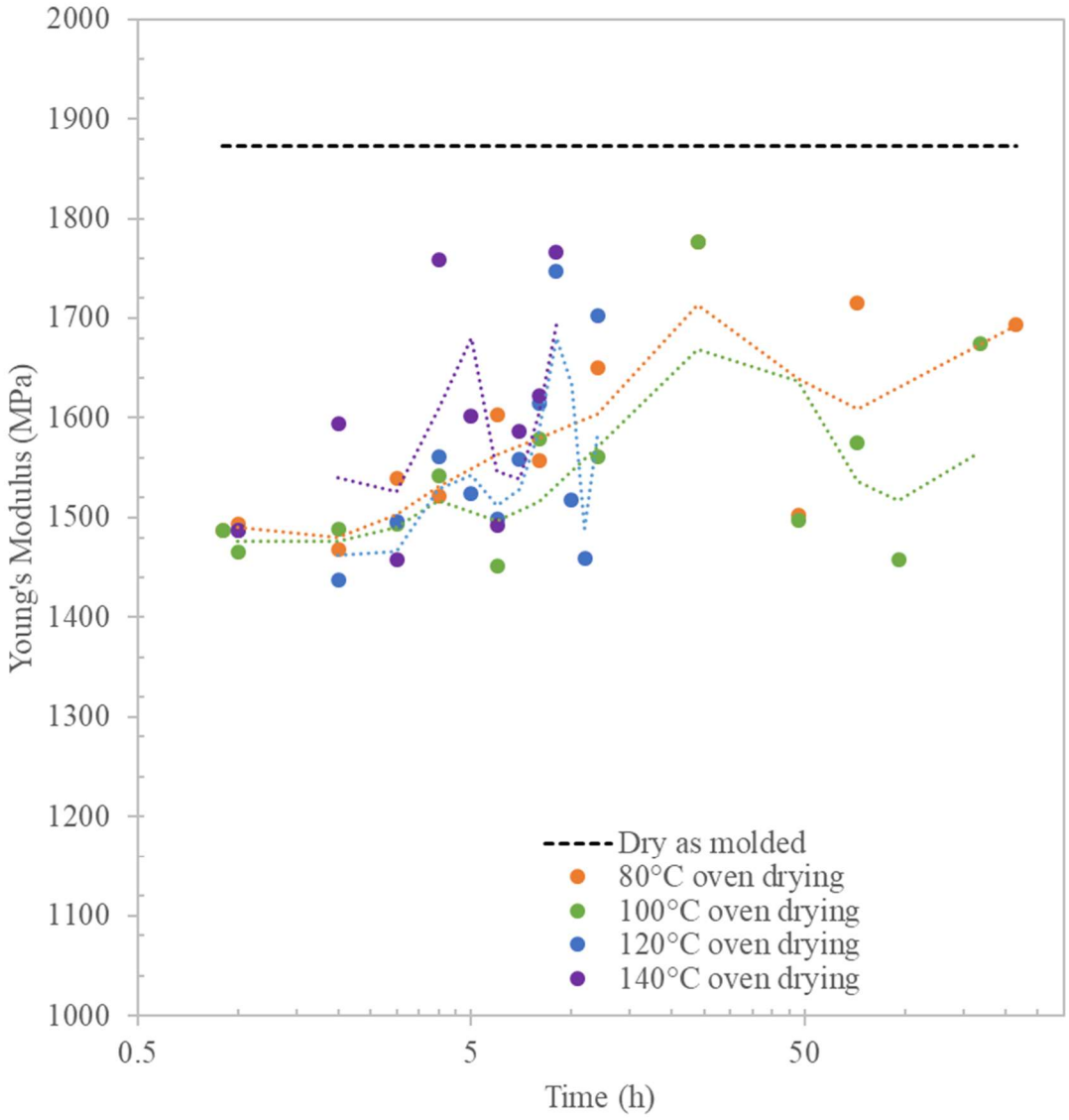

Figure 4.48: PA MACM12 Young's Modulus Dried from Conditioned

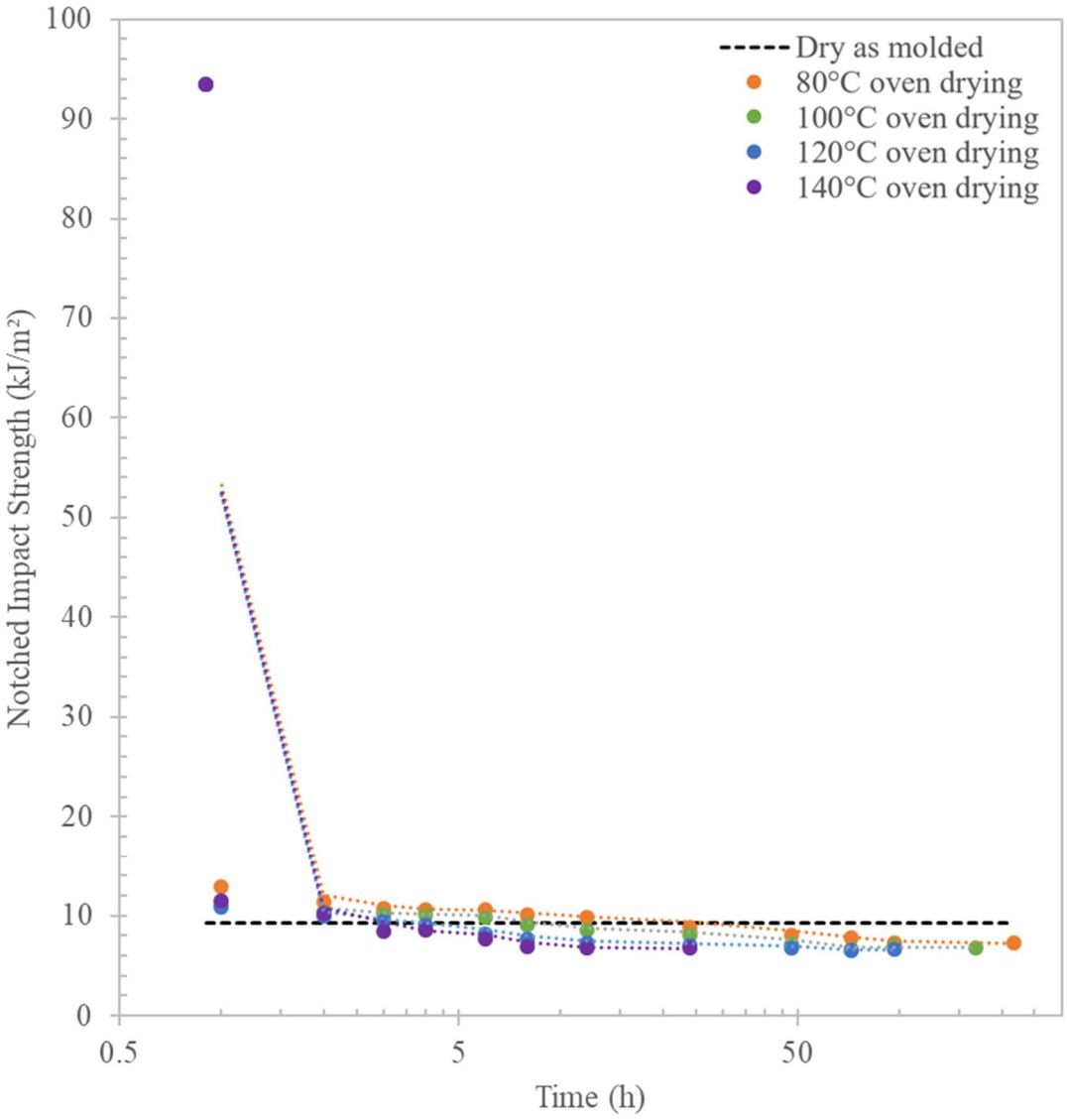

Figure 4.49: PA MACM12 Charpy Impact Dried from Conditioned

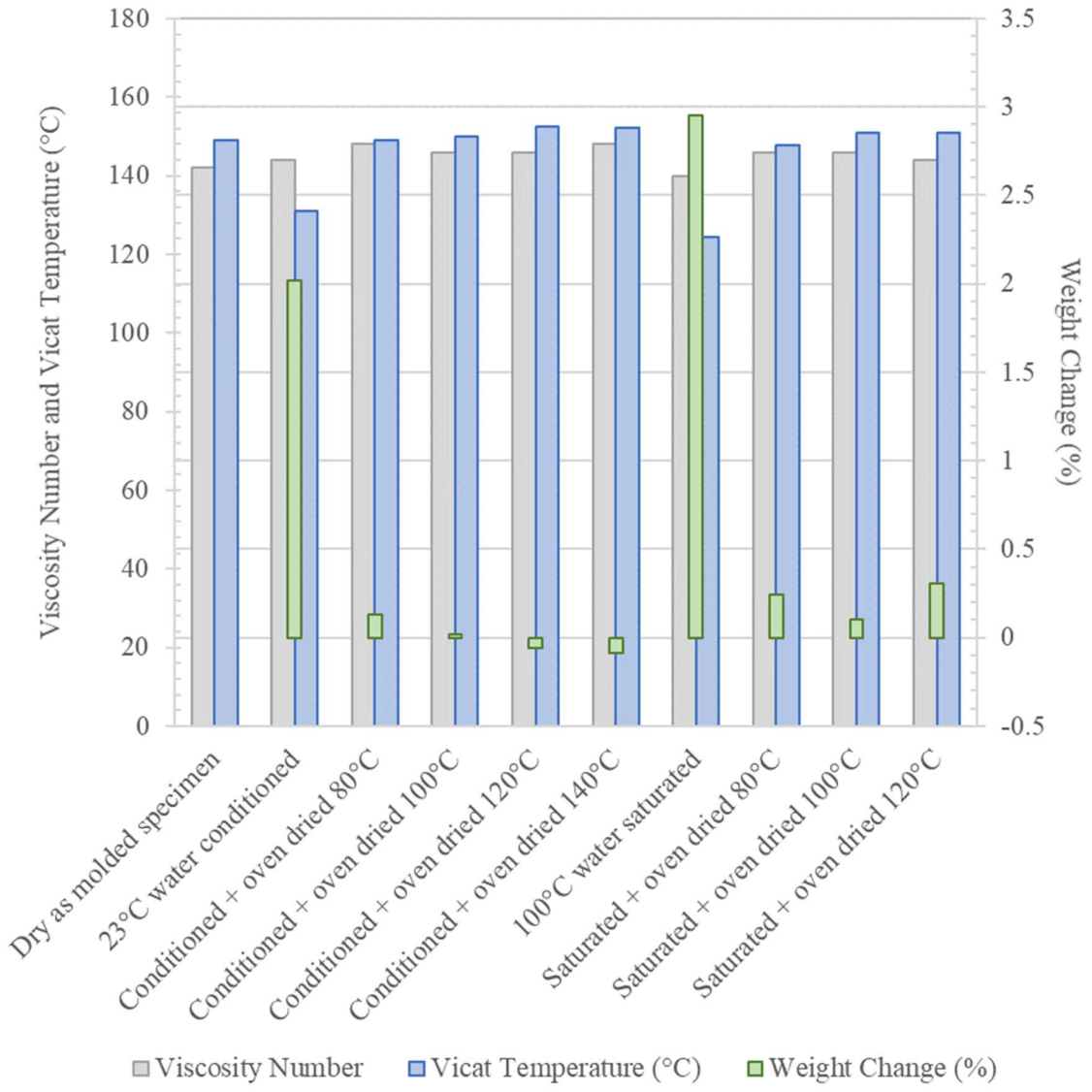

Figure 4.50: PA MACM12 Viscosity Number and Vicat Temperature

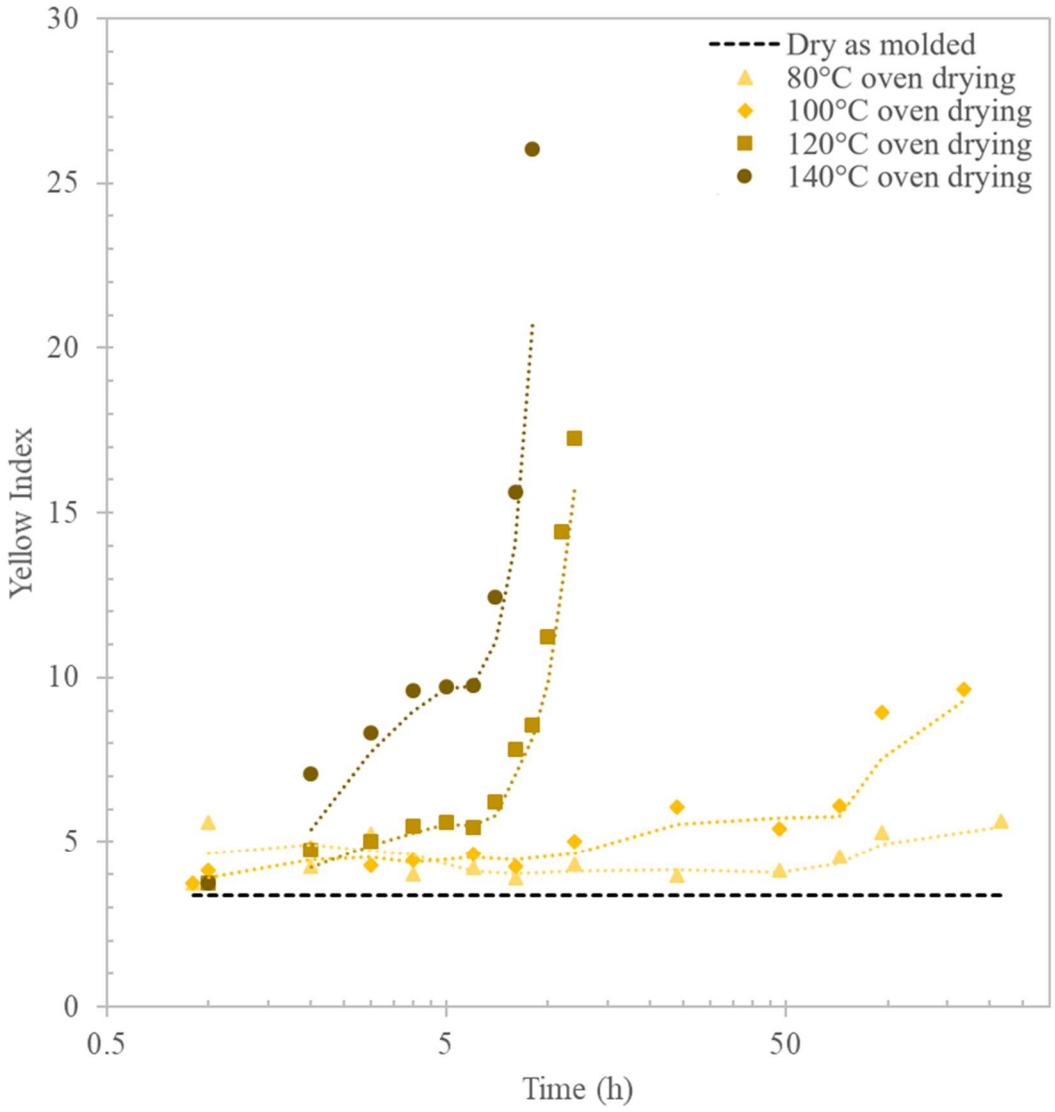

Figure 4.51: PA MACM12 Yellowness Index Dried from Conditioned

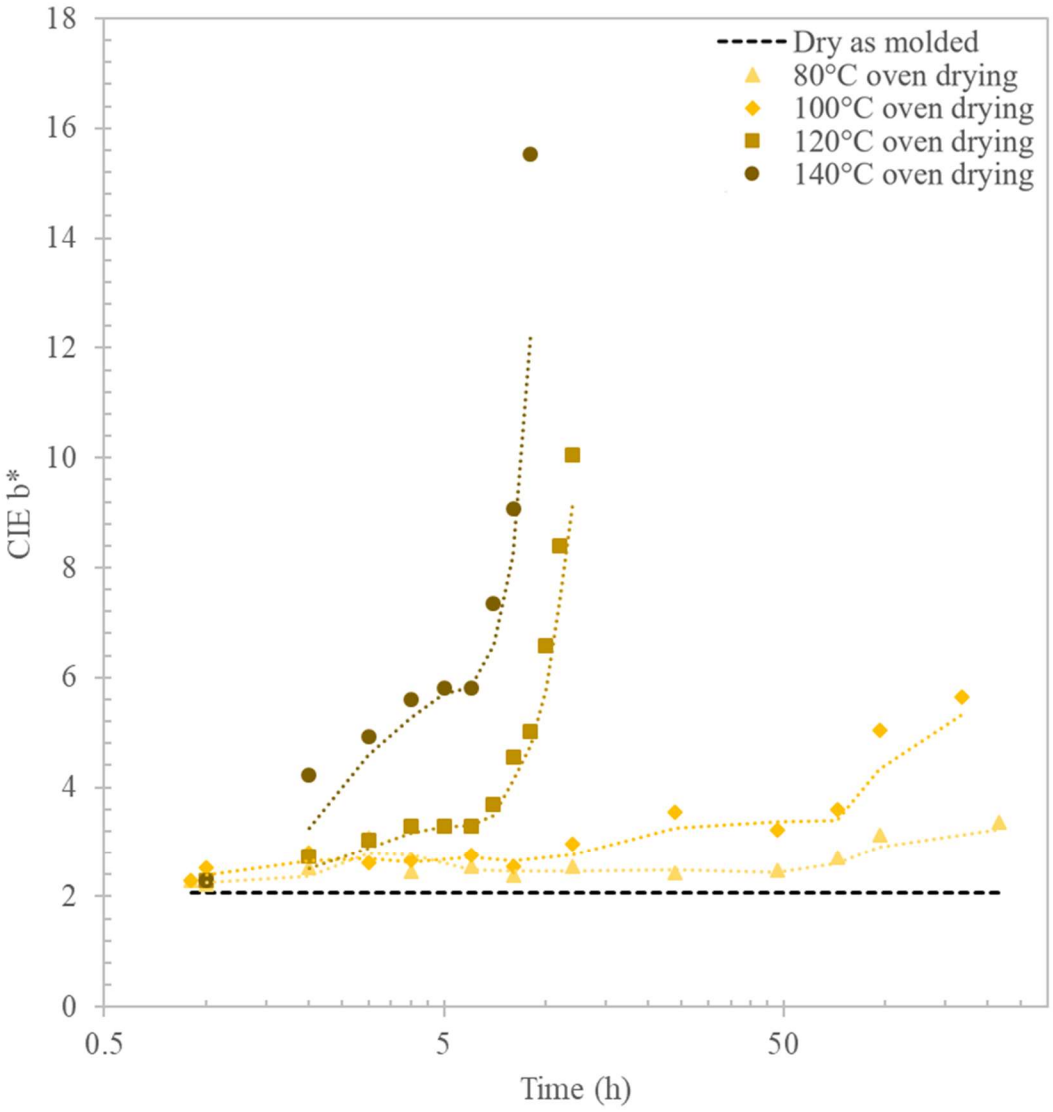

Figure 4.52: PA MACM12 CIE b-Value Dried from Conditioned

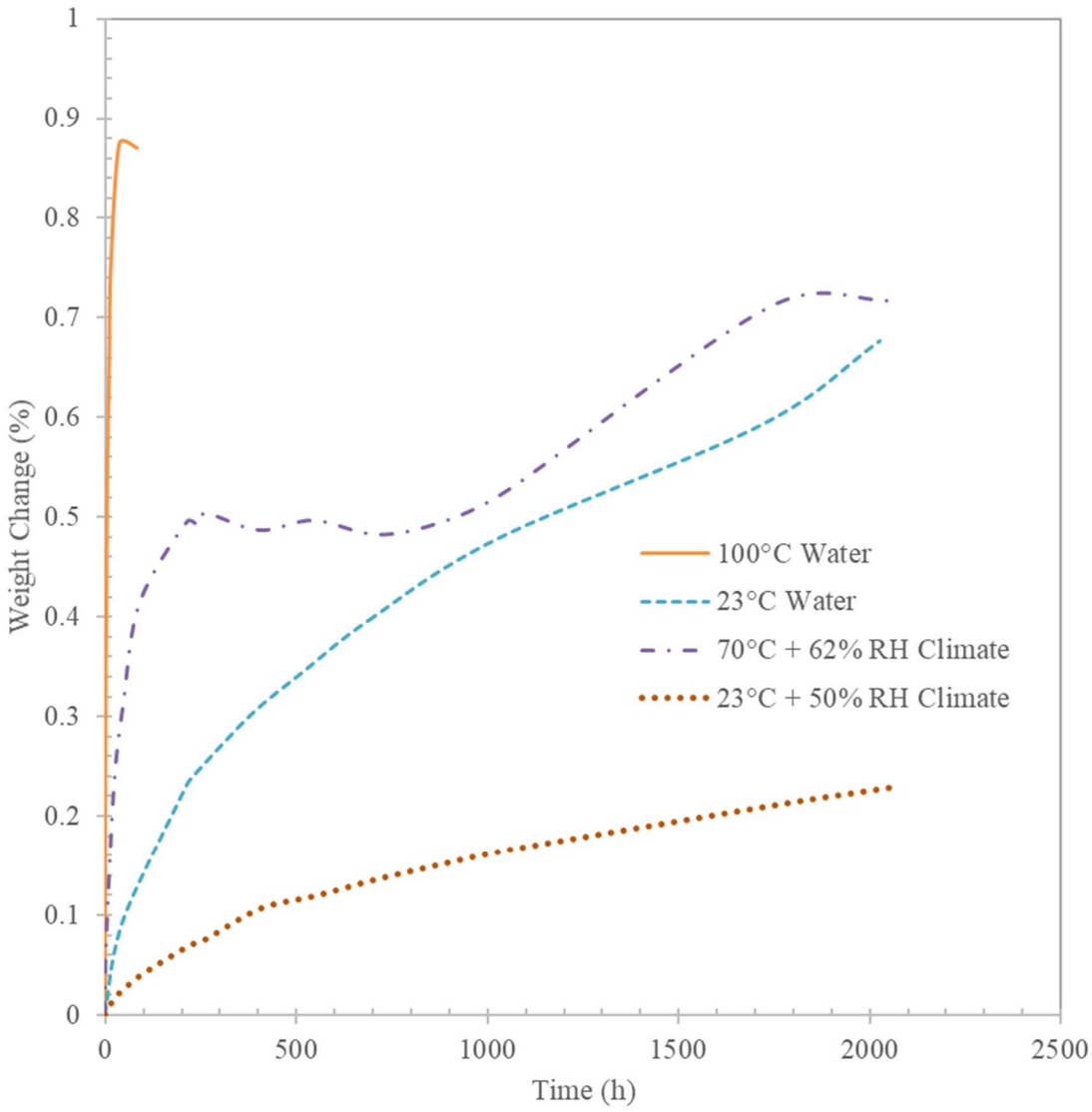

Figure 4.53: 50% GF Reinforced PA12 Absorption Comparison

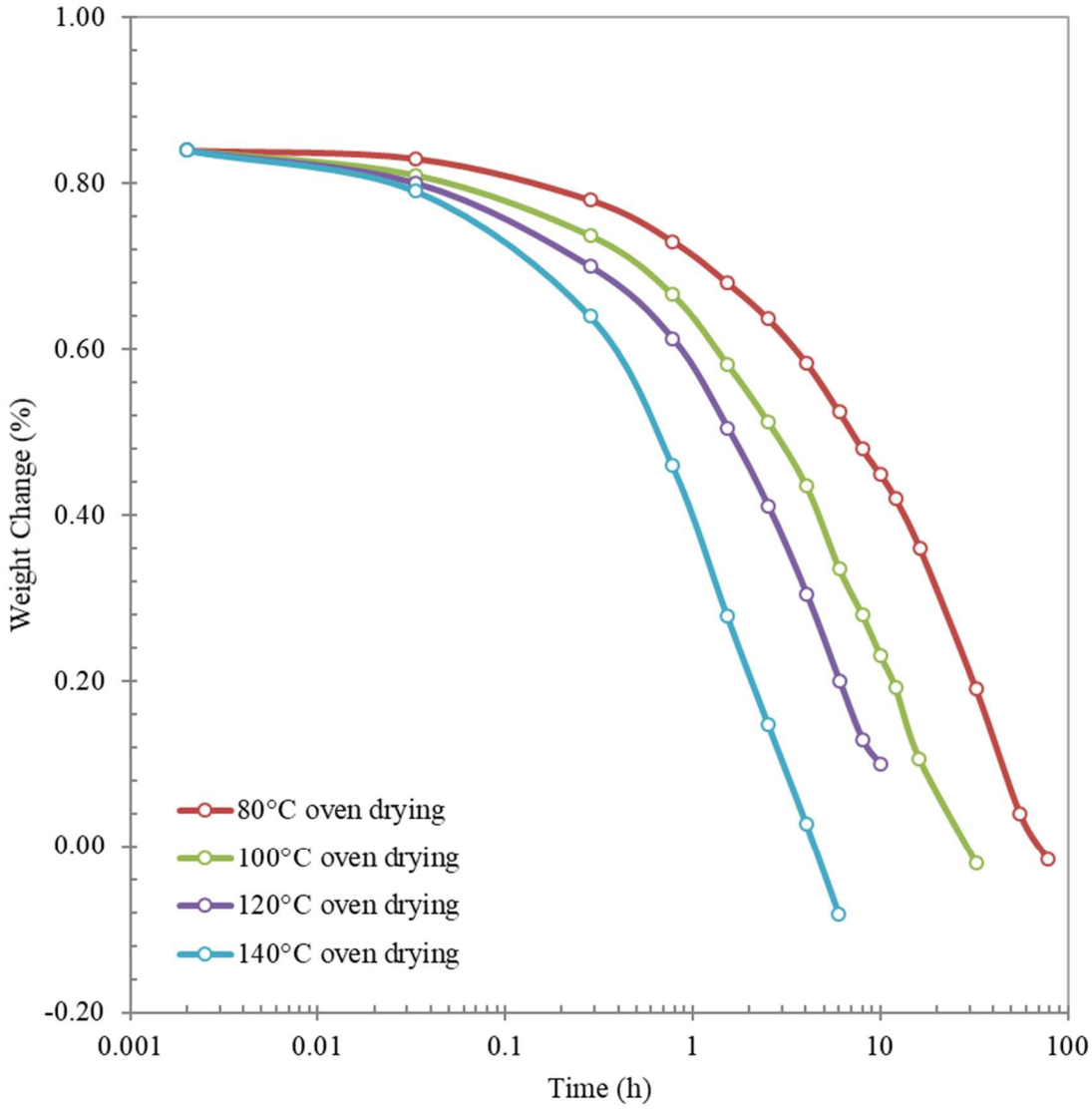

Figure 4.54: Desorption of Saturated 50% GF PA12 Samples

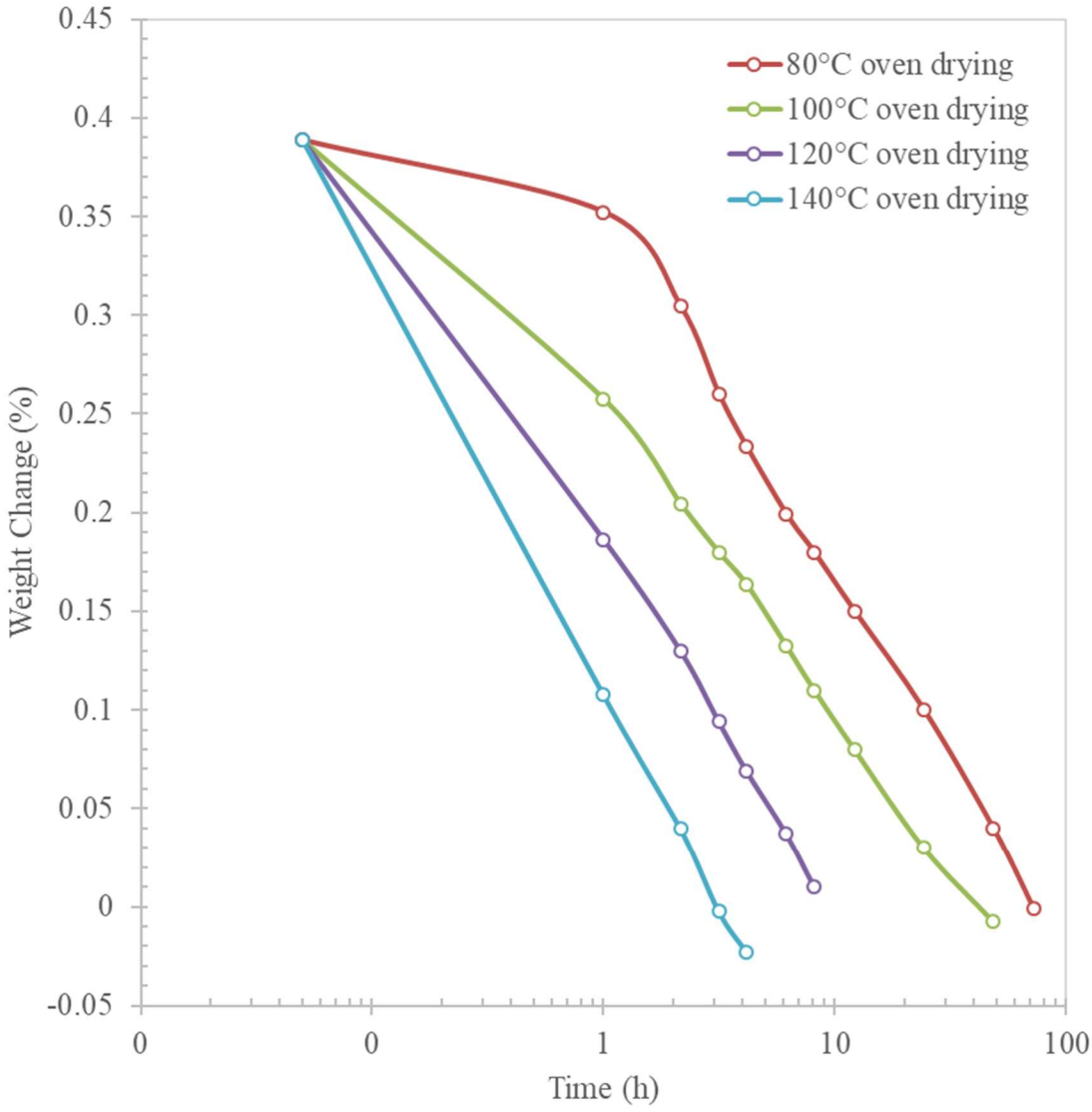

Figure 4.55: Desorption of Conditioned 50% GF PA12 Samples

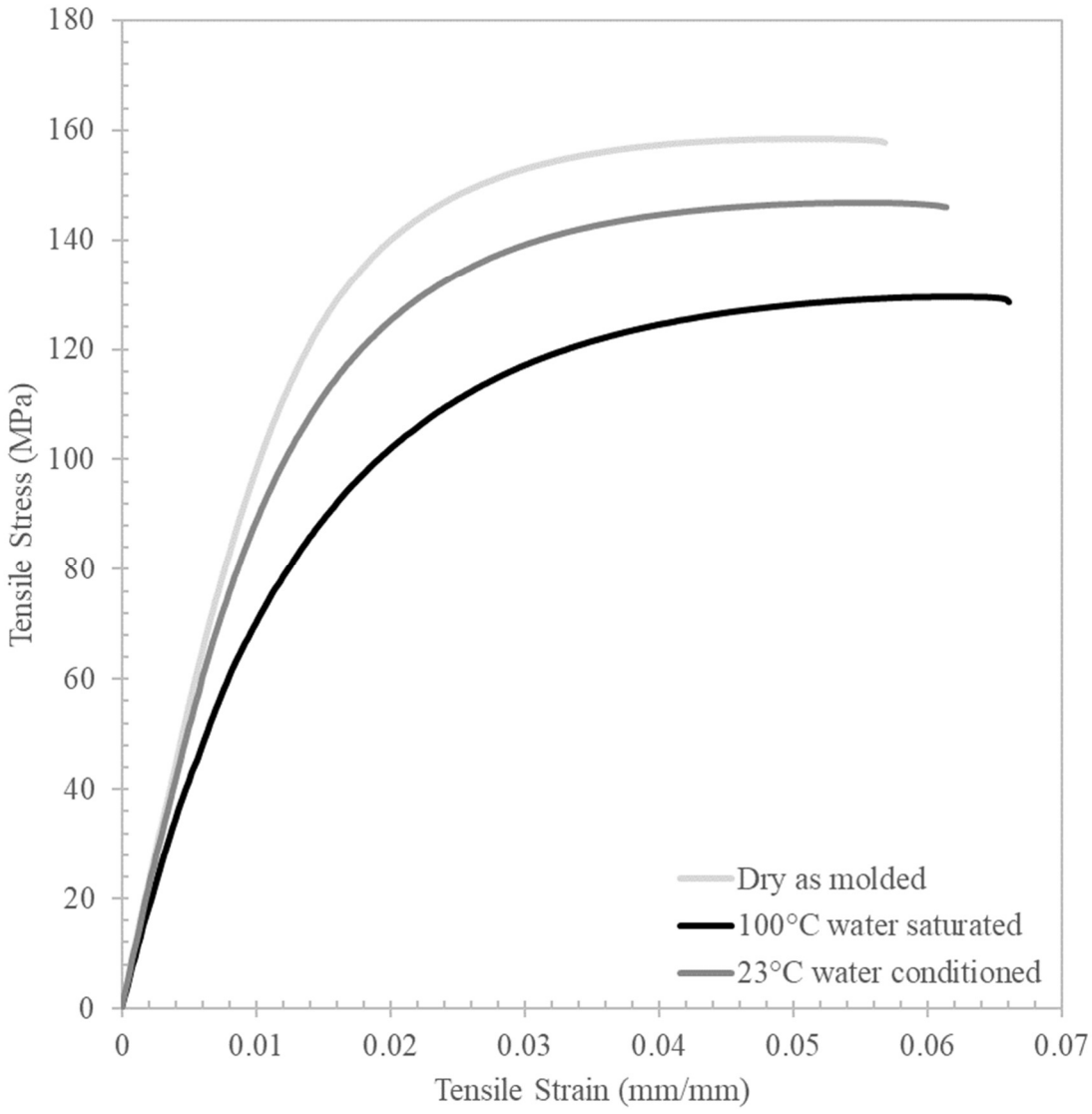

Figure 4.56: 50% GF PA12 Tensile Stress-Strain DAM vs Water Samples

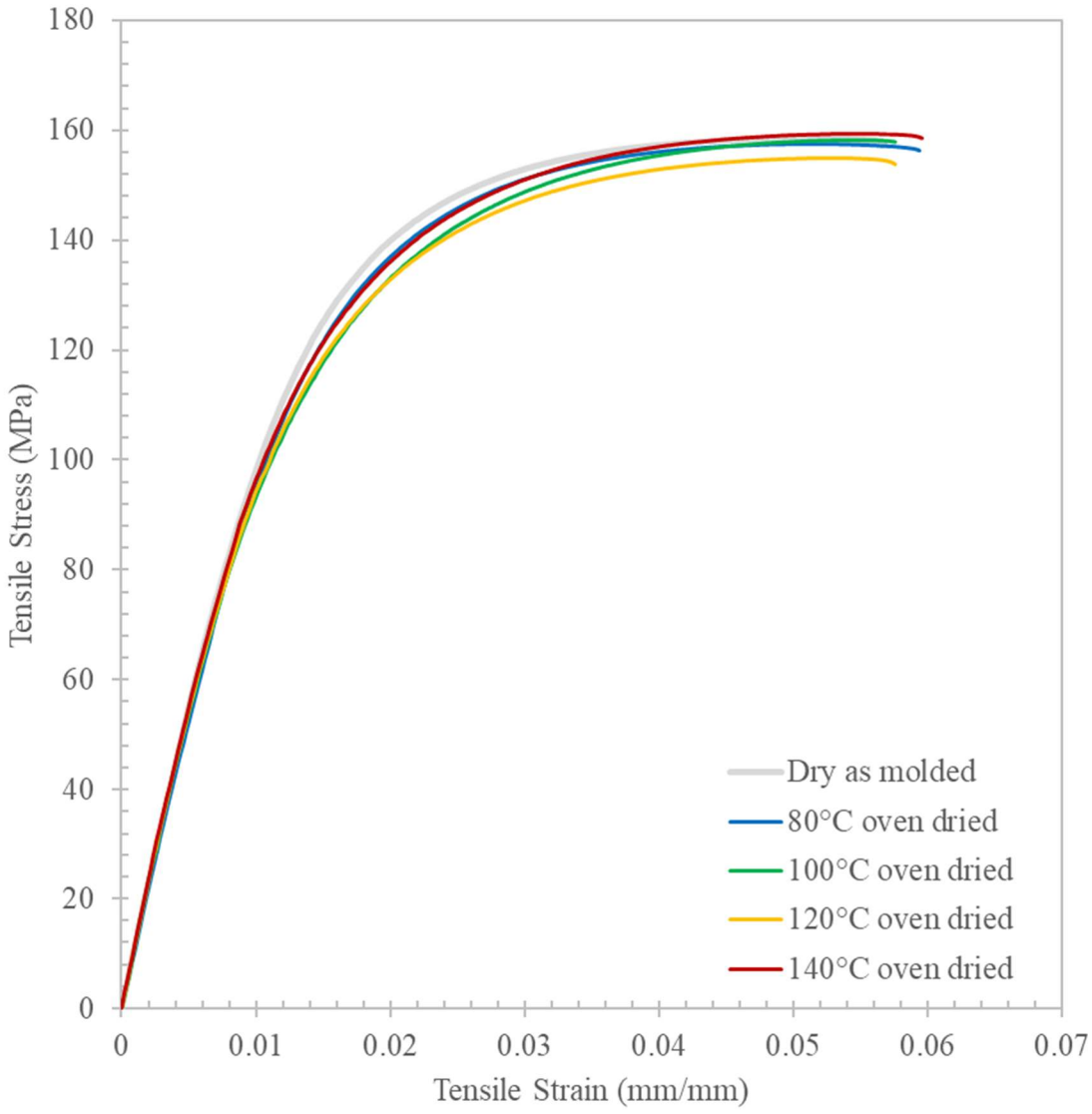

Figure 4.57: 50% GF PA12 Tensile Stress-Strain DAM vs Dried from Saturated

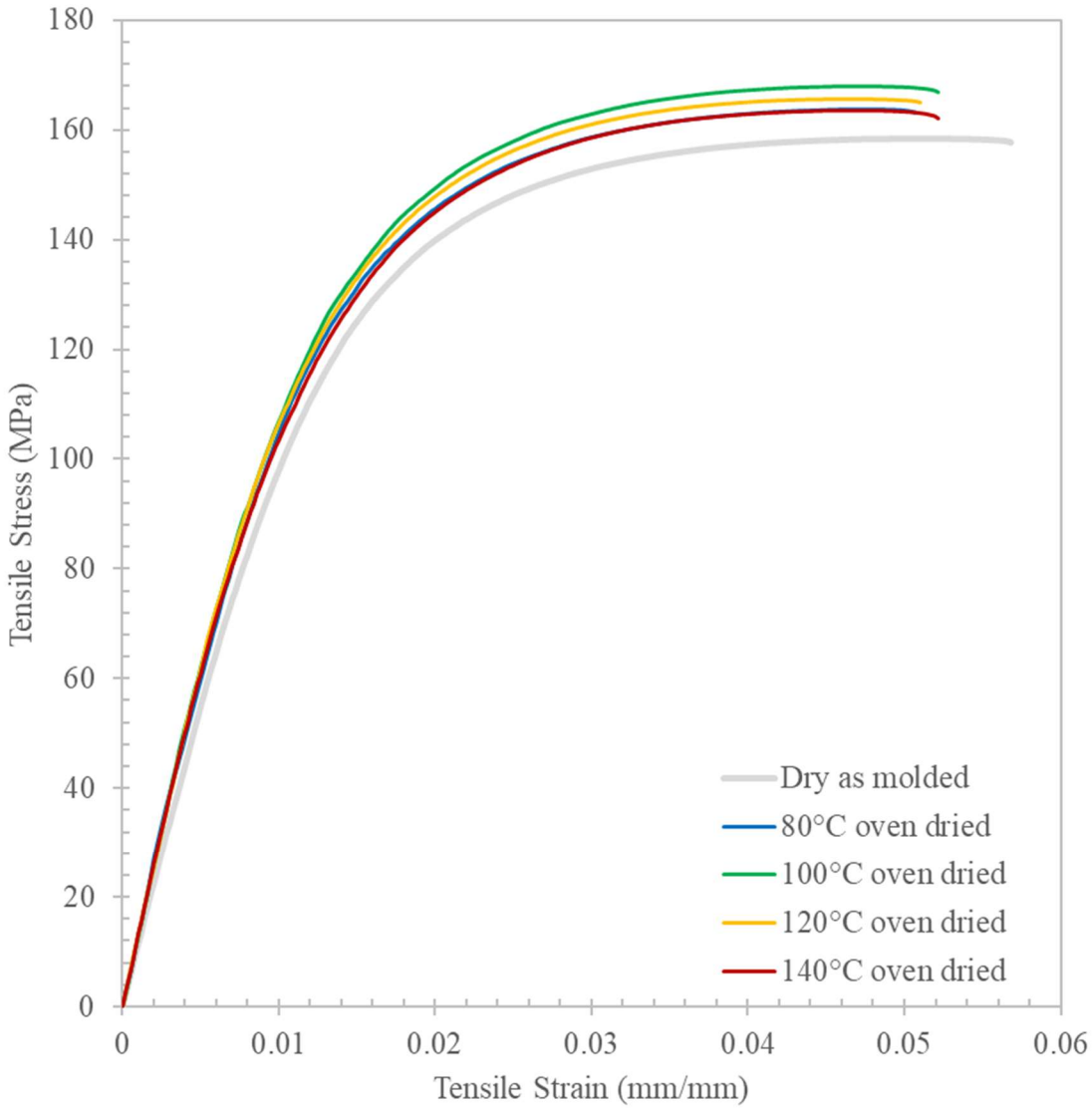

Figure 4.58: 50% GF PA12 Tensile Stress-Strain DAM vs Dried from Conditioned

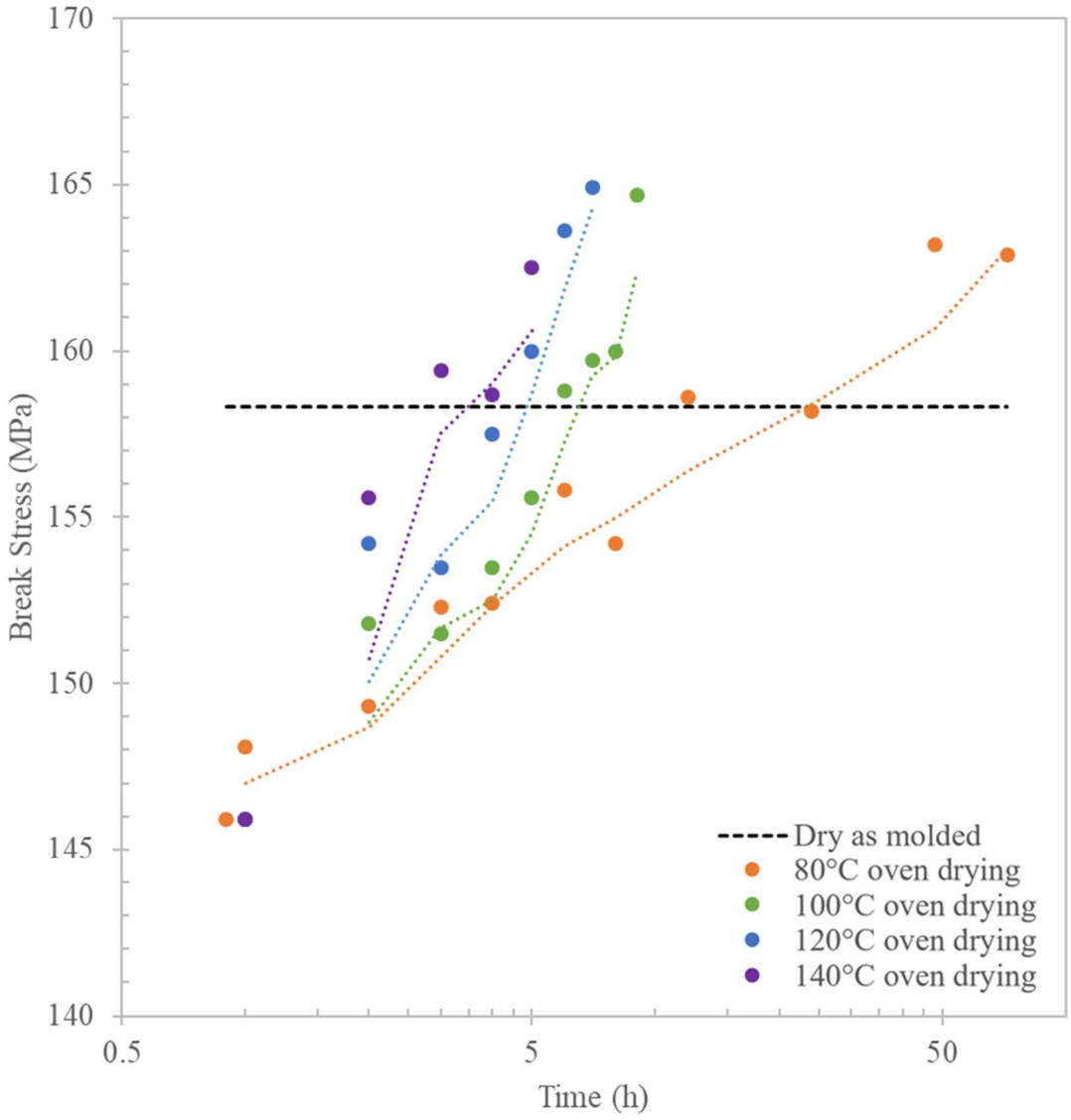

Figure 4.59: 50% GF PA12 Tensile Break Stress Dried from Conditioned

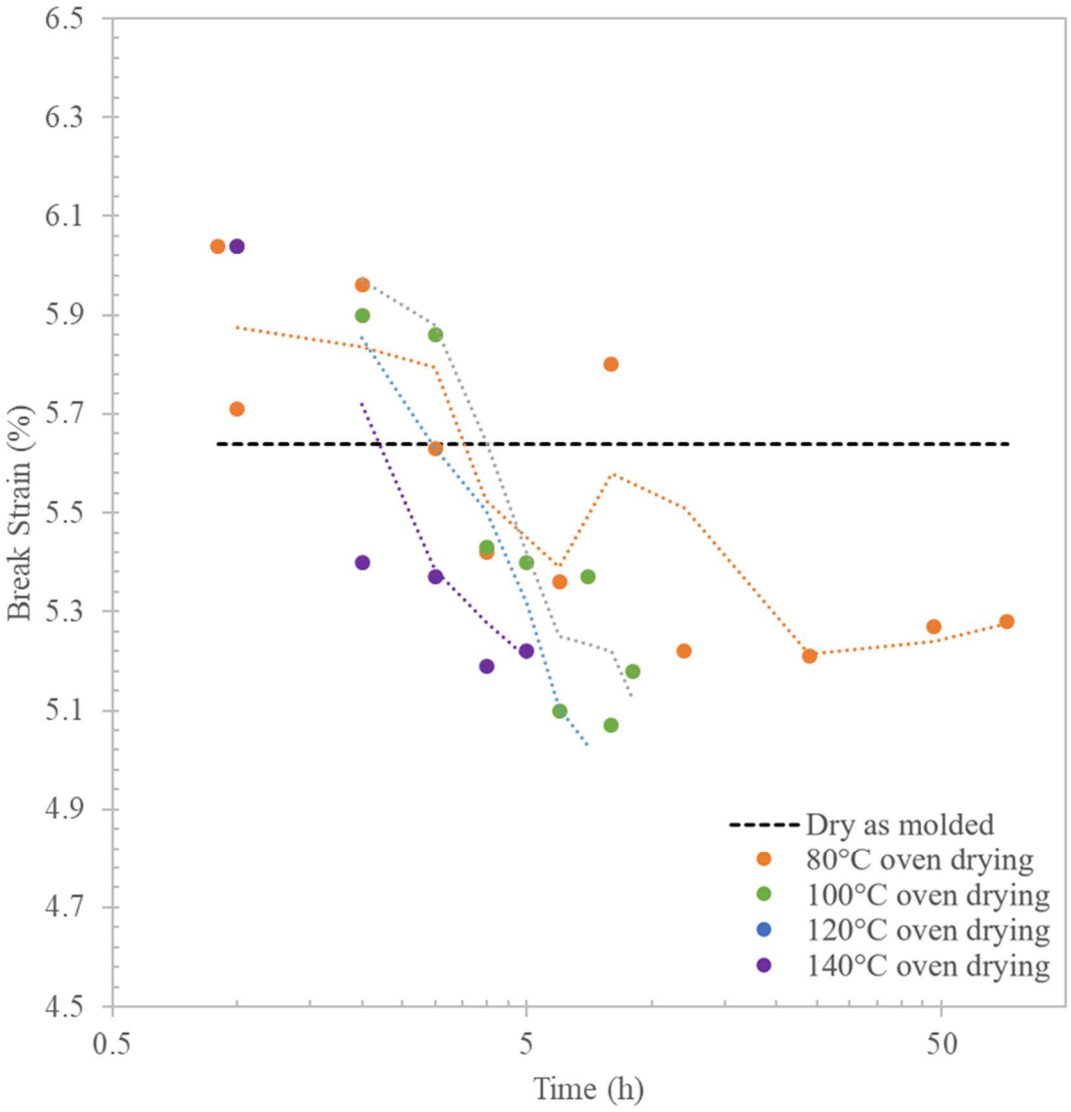

Figure 4.60: 50% GF PA12 Tensile Break Strain Dried from Conditioned

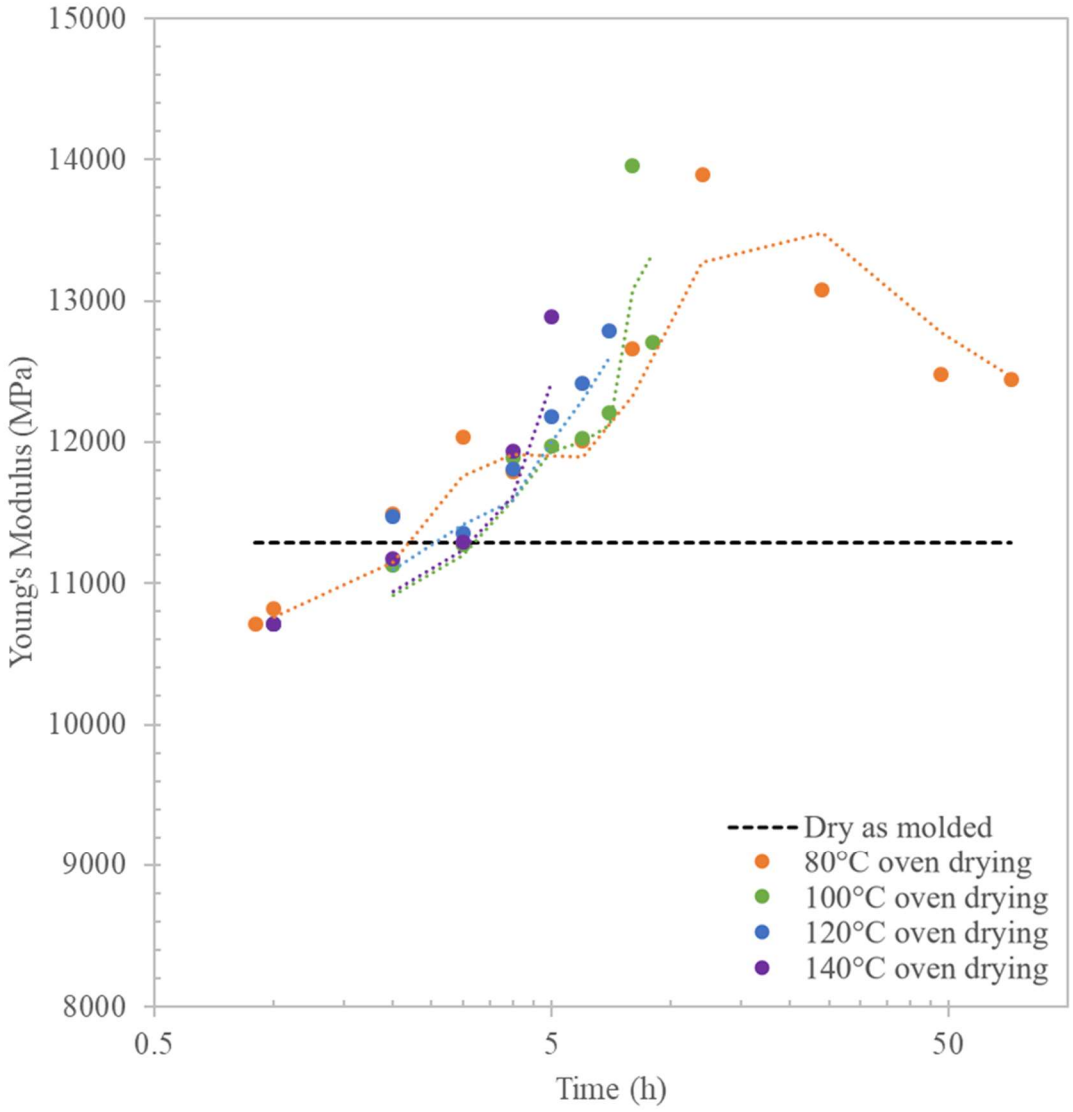

Figure 4.61: 50% GF PA12 Young's Modulus Dried from Conditioned

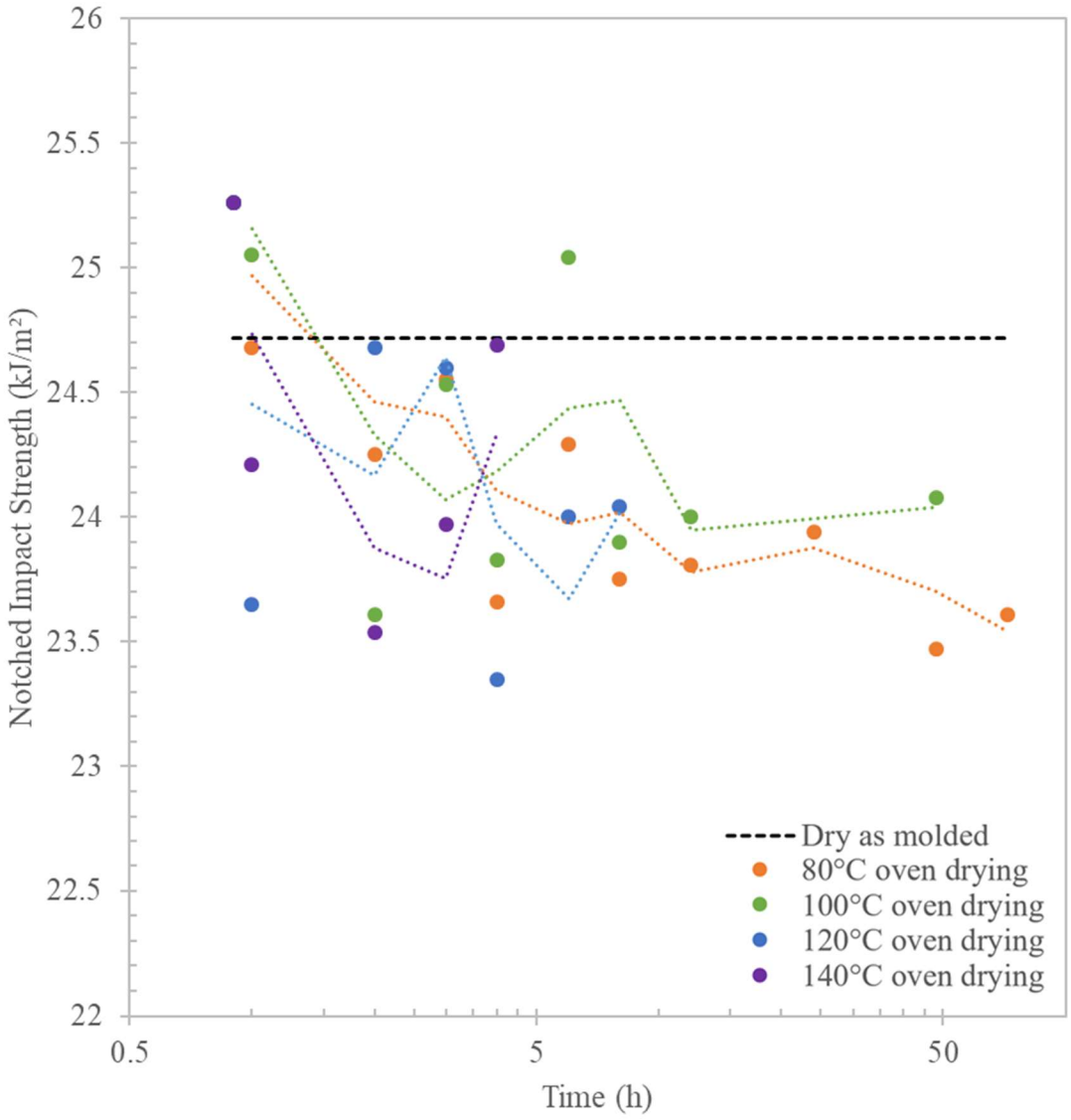

Figure 4.62: 50% GF PA12 Charpy Impact Dried from Conditioned

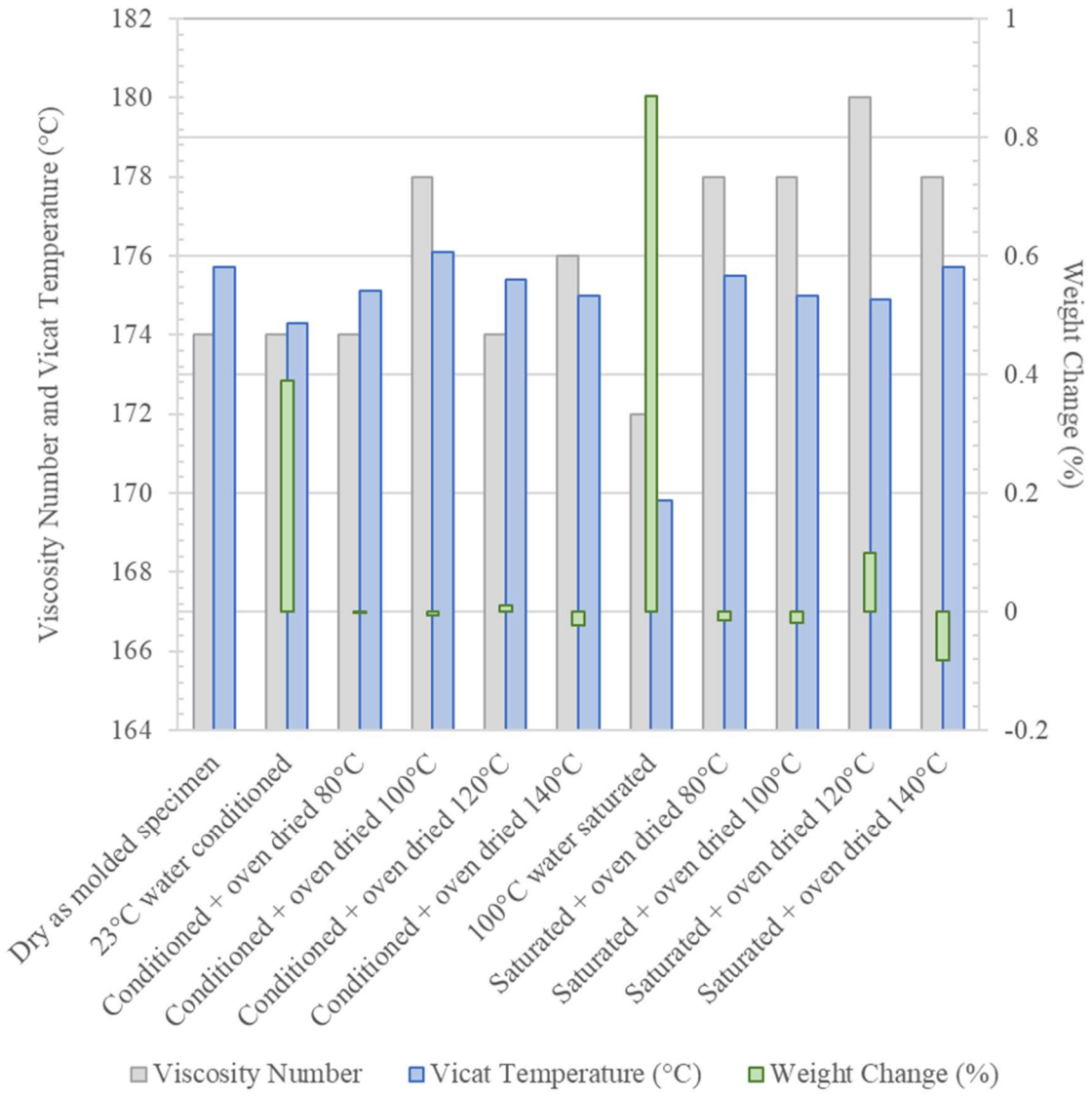

Figure 4.63: 50% GF PA12 Viscosity Number and Vicat Temperature

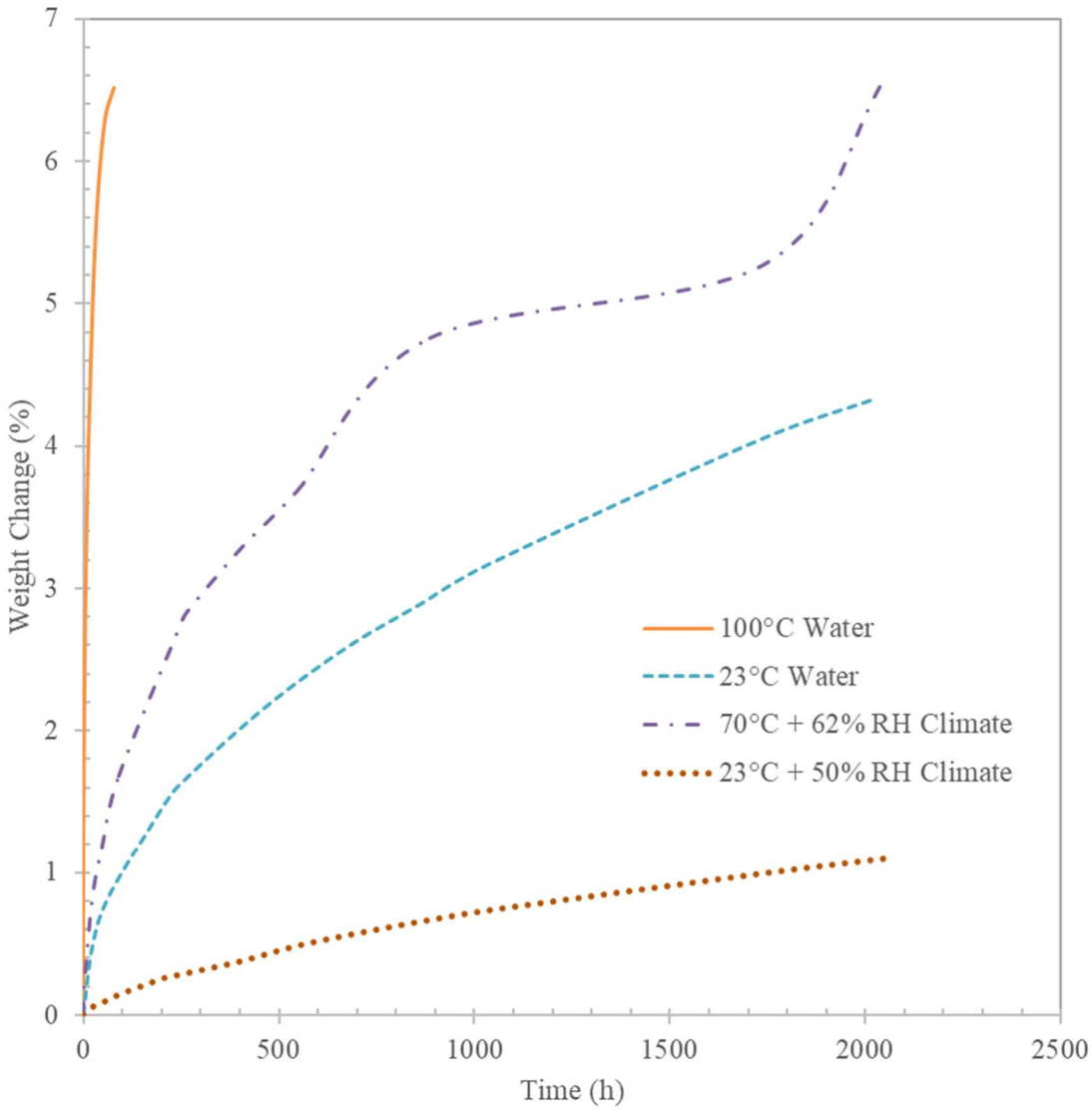

Figure 4.64: Unreinforced PA6I/6T Absorption Comparison

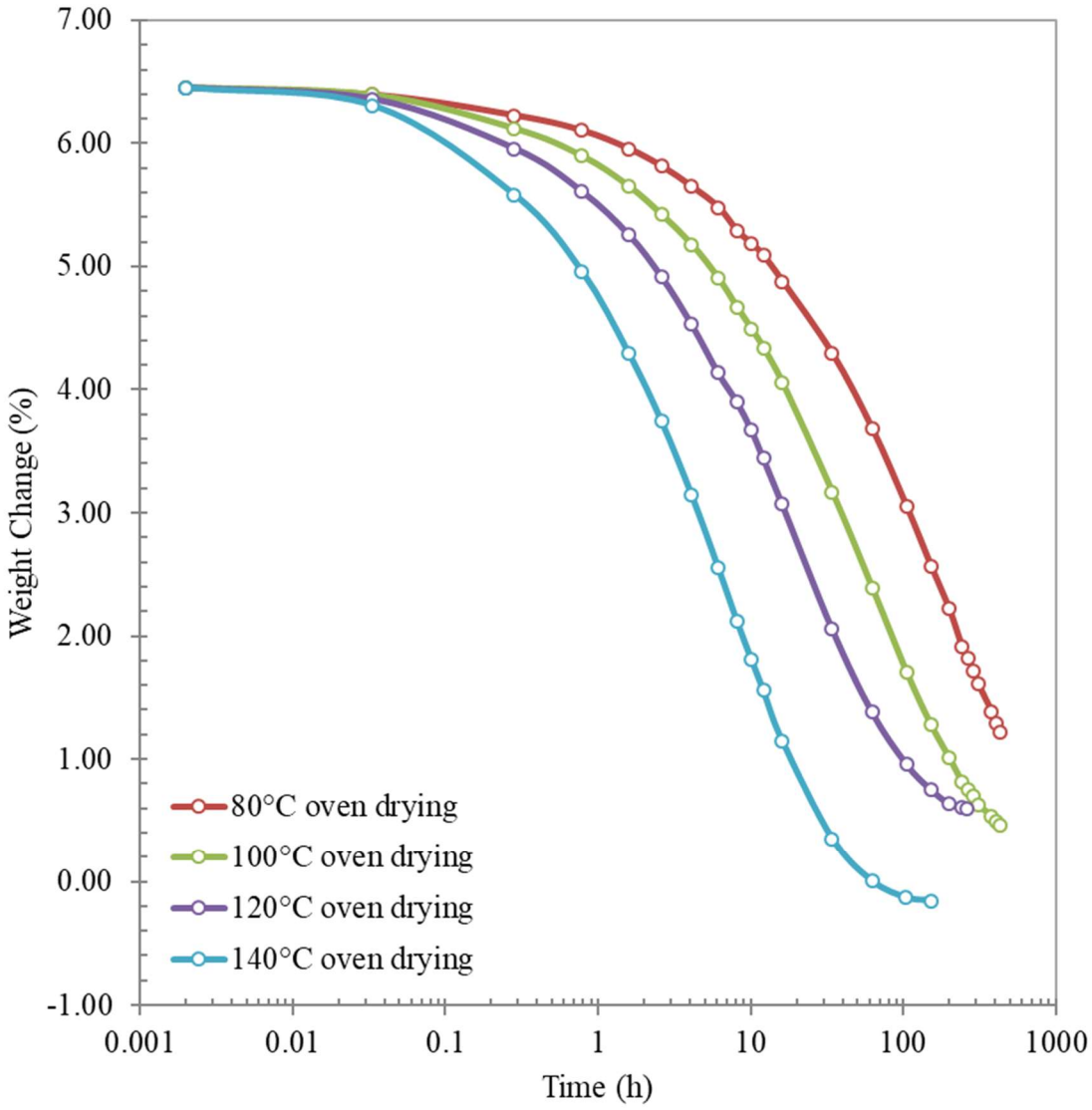

Figure 4.65: Desorption of Saturated PA6I/6T Samples

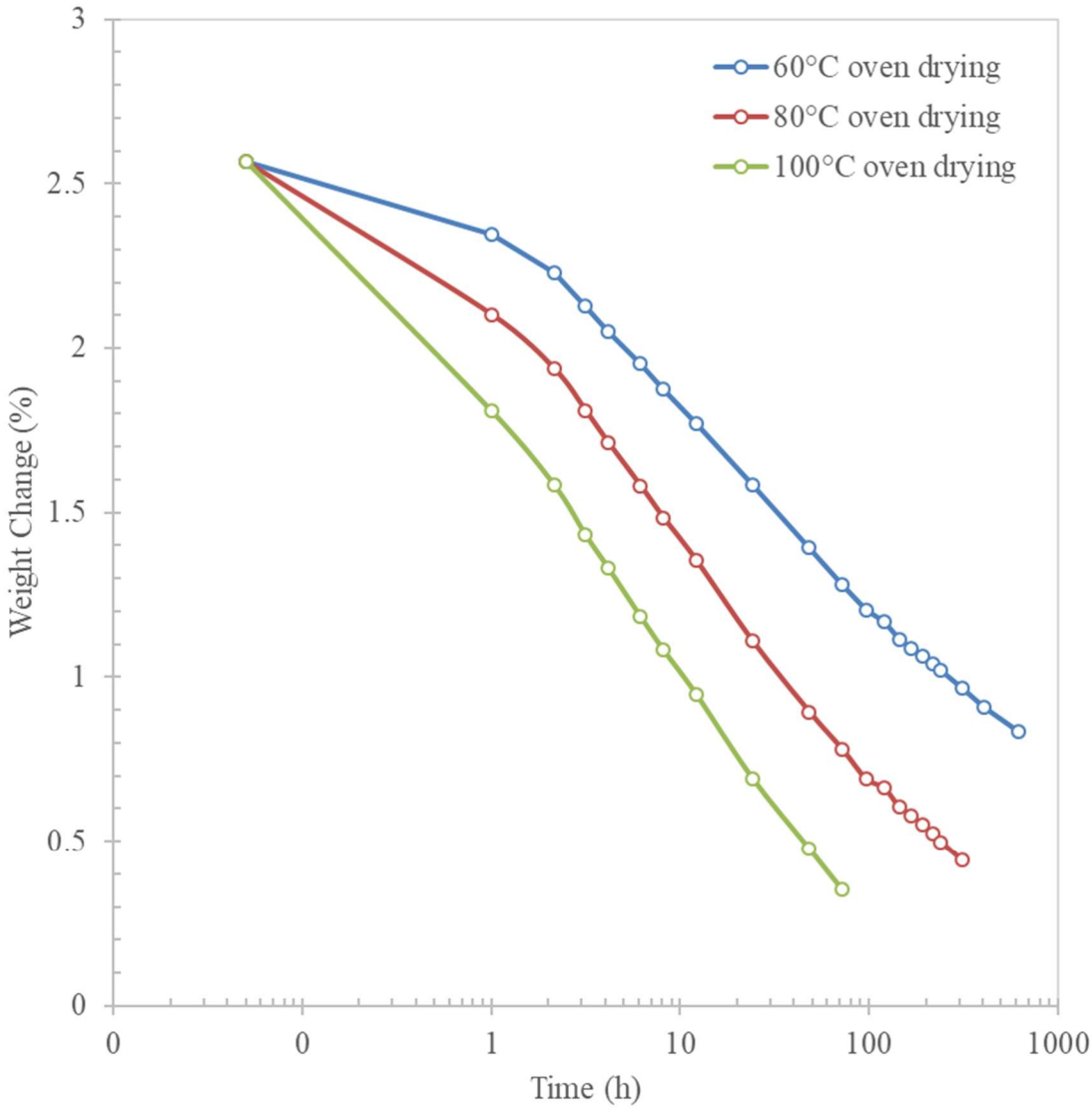

Figure 4.66: Desorption of Conditioned PA6I/6T Samples

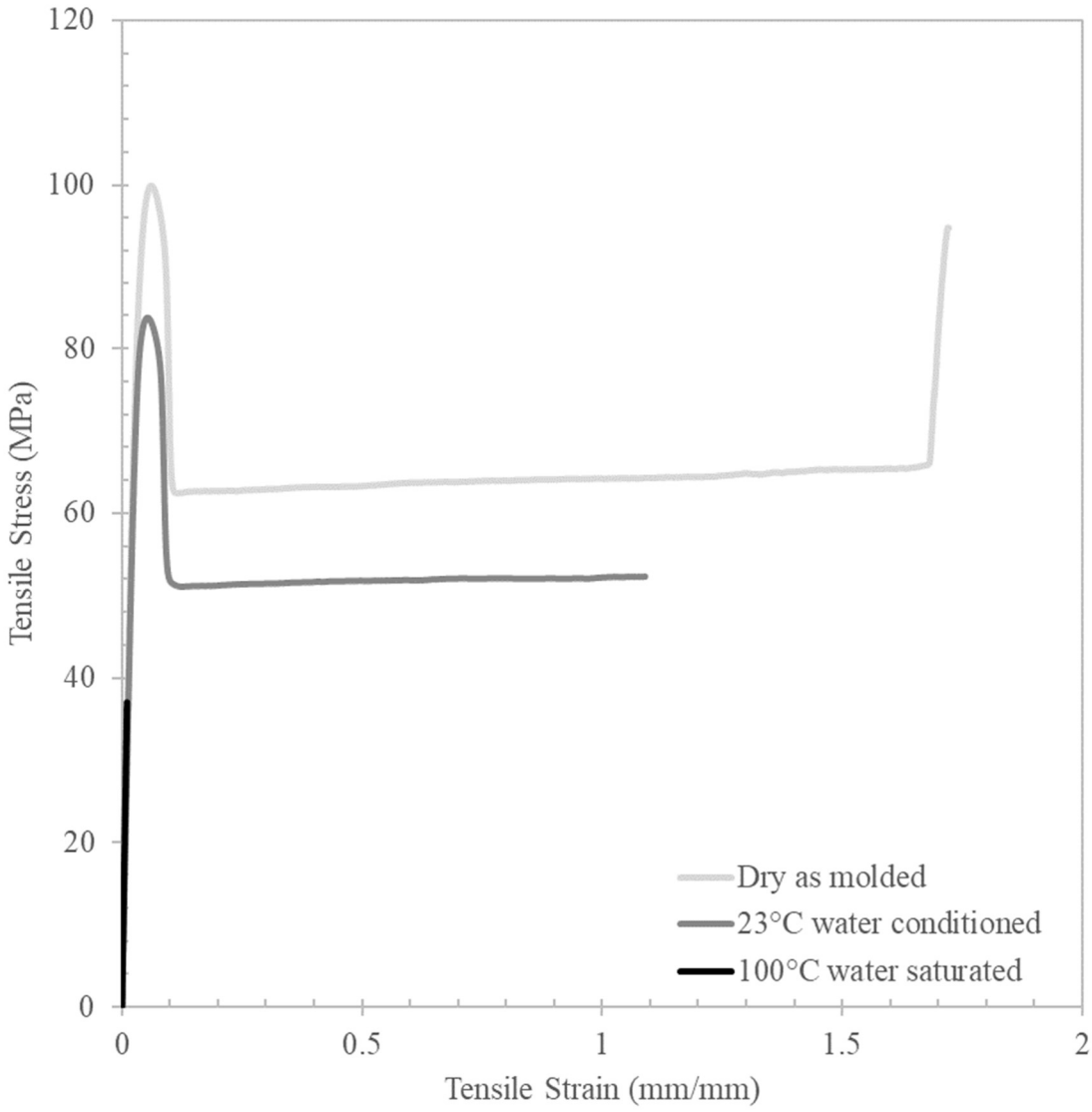

Figure 4.67: PA6I/6T Tensile Stress-Strain DAM vs Water Samples

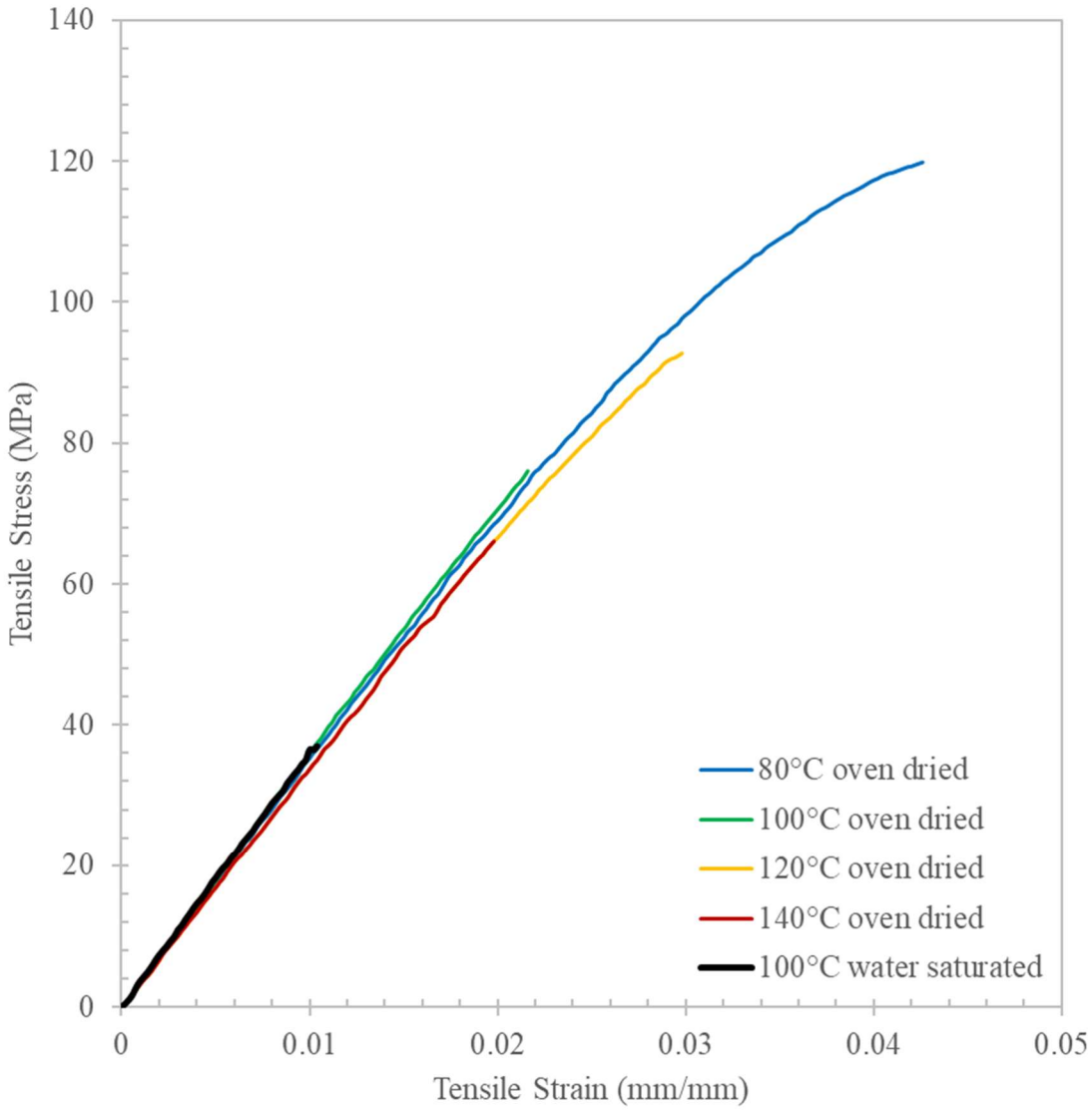

Figure 4.68: PA6I/6T Tensile Stress-Strain DAM vs Dried from Saturated

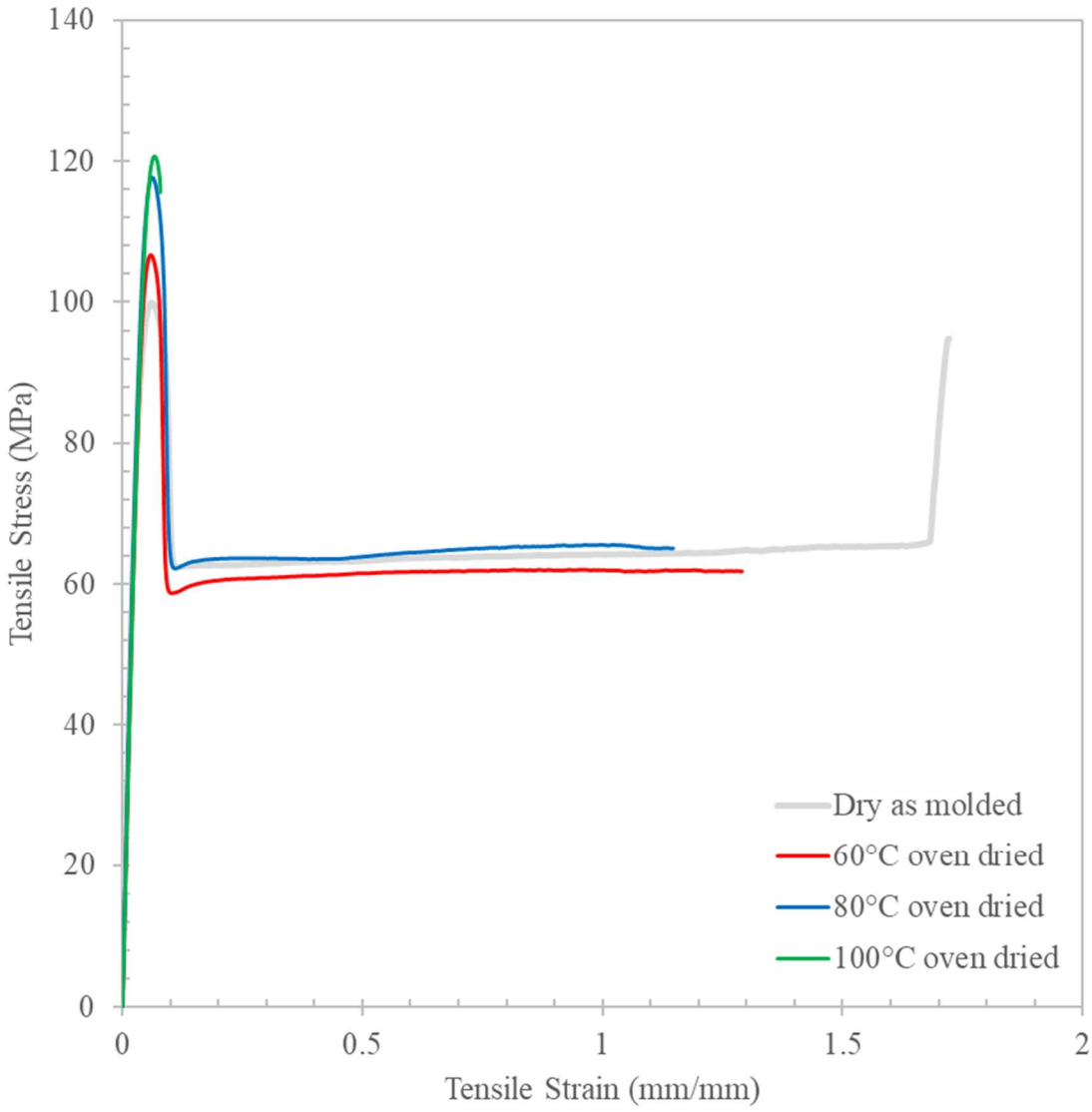

Figure 4.69: PA6I/6T Tensile Stress-Strain DAM vs Dried from Conditioned

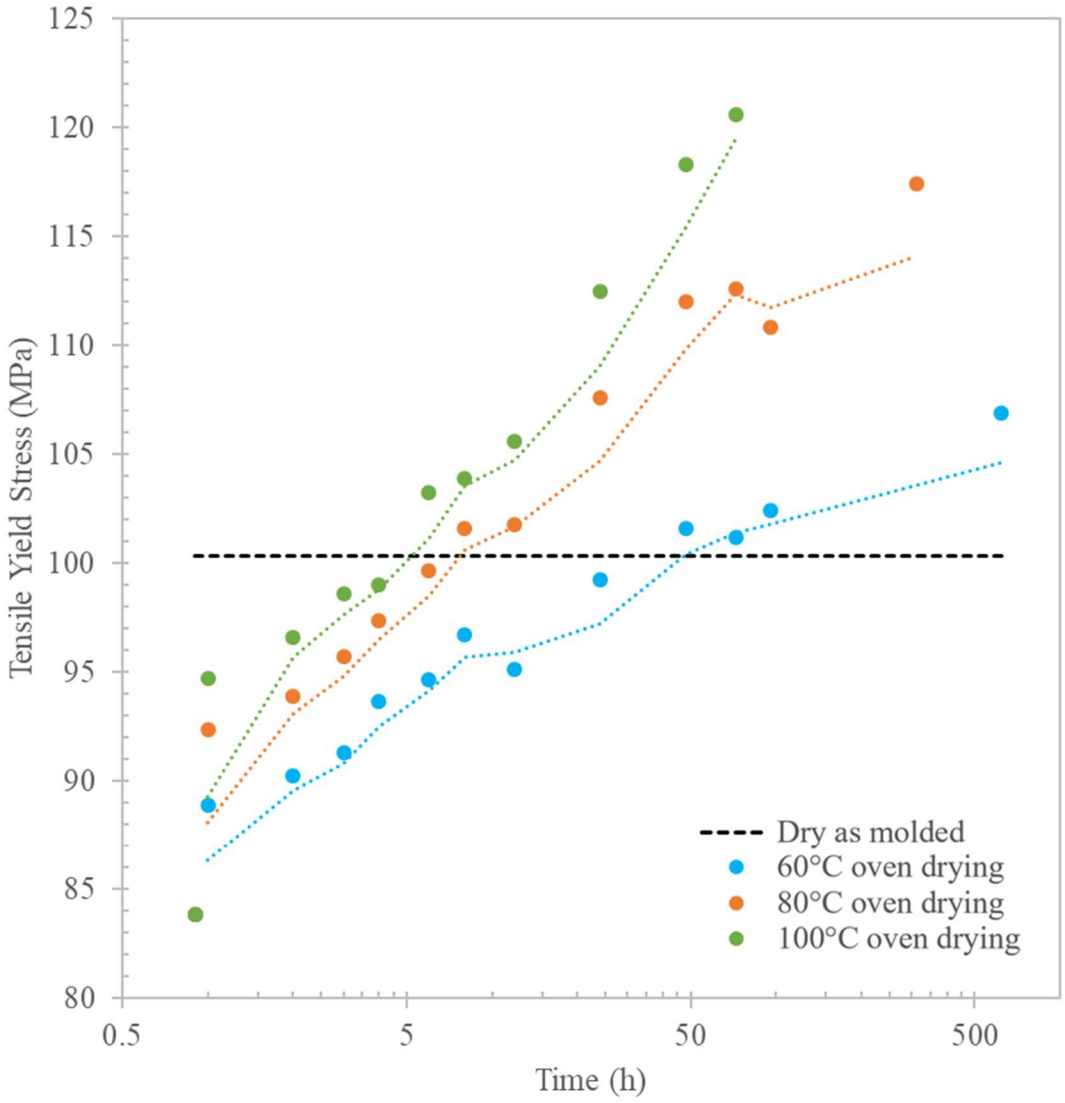

Figure 4.70: PA6I/6T Tensile Yield Stress Dried from Conditioned

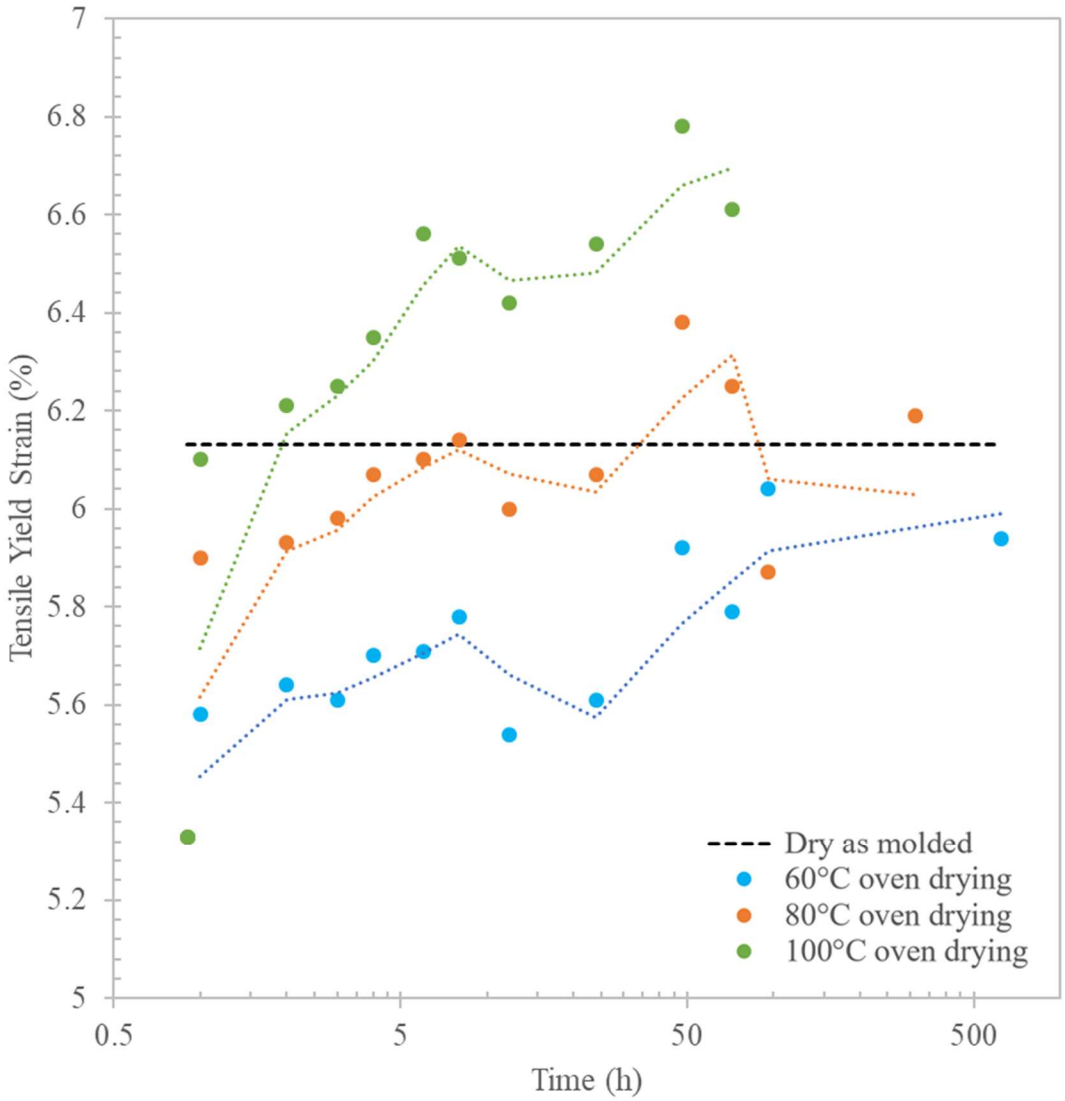

Figure 4.71: PA6I/6T Tensile Yield Strain Dried from Conditioned

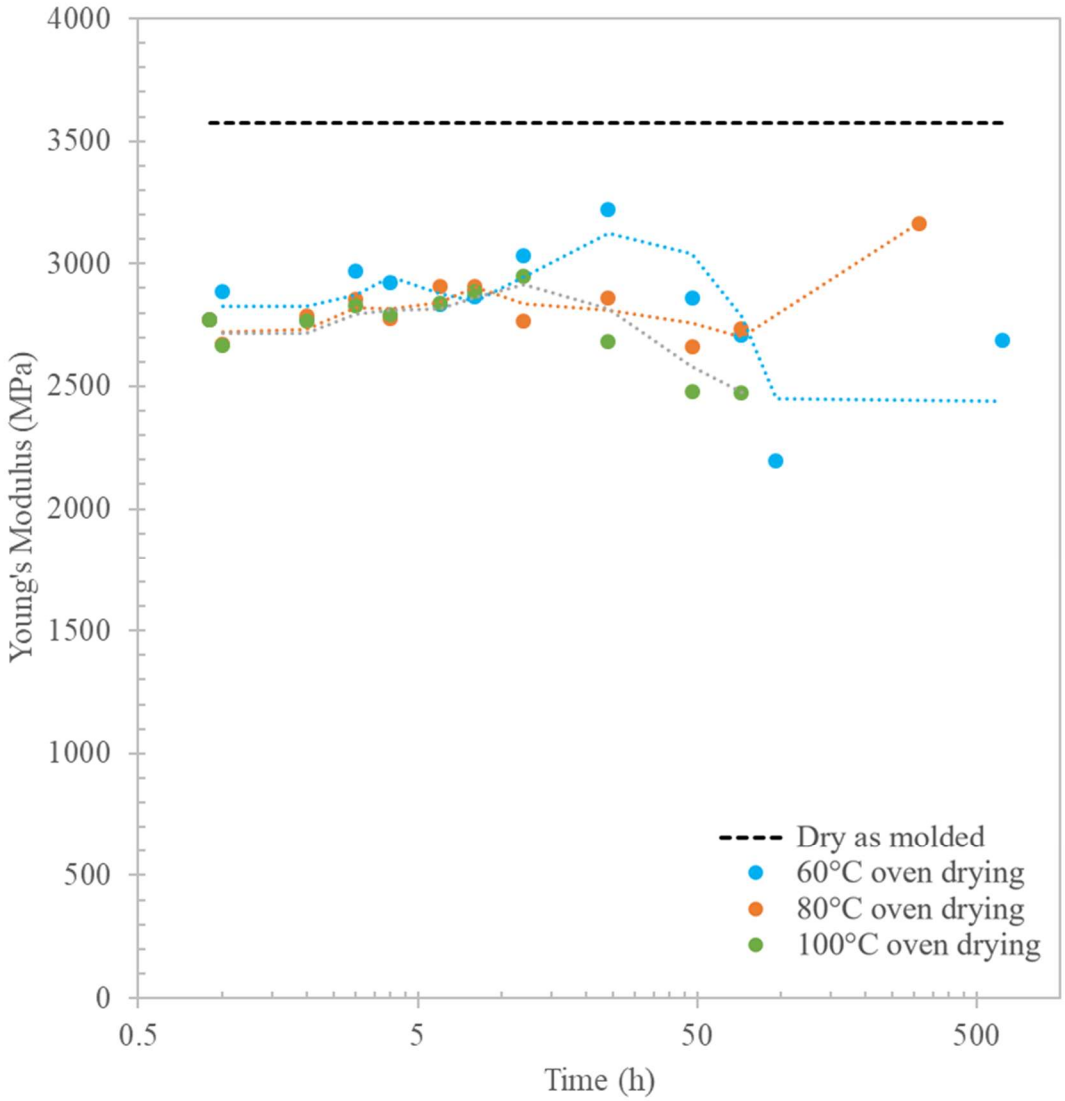

Figure 4.72: PA6I/6T Young's Modulus Dried from Conditioned

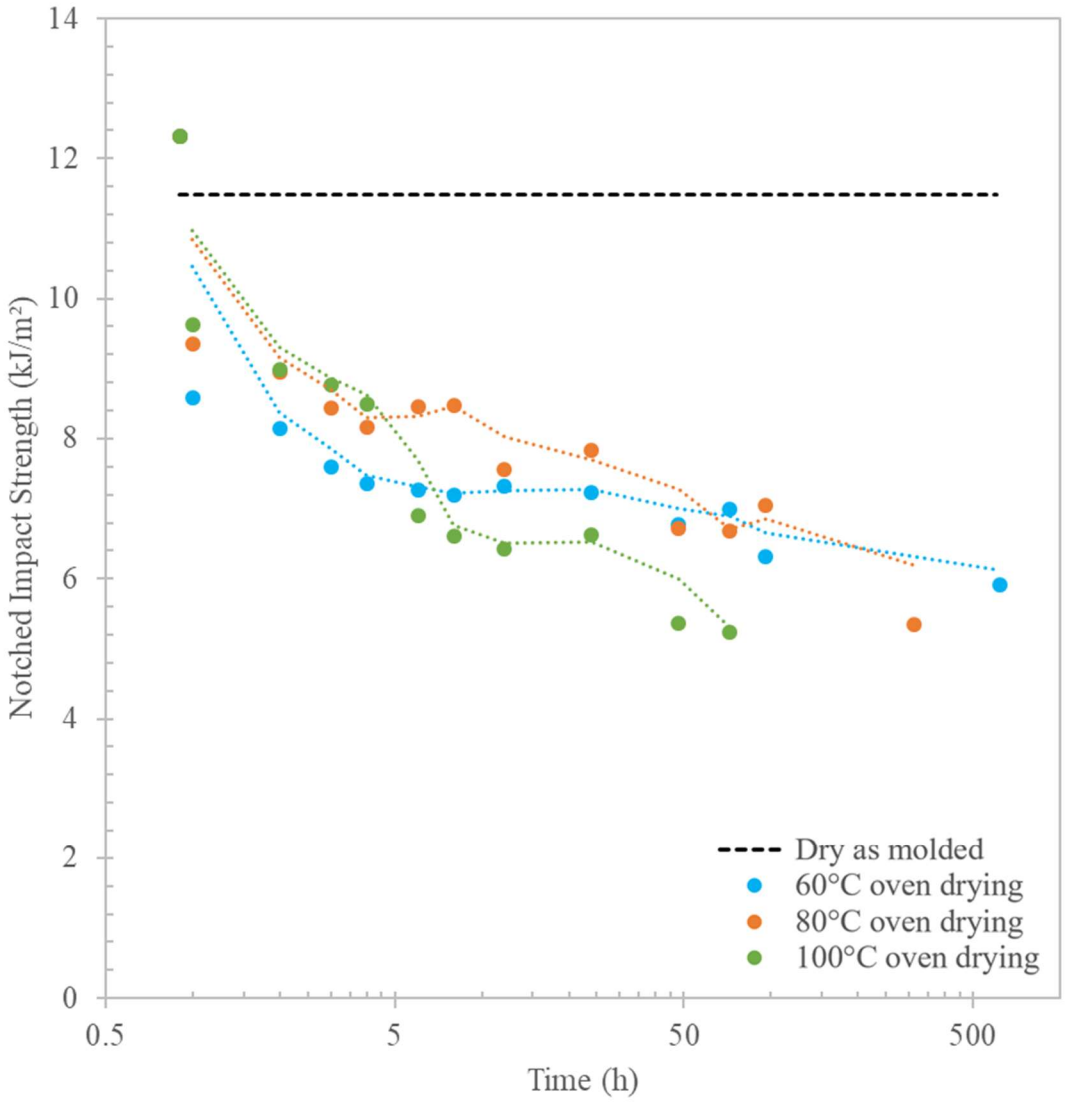

Figure 4.73: PA6I/6T Charpy Impact Dried from Conditioned

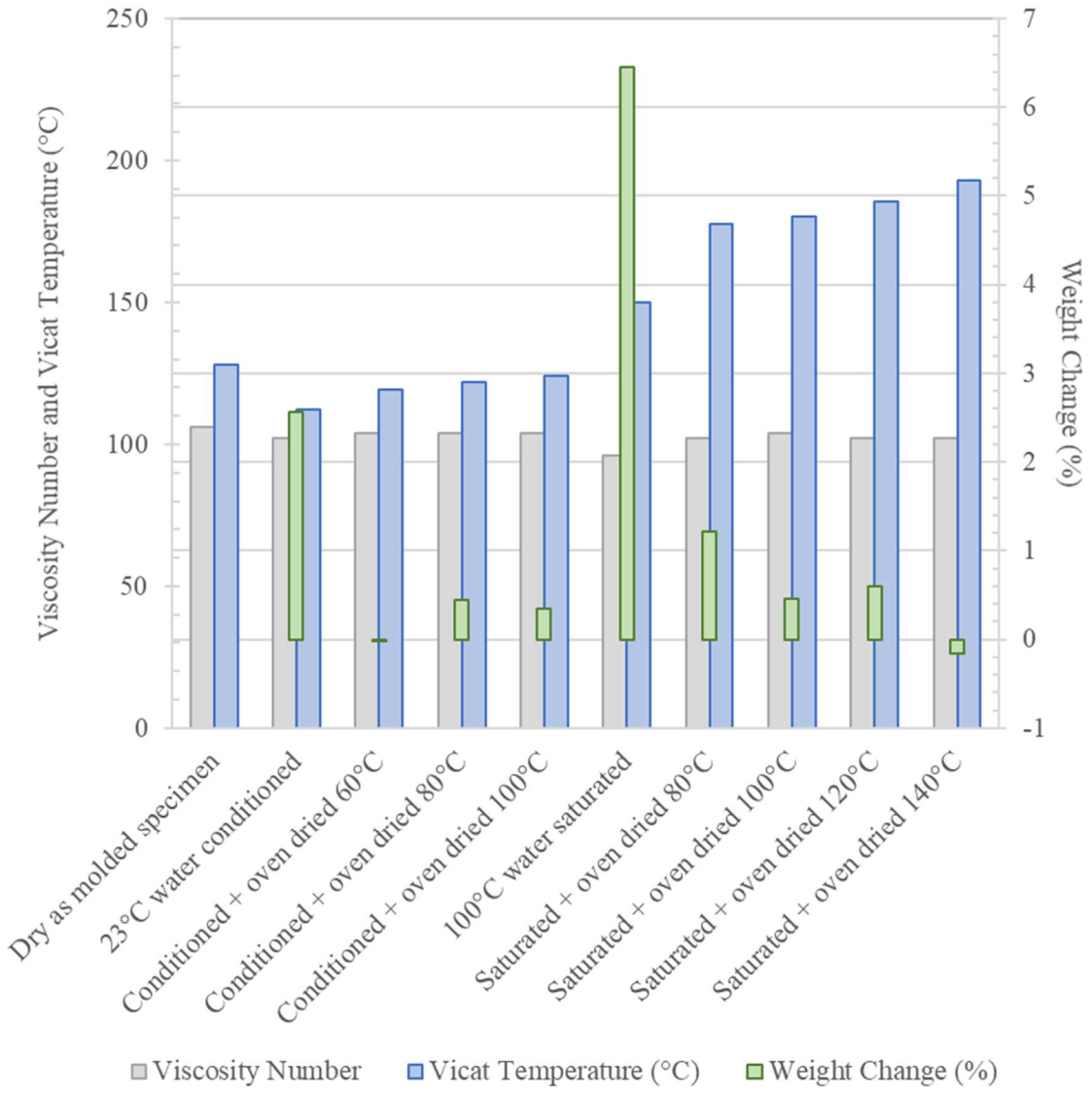

Figure 4.74: PA6I/6T Viscosity Number and Vicat Temperature

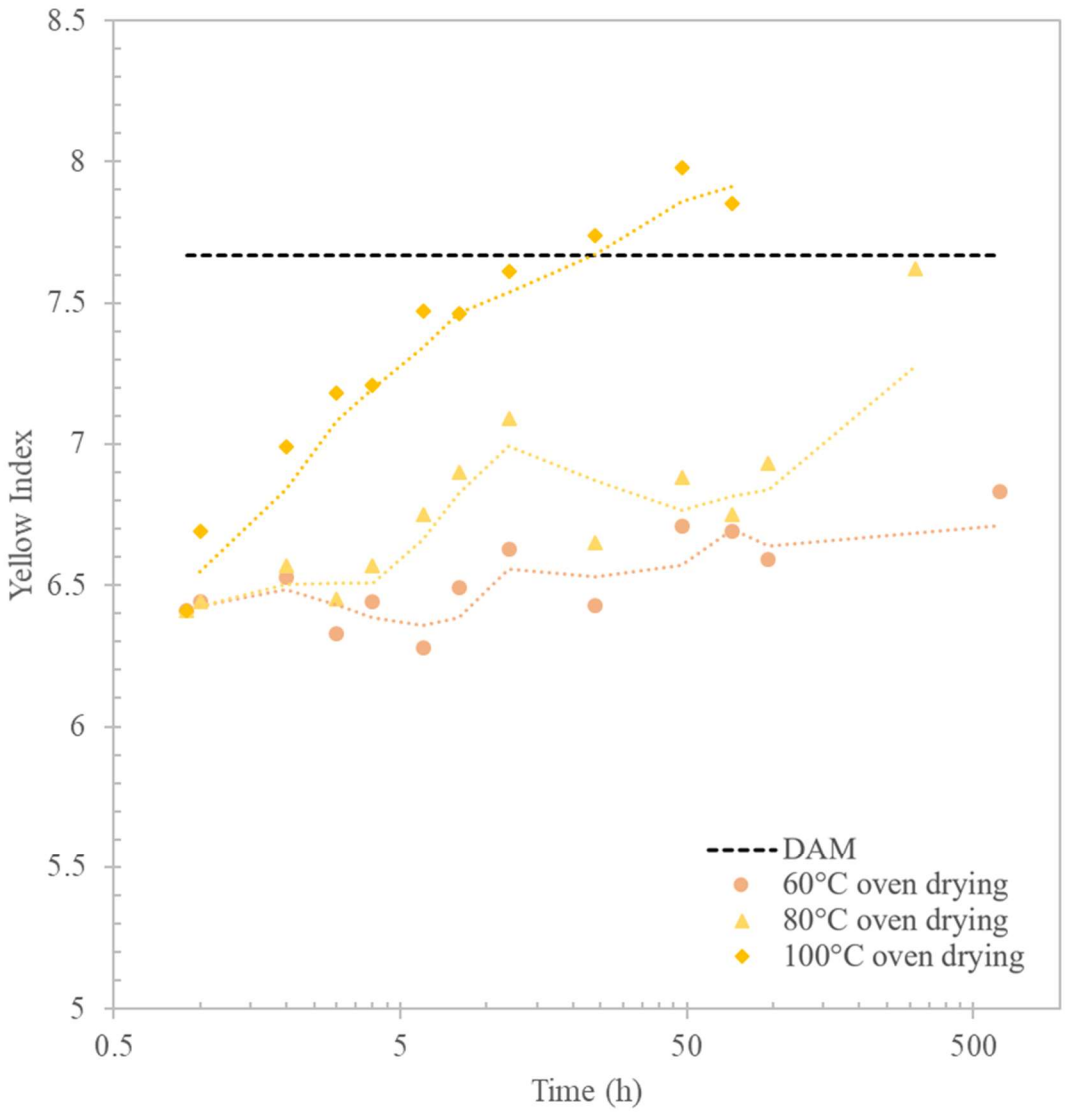

Figure 4.75: PA6I/6T Yellowness Index Dried from Conditioned

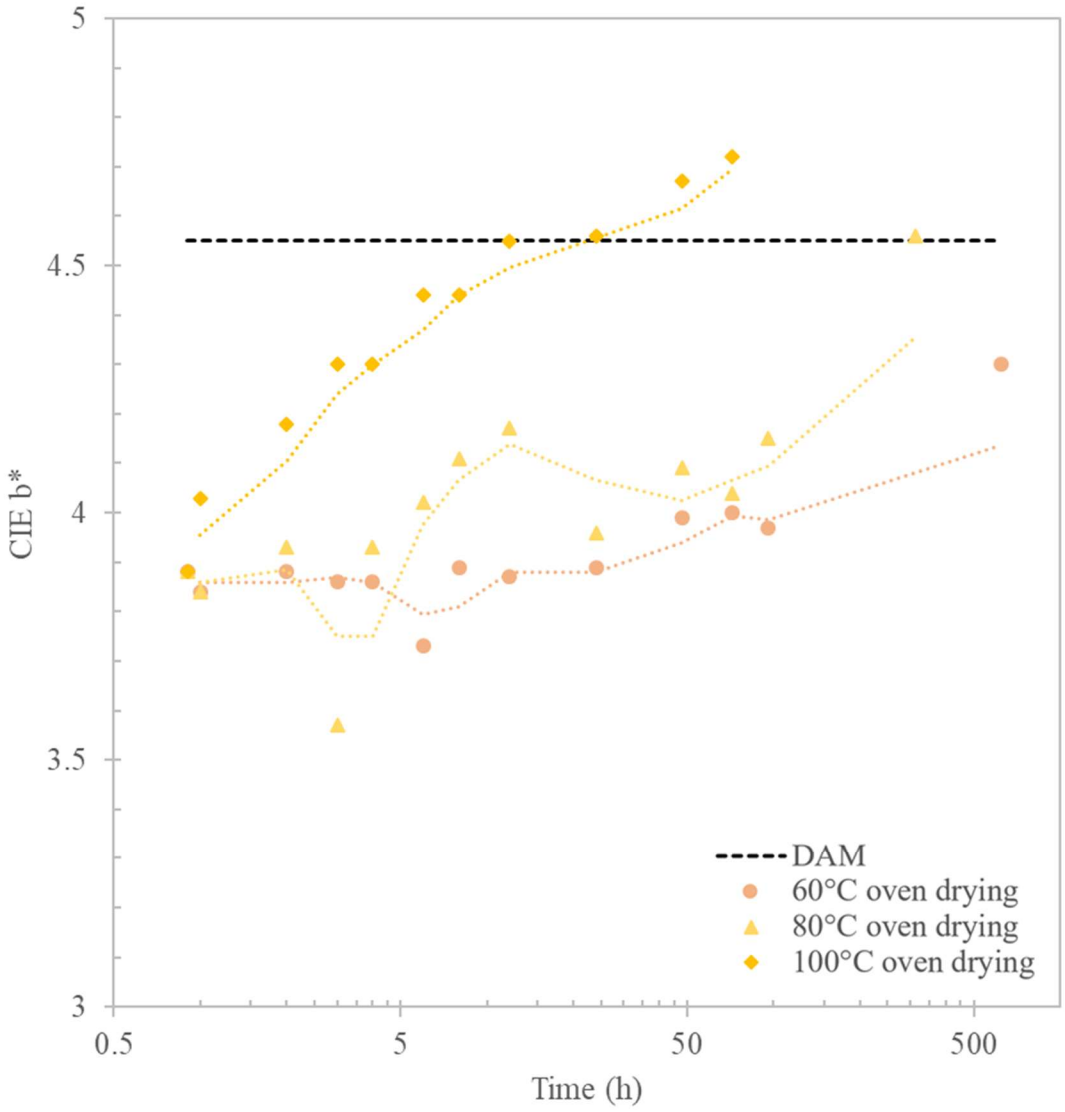

Figure 4.76: PA6I/6T CIE b-Value Dried from Conditioned

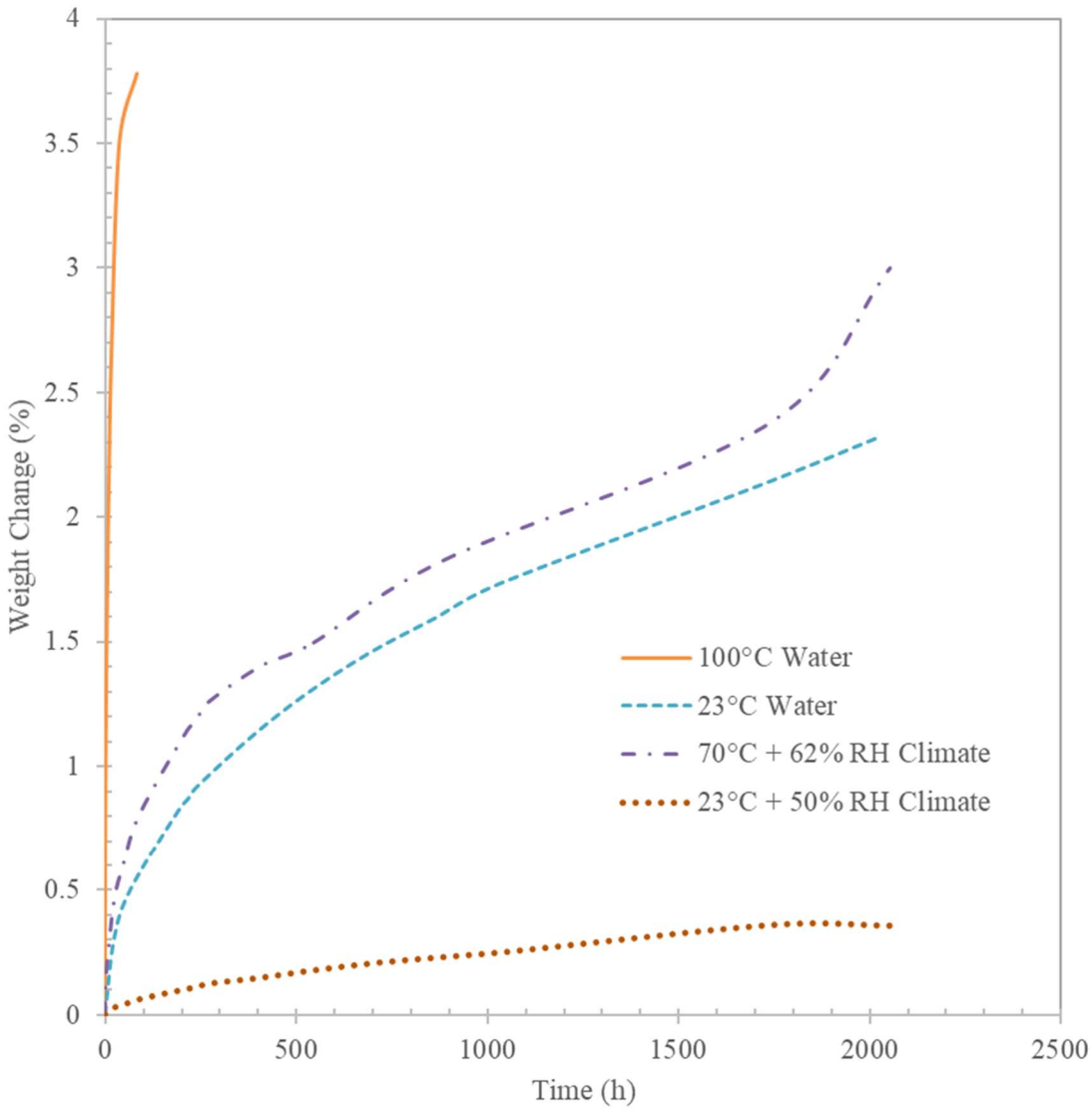

Figure 4.77: 50% GF Reinforced PA66+PA6I/X Absorption Comparison

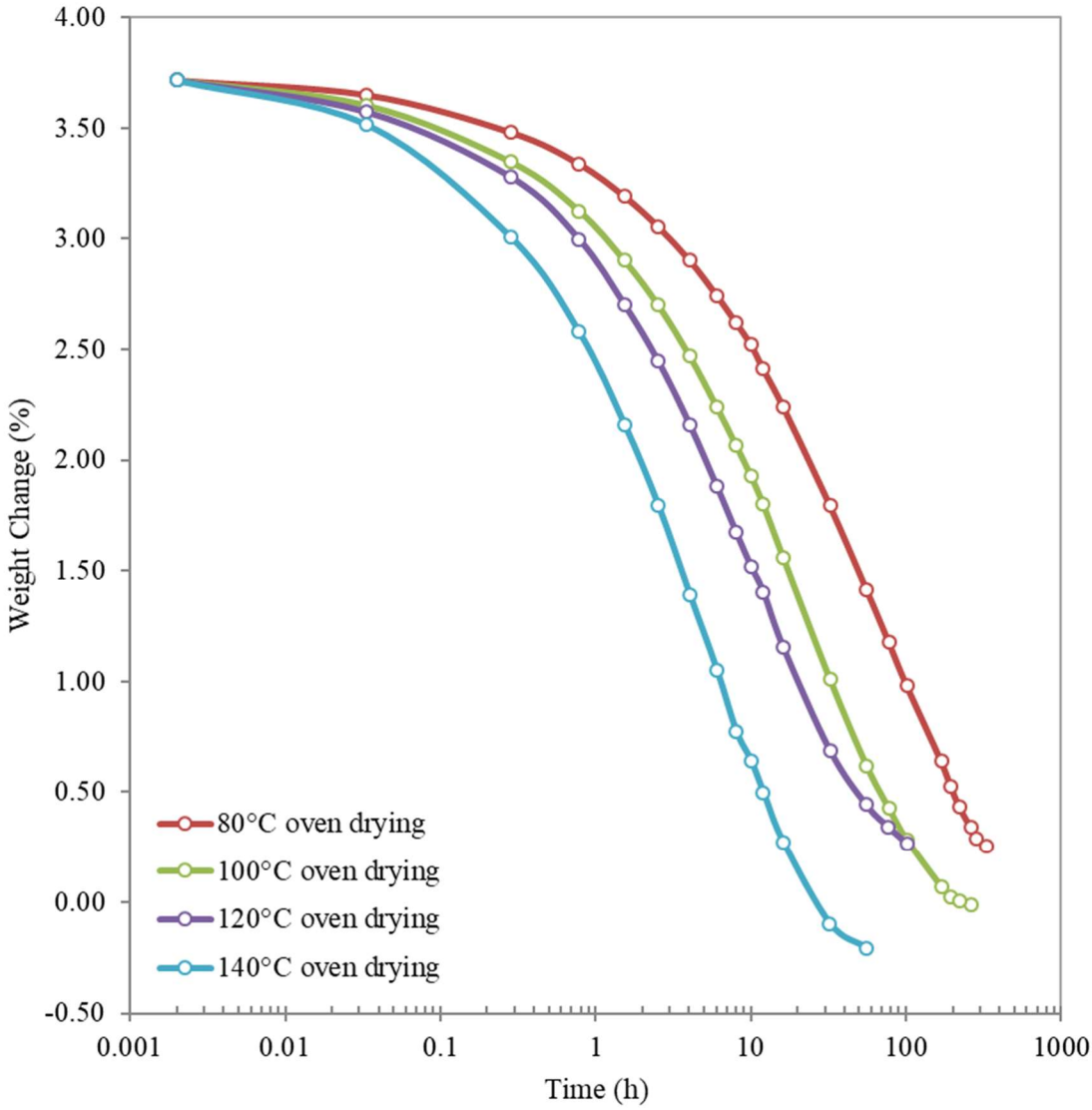

Figure 4.78: Desorption of Saturated 50% GF PA66+PA6I/X Samples

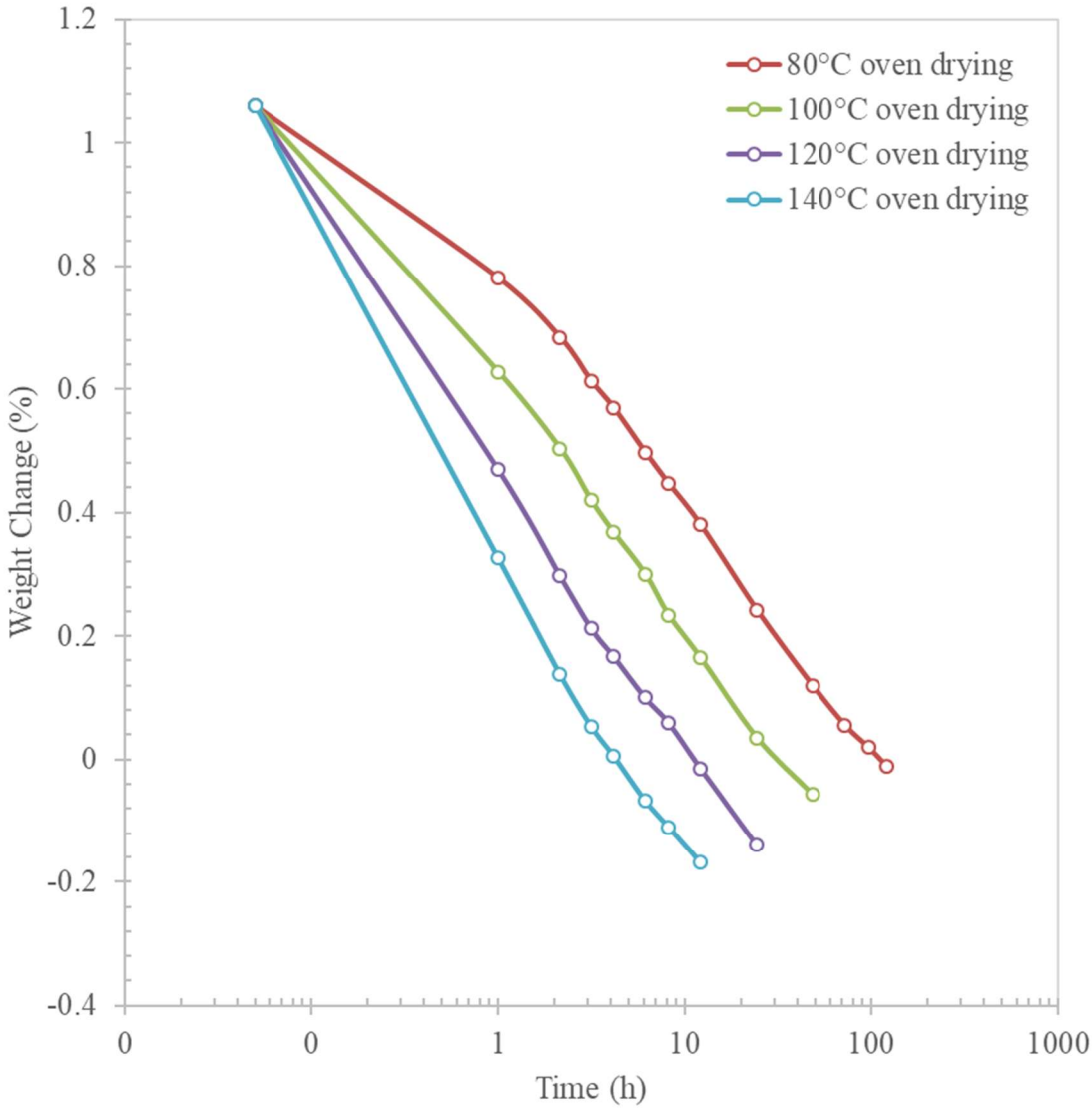

Figure 4.79: Desorption of Conditioned 50% GF PA66+PA6I/X Samples

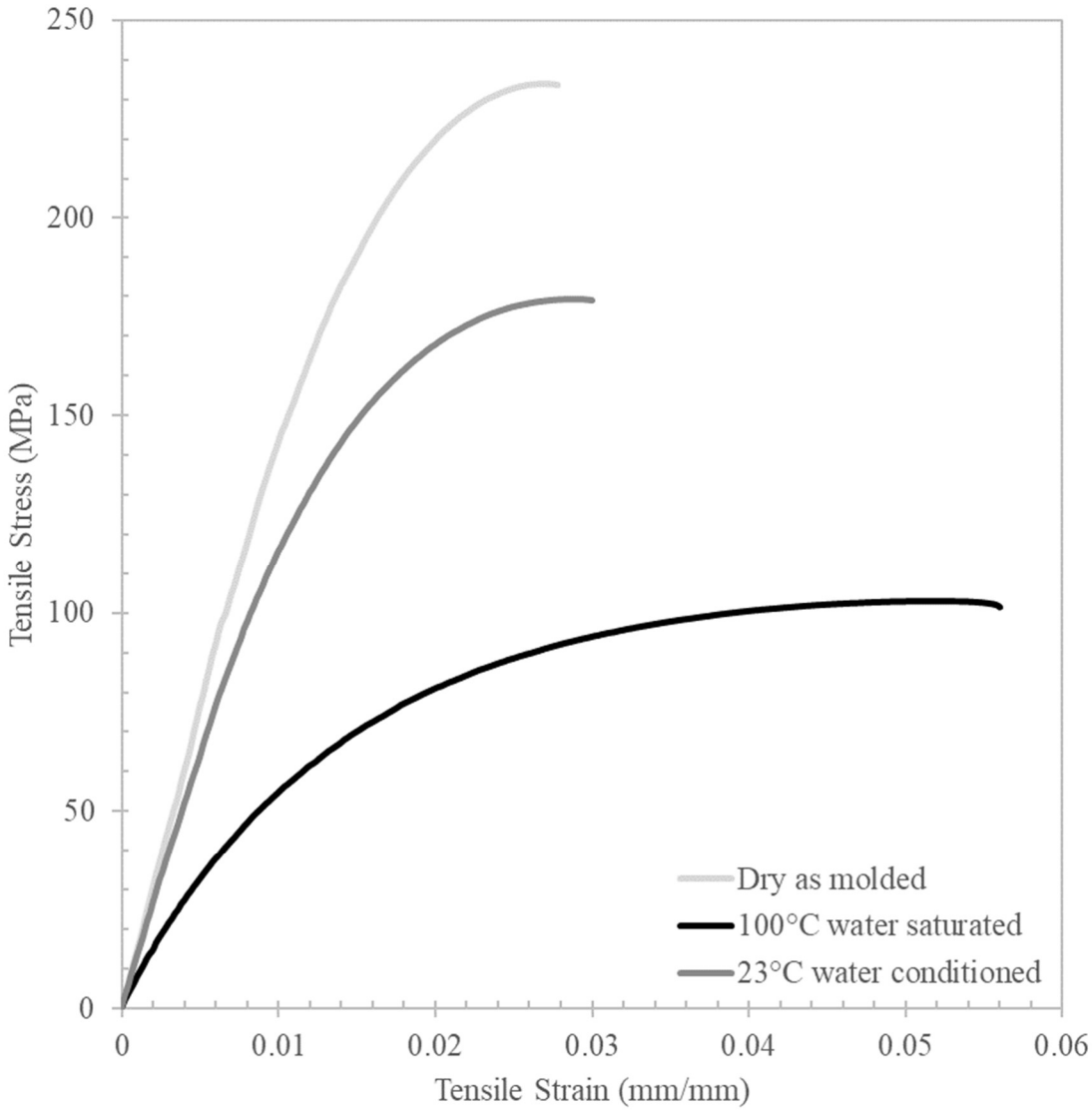

Figure 4.80: 50% GF PA66+PA6I/X Tensile Stress-Strain DAM vs Water Samples

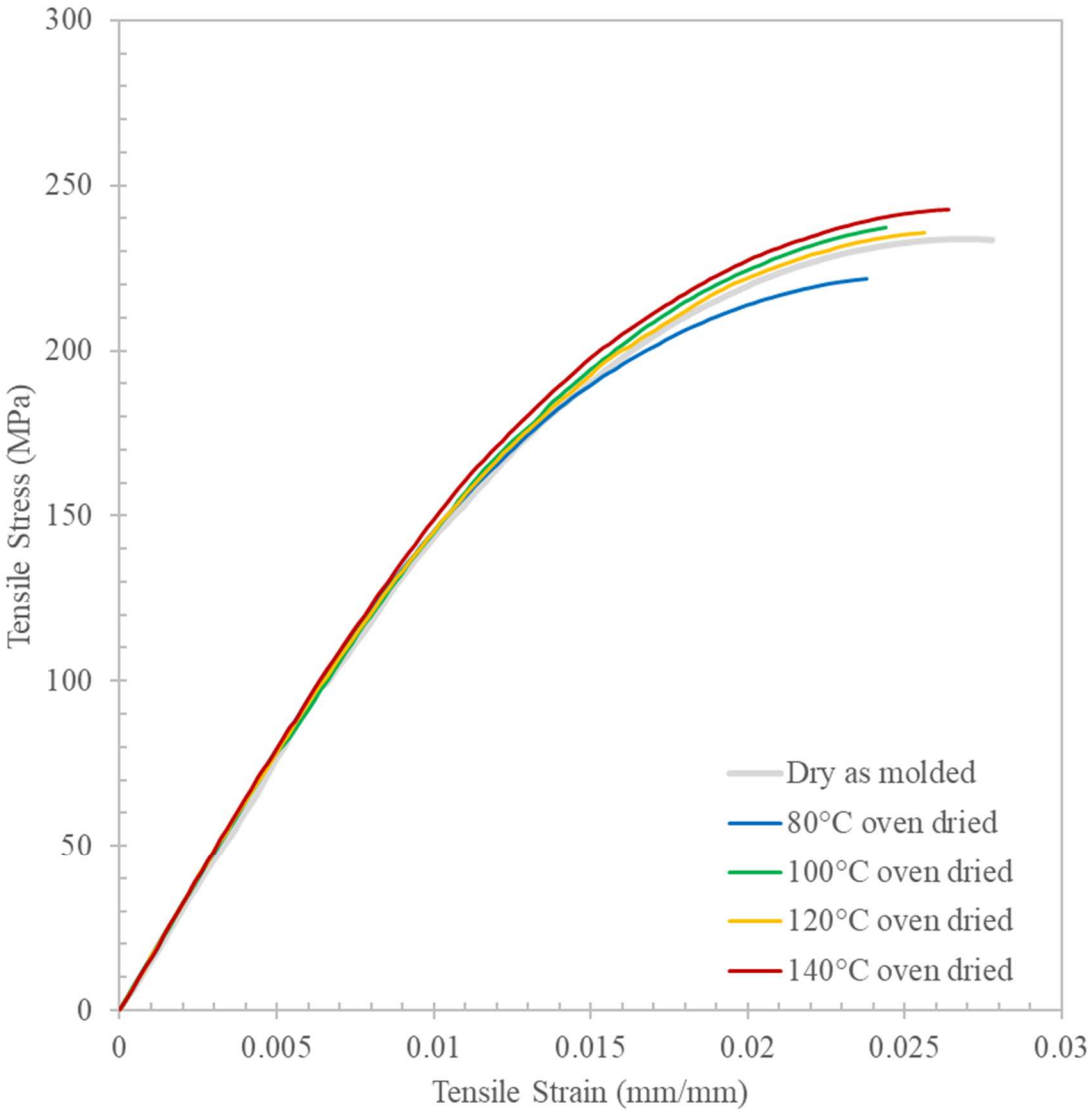

Figure 4.81: 50% GF PA66+PA6I/X Tensile Stress-Strain DAM vs Dried from Saturated

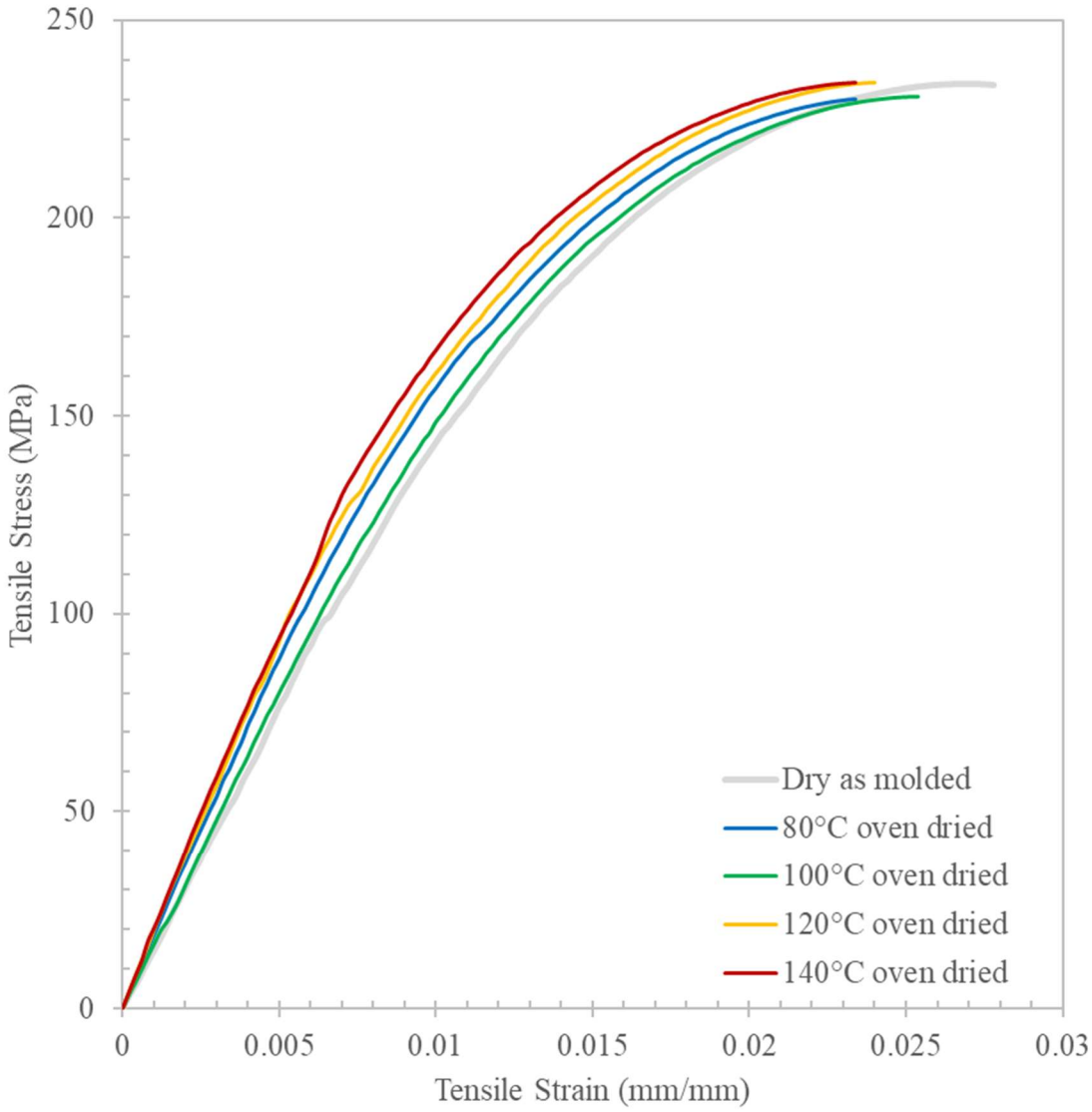

Figure 4.82: 50% GF PA66+PA6I/X Tensile Stress-Strain DAM vs Dried from Conditioned

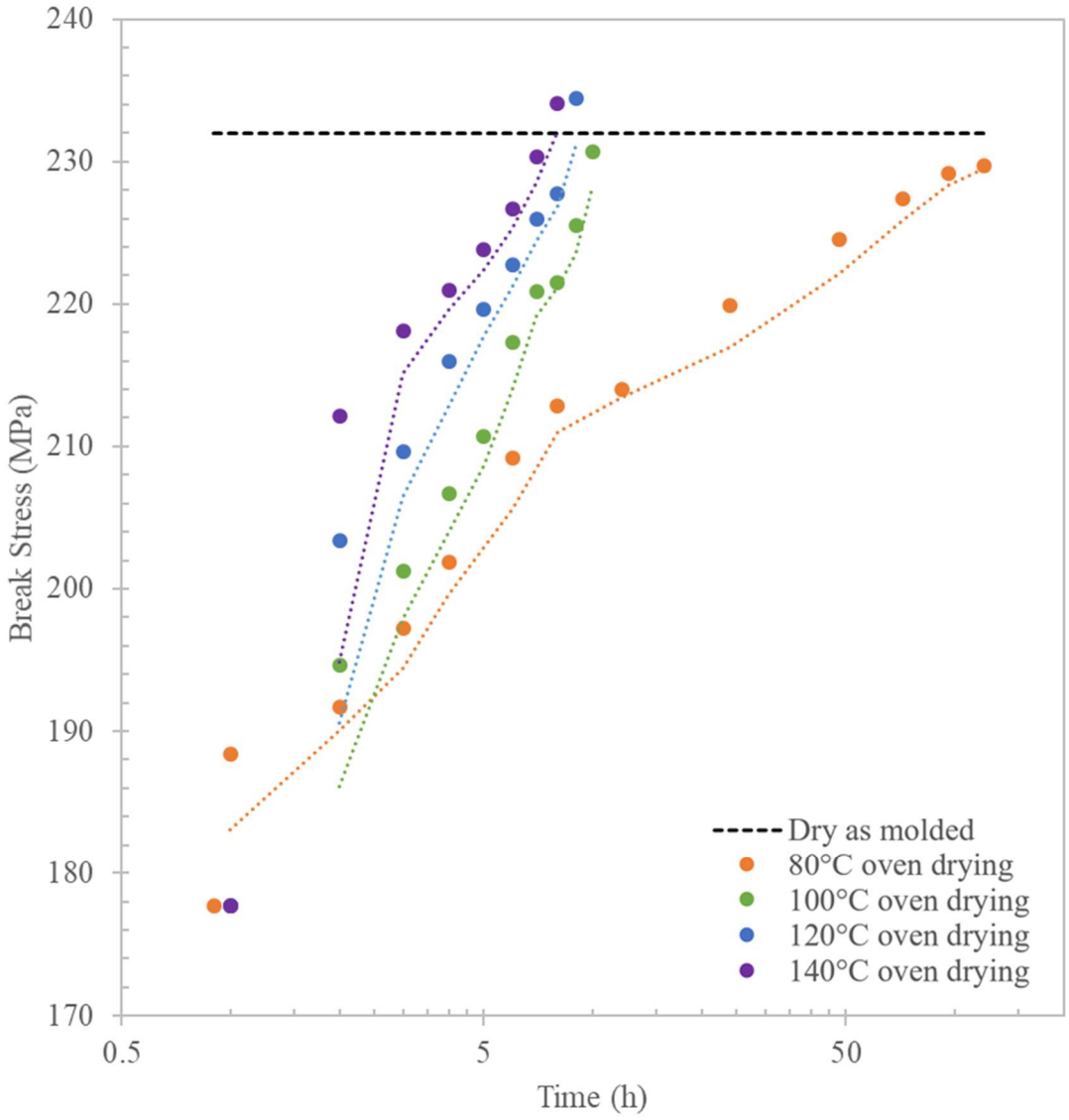

Figure 4.83: 50% GF PA66+PA6I/X Tensile Break Stress Dried from Conditioned

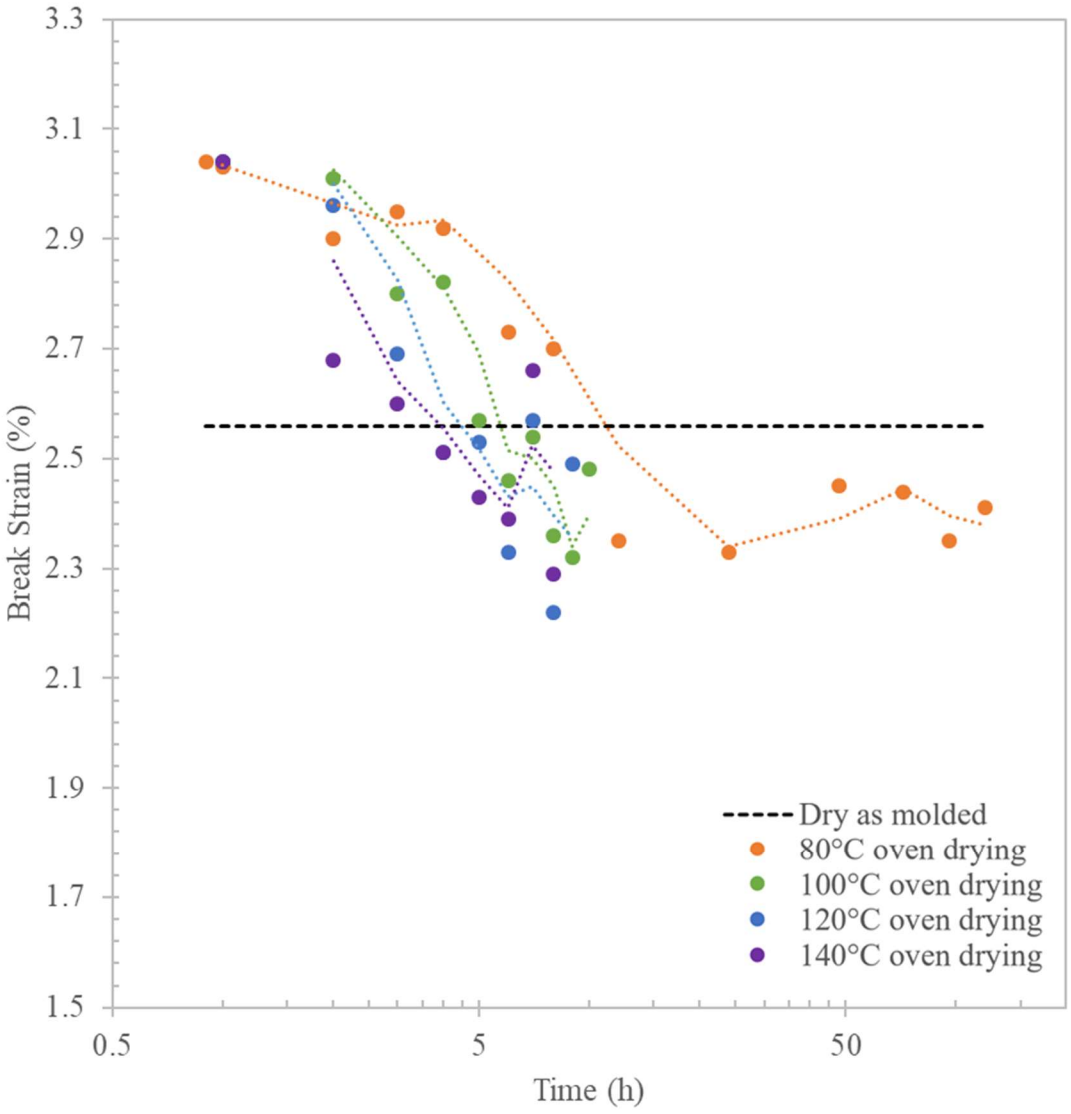

Figure 4.84: 50% GF PA66+PA6I/X Tensile Break Strain Dried from Conditioned

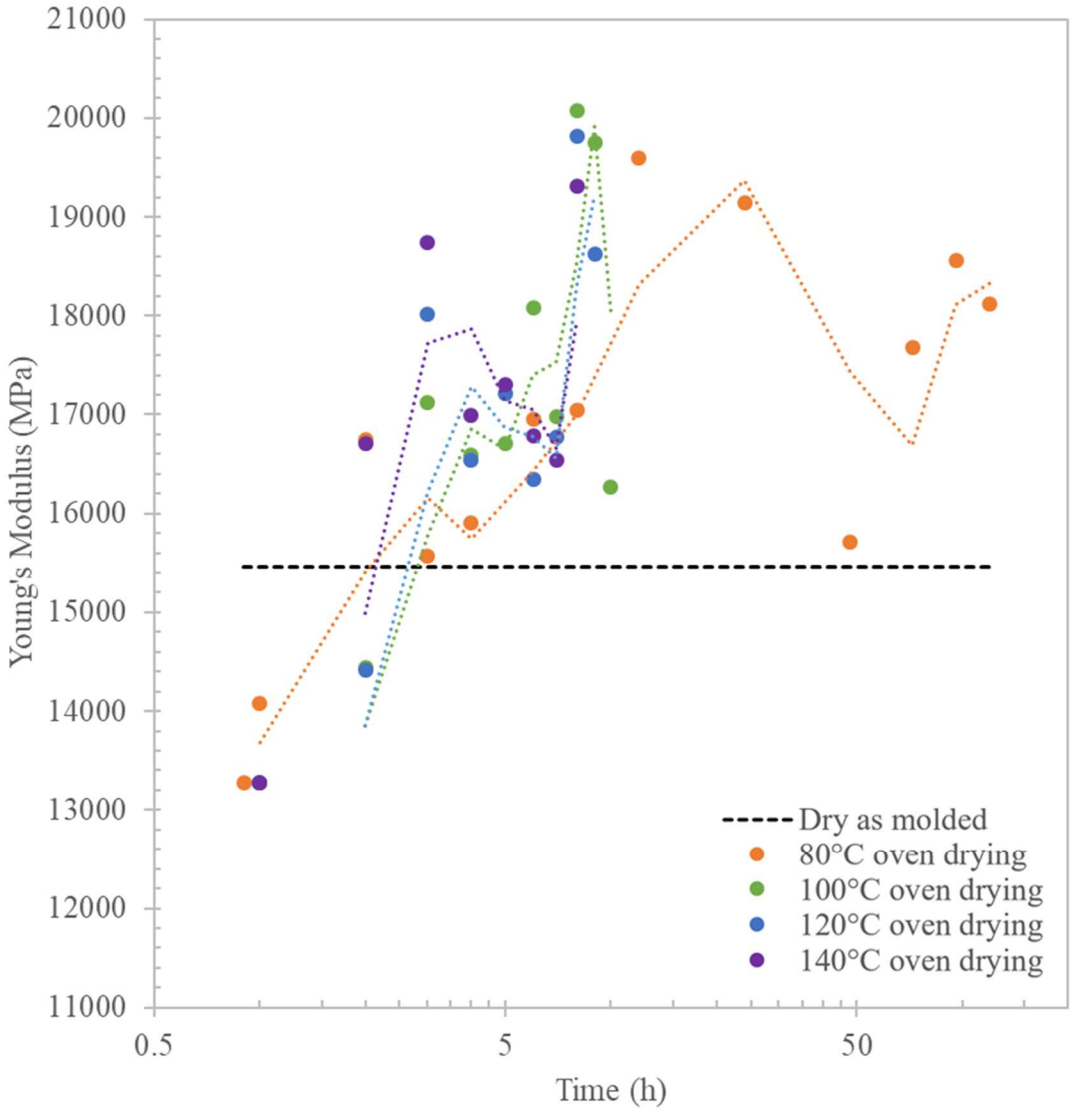

Figure 4.85: 50% GF PA66+PA6I/X Young's Modulus Dried from Conditioned

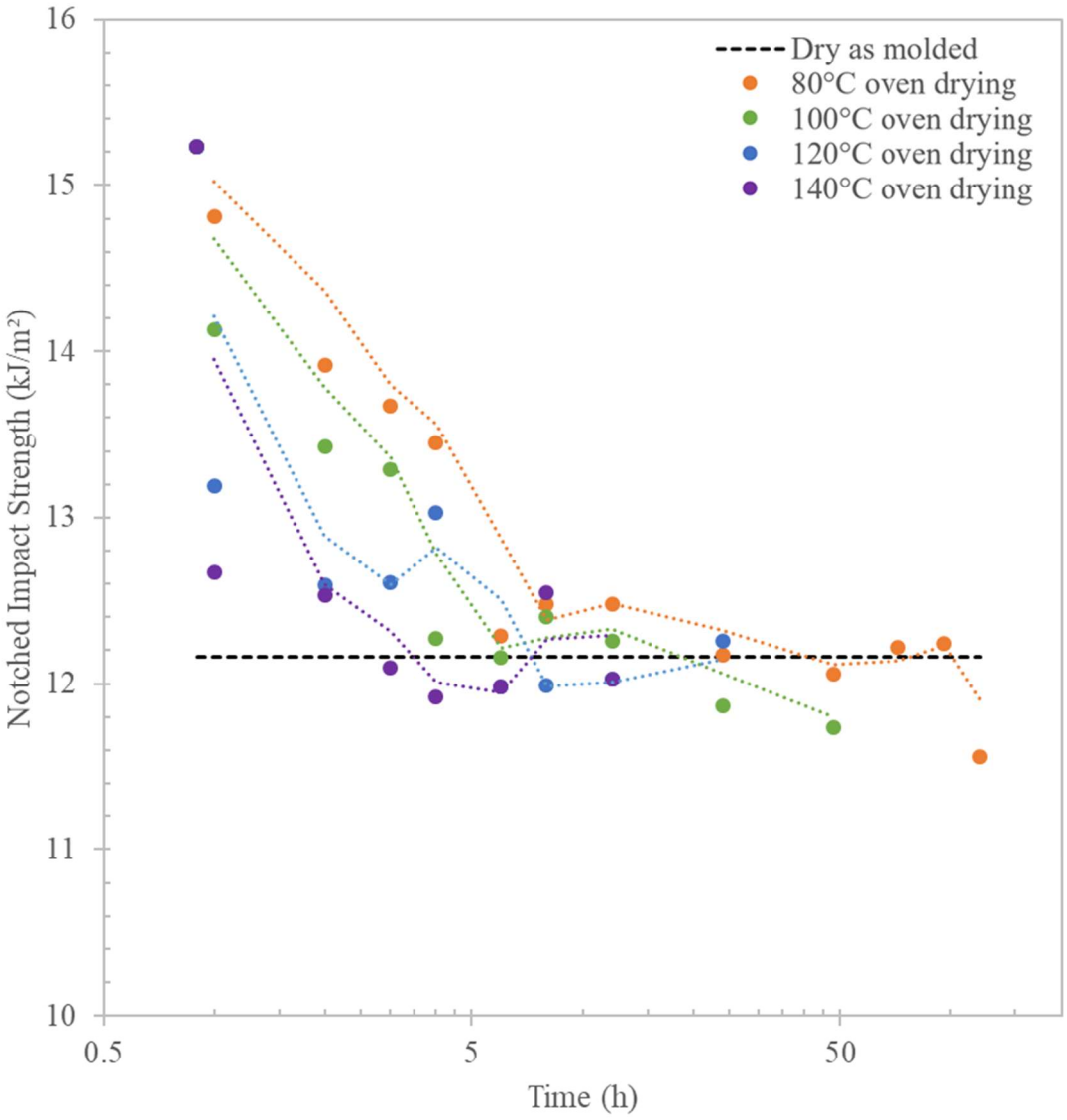

Figure 4.86: 50% GF PA66+PA6I/X Charpy Impact Dried from Conditioned

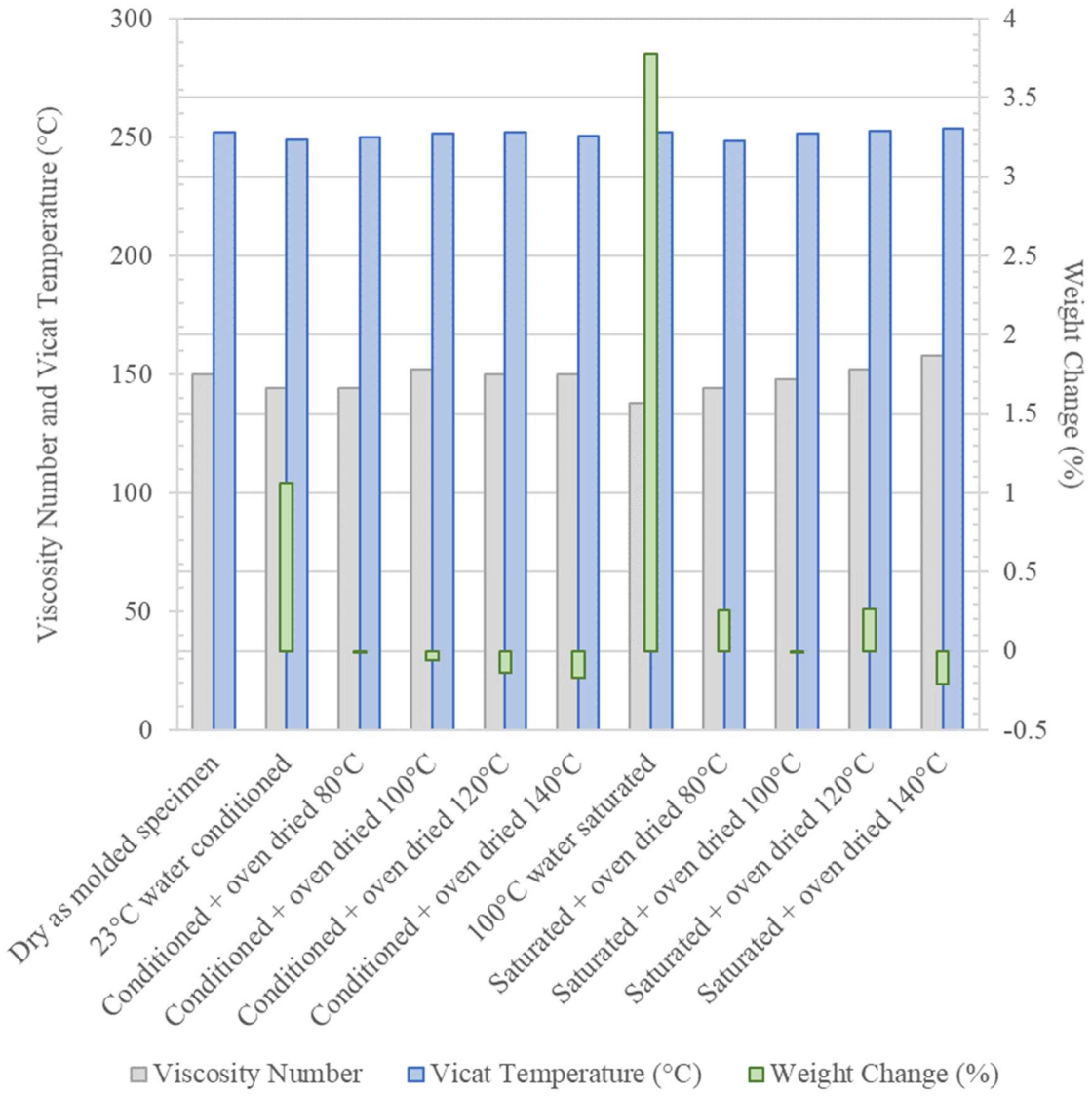

Figure 4.87: 50% GF PA66+PA6I/X Viscosity Number and Vicat Temperature

VITA

Michelle D. Brown

EDUCATION

Master of Science in Polymer Science & Engineering at Lehigh University, August 2015 – present. Thesis title: "Moisture Absorption and Desorption Effects on Mechanical Behavior in Specialty Polyamide Products"

Bachelor of Science (August 1999) in Chemistry, University of South Carolina, Columbia, South Carolina

PROFESSIONAL EMPLOYMENT

Material Testing Supervisor, EMS-CHEMIE (North America), Inc., January 2005 – present. Responsibilities include conduct mechanical testing on specialty polyamide products, monitor injection molding and film extrusion operations, and assist engineers with data compilation for customer presentation

Technical Assistant, Carolina Filters, Inc., April 1994 – April 2004. Responsibilities include investigate customer complaints, develop production process improvements, and generate trial and technical reports for corporate review.